



Building Technologies & Urban Systems Division
Energy Technologies Area
Lawrence Berkeley National Laboratory

Passive cooling designs to improve heat resilience of homes in vulnerable communities

Kaiyu Sun¹, Wannan Zhang¹, Zhaoyun Zeng¹, Ronnen Levinson¹, Max Wei^{2,*},
Tianzhen Hong¹

¹ Building Technology and Urban Systems Division, Lawrence Berkeley National Laboratory, One Cyclotron Road, Berkeley, California

² Energy Analysis & Environmental Impacts Division, Lawrence Berkeley National Laboratory, One Cyclotron Road, Berkeley, California

Energy Technologies Area
December 2021

<https://doi.org/10.1016/j.enbuild.2021.111383>



This work was supported by the Assistant Secretary for Energy Efficiency and Renewable Energy,
Building Technologies Office, of the U.S. Department of Energy
under Contract No. DE-AC02-05CH11231.

Disclaimer:

This document was prepared as an account of work sponsored by the United States Government. While this document is believed to contain correct information, neither the United States Government nor any agency thereof, nor the Regents of the University of California, nor any of their employees, makes any warranty, express or implied, or assumes any legal responsibility for the accuracy, completeness, or usefulness of any information, apparatus, product, or process disclosed, or represents that its use would not infringe privately owned rights. Reference herein to any specific commercial product, process, or service by its trade name, trademark, manufacturer, or otherwise, does not necessarily constitute or imply its endorsement, recommendation, or favoring by the United States Government or any agency thereof, or the Regents of the University of California. The views and opinions of authors expressed herein do not necessarily state or reflect those of the United States Government or any agency thereof or the Regents of the University of California.

Passive cooling designs to improve heat resilience of homes in vulnerable communities

Kaiyu Sun¹, Wannan Zhang¹, Zhaoyun Zeng¹, Ronnen Levinson¹, Max Wei^{2,*}, Tianzhen Hong^{1,*}

¹ Building Technology and Urban Systems Division, Lawrence Berkeley National Laboratory, One Cyclotron Road, Berkeley, California, USA

² Energy Analysis & Environmental Impacts Division, Lawrence Berkeley National Laboratory, One Cyclotron Road, Berkeley, California, USA

*Corresponding authors: T. Hong, thong@lbl.gov; M. Wei, mwei@lbl.gov

Abstract

Disadvantaged communities face a growing threat to staying safe during heat waves, especially during coincident power outages. This study develops a methodology to evaluate the effectiveness of passive cooling measures (those that operate without power) to improve residential building heat resilience. Building performance is simulated for representative homes and on district scales in two disadvantaged communities in Fresno, California. Eleven passive measures are evaluated using four heat resilience metrics with and without grid power. Results show performance of the mitigation measures varies by building characteristics, surrounding environment, and power scenario. The two most effective measures were installing solar-control window films and adding roof insulation. For pre-1978 single-family homes, these two measures can reduce unmet degree-hours (UDH) by 12% and 11% respectively without grid power, or 28% and 37% with grid power. Their respective UDH reductions on district scale typically range 8% — 20% and 4% — 12% without grid power, or 13% — 40% and 8% — 42% with grid power. The top floors are more dangerous than lower floors during extreme heat events with coincident power outages. Natural ventilation can significantly help, reducing UDH by 21% — 26%. The methodology and findings from this study can help cities, communities, and utilities develop effective and targeted strategies to promote greater residential heat resilience.

Keywords: heat resilience; heat wave; passive measures; residential building; occupant health; occupant safety; vulnerable community; power outage; Fresno, California;

Abbreviations

AC	Air conditioning or air conditioner
ACH	Air changes per hour

ACM	Alternative calculation method
BEopt	Building Energy Optimization Tool
CBECC-RES	California Building Energy Code Compliance - Residential
DAC	Disadvantaged community
ECM	Energy conservation measure
Fresno EOC	Fresno Economic Opportunities Commission
HAP	Heat action plan
HI	Heat index
HIHH	Heat index hazard hours
IECC	International Energy Conservation Code
LEED	Leadership in Energy and Environmental Design
PMV	Predicted mean vote
PMVET	Predicted mean vote exceedance hours
NOAA	National Oceanic and Atmospheric Administration
RECS	Residential Energy Consumption Survey
RH	relative humidity
SET	Standard effective temperature
SETUDH	Standard effective temperature unmet degree-hours
SHGC	Solar heat gain coefficient
SR	Solar reflectance
TE	Thermal emittance
TMY	Typical meteorological year
UDH	Unmet degree-hours
VT	Visible transmittance

1. Introduction

Extreme heat is one of the leading causes of weather-related deaths globally, and the leading cause in the United States [1,2], where extreme heat events were responsible for nearly 8,000 excess deaths from 1999 to 2009. Extreme heat events are expected to occur 5 to 10 times more frequently by the end of the 21st century [3]. In 2006, more than 600 people in California died due to heat-related conditions during a 10-day heat wave in 2006 [4], and during the U.S. Labor Day holiday in 2017, there were six heat-related deaths in San Francisco (a moderate climate) when the outside air temperature reached 41 °C (106 °F) [5], breaking the 140-year record for high temperature in San Francisco.

In a review for California's Fourth Climate Change Assessment [6], Seville et al. [7] reported that by 2100, California summers are expected to be 2 – 3 °C (4 – 5 °F) warmer than today, with 25 to 50 extreme heat days (defined as weather that is much hotter than average for a particular time and place [8]) per year by 2050, and over 100 such days annually by 2100. They estimate that heat-related deaths in the state could increase two to threefold by 2050, and that mortality for seniors could rise tenfold by the end of the century. Air conditioning demand is projected to increase due to warmer weather and wider use of cooling equipment [9,10], increasing customer utility cost. These events and trends also strain the electric grid by increasing demand for air conditioning, reducing output from inadequately cooled power plants, and lowering the efficiency of electrical transmission [11].

Residents of disadvantaged communities (DACs) who live in older homes with poor insulation, single-pane windows, leaky envelopes, inefficient lighting, and/or inefficient appliances are especially vulnerable to extreme heat events, because such homes suffer from high solar heat gains (through roof, walls, and windows), and/or high internal heat gains (from in-efficient lighting and appliances). Such homes may also have antiquated (if any) air conditioning equipment with limited cooling capacity, low efficiency, and high operating costs. The public health threat of heat gains in such homes will grow more severe as California warms, raising the number of hours each year in which buildings need cooling, as well as the number of extreme heat days each year in which lack of adequate cooling threatens occupant health. Therefore, there is an urgent need to boost resilience to heat waves in California's neighborhoods and cities, especially for the state's most vulnerable populations, such as low-income residents and elderly residents who live in DACs.

Both weather related grid disturbance events and overall electric grid disturbance events in the U.S. have been trending higher since 2000 [12] and the U.S. Department of Energy has launched efforts to enhance the resilience of the electricity grid to reduce the impact from natural disasters and climate change [13]. Starting in 2019, after catastrophic wildfires in 2018, California residents have been subject to "public safety power shutoff" events [14] in the fire season during periods of very high wind speeds where utilities have de-energized portions of the grid to prevent wildfires from being started by electrical equipment. In the summer of 2020, some residents in California experienced either rolling blackouts—the first non-wildfire ones in 19 years—or the threat of rolling blackouts due to intense heat across the Western U.S. and constrained supply resources due to the shutdown of fossil fuel plants [15]. All of these threats

and events highlight the need for greater resilience to extreme heat and potential grid power outages.

Multiple challenges exist in Fresno and the Central Valley for disadvantaged communities. Fresno belongs to ASHRAE Climate Zone 3B according to ASHRAE Standard 169 [16]. Residents suffer from the worst air quality in the state [17] and have the highest utility bills in the state [18]. Residents will experience more extreme heat days each year, likely tripling by 2030 (to 20 days from 6) [19]. In January 2017, the California Environmental Protection Agency released version 3.0 of the California Communities Environmental Health Screening Tool [20]. CalEnviroScreen 3.0 ranks the disadvantages of California communities by census tract using a holistic set of metrics covering sources of pollution (e.g., PM2.5, pesticides, toxic releases), water, traffic, health indicators (e.g., asthma, low birth weight, cardiovascular health), and social metrics (e.g., unemployment, education, poverty, linguistic isolation). The higher the score, the more disadvantaged the community in this tool. CalEnviroScreen 3.0 identifies most areas of southwest and south Fresno as highly disadvantaged communities, scoring in the top decile. The housing stock in southwest Fresno is largely made up of older buildings with over 90% of its homes built before 1980, placing it at greater risk for having older HVAC equipment and limited envelope insulation as described above. This coincidence of poor underlying respiratory and cardiovascular health in the community, older building stock, a future with much greater incidence of heat waves, and the increased threat of power outages make this area particularly vulnerable to heat waves, and an important test case to model and better understand heat resilience measures.

Passive (no energy) cooling measures for buildings [21–32] can reduce envelope heat gain, modulate (time shift) indoor temperature changes by storing and releasing heat, or remove heat from the building. Unwanted heat gain through the envelope can be reduced with cool envelope materials, including light-colored [33–37] and cool-colored [35,37–43] roof and wall products, fluorescent materials [44,45], thermochromic materials [33,46–48], directionally reflective materials [49–51], solar-retroreflective materials [52,53], and daytime sky radiators [54–56]; advanced windows and shading solutions, including innovative glass technologies to passively and actively control thermal and solar energy flows [57–65], fixed and operable shading solutions both interior and exterior to the glazing [66–76], and glazing/shading technologies that convert incident solar energy to electric power [77–80]; thermal insulation, including bulk materials [81–84] and radiant barriers [84–88]; evaporative envelope surfaces, including green roofs and green façades [89,90] and roof ponds [91–93]; and ventilated envelope surfaces, including closed cavity façades; exhaust air façades; outdoor air curtain façades, ventilated roofs, and ventilated double-skin facades [94–96]. Heat gain can be modulated with phase-change materials [97–101] and removed via natural ventilation [102–104]. The strategies listed in this paragraph are illustrative but not exhaustive. Guidelines for the use of passive cooling measures are provided by a variety of general-audience primers [84,88,105–122].

Overheating propensity and the risk that it poses to building occupants has been assessed for buildings in Australia [31,123], Canada [124], Chile [125], England [126–134], Greece [135], Norway [136], Spain [137], Taiwan [138], and the United States [139–142]. Some research evaluates risks or potential adaptations during heat waves [31,126,135,141,143–146] or in disadvantaged communities [123,130,133,135,147,148].

Many case studies compare the efficacies of alternative passive cooling measures in a specific location, such as Algiers [149], Australia [102,150,151], Brazil [32], Canada [152], China [153–155], Egypt [105,156–158], England [126,159,160], Greece [105,161], Hong Kong [26,162,163], India [164–166], Indonesia [167], Iran [106,168,169], Italy [26,156], Japan [170], Kenya [164], Malaysia [171,172], Mexico [30], Morocco [86,173], New Zealand [174], Oman [175], Poland [176], Portugal [26,164], Saudi Arabia [26,177], Singapore [26], South Africa [178], Spain [156,179], Sri Lanka [180], Tunisia [181], the United Arab Emirates [182], and the United States [142]. Meanwhile, a vast body of literature reports the cooling energy savings, indoor temperature reduction, and/or occupant comfort improvement from individual measures. For example, there are well over 100 such studies just for cool envelope materials [183]. Individual-measure benefits explored in California (the venue of the current work) include those of cool roofs [34,184–194], cool walls [185,195,196], advanced windows [197,198], and shading [70].

From the perspectives of policy makers and residents, it is important to estimate the benefits and potential drawbacks of the proposed solutions quantitatively before selecting and applying them to DACs. Governments and researchers have explored potential solutions to improve heat resilience during extreme heat events and evaluated their effectiveness at different scales. The United States Environmental Protection Agency provided a suite of adaptation strategies to help with emergency response to extreme heat events [199]. The Heatwave Plan issued by the Department of Health in England advocated high-level strategies to keep residents cool in the building during heat waves [200]. The public health officials in Canada have been developing the Heat Alert and Response Systems, which provide guidelines of preventative approach to reducing urban heat island effect and building heat resiliency by modifying the built environment. Strategies include increasing vegetative cover, retrofitting buildings, and installing cool surface materials [201]. Hatvani-Kovacs et al. [202] proposed a range of integrated policy measures to increase the heat stress resilience of urban populations in Australian cities. Maru et al. [203] developed a framework for exploring adaptation pathways to climate change among people in remote and marginalized regions who are disadvantaged and vulnerable. However, the above research covers mainly policy measures with qualitative evaluation, but investigated few building retrofit measures targeting at heat resilience, and none of these resources quantified the expected effectiveness or prioritized the strategies.

There is also research that focuses more on building retrofit measures, especially passive strategies, to improve resilience during heat waves or cold snaps. For example, Katal et al. [204] developed an integrated platform that combines urban building energy modeling with urban-scale microclimate modeling. They used the platform to evaluate building retrofit strategies to improve resilience against winter power outages, as well as evaluate the impact of microclimate on the effectiveness of measures. Short et al. [205] evaluated five retrofit options on their effectiveness on improving hospital buildings' heat resilience as well as impact on energy demands and CO₂ emission. A representative hospital tower building from the late 1960s was used for simulation. Flores-Larsen and Filippin [206] studied the indoor environment in low-income housing from the perspectives of energy and heat resilience during extreme hot periods, and evaluated passive cooling measures to improve both heat resilience and energy efficiency. They performed a case study in a representative social housing in a low-income neighborhood in central Argentina. Sun et al. [142] evaluated the effectiveness of passive and

active energy conservation measures (ECMs) on improving heat resilience and their impact on energy consumption in a Florida nursing home. Hess et al. [207] evaluated the impact of India's first heat action plan (HAP) on mortality caused by heat waves. They found the HAP strategies are effective in reducing mortality rates during extreme heat events. However, the majority of the above research focused on individual buildings and few targeted at district scale, especially DACs.

In summary, there are three major gaps in existing research. First, previous studies focused mostly on building-scale case studies under only one power scenario (either grid on or grid off). However, results from individual buildings cannot provide sufficient information for policy makers to make comprehensive decisions for broader scales like districts/neighborhoods, where there are thousands of buildings and their characteristics vary substantially. Second, few studies performed quantitative analysis at the neighborhood level, which reveals the variations of individual house's resilience to heat waves considering their characteristics, efficiency level, and inter-building impacts (e.g., solar shading). Third, even fewer studies focused on DACs. To address these three gaps, approaches and methodologies should be developed for quantitative analysis of the effectiveness of passive measures on improving heat resilience of DACs at the district scale.

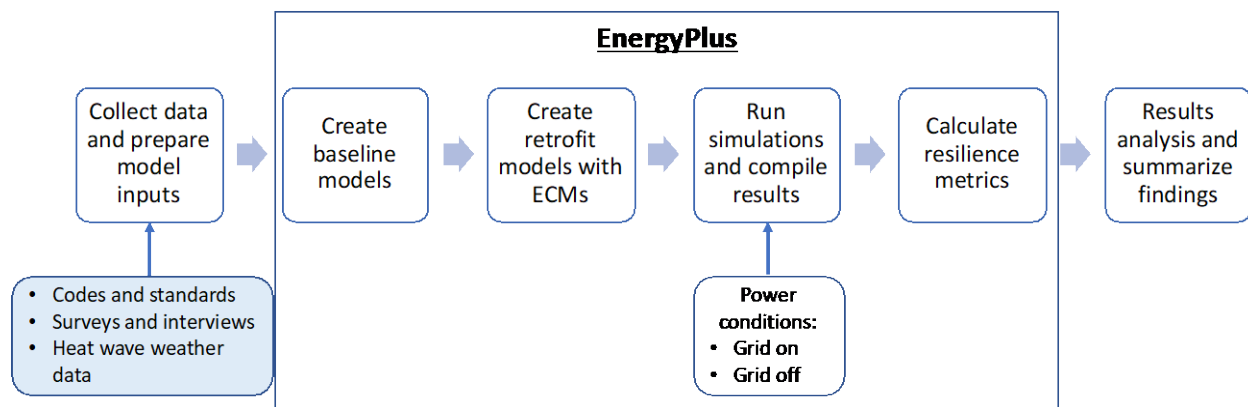
This study addressed the urgent need to boost resilience to heat waves at both the building-scale and the neighborhood-scale, and for two power scenarios: grid-on and grid-off. While the building-scale analysis delivers deterministic values, the neighborhood-scale analysis is able to provide statistical distributions of the measures' effectiveness in the local area, which could help inform more comprehensive decision-making. To fill the second gap regarding lack of quantitative analysis, we developed a methodology to quantitatively evaluate and prioritize passive measures in DACs using four complementary metrics, for both individual buildings and neighborhoods. To close the third gap, our study focuses on DACs and applies the methodology to two DACs in southwest Fresno.

The overall methodology is illustrated in Section 2. We review existing resilience metrics and developed complementary metrics for evaluating the impact of passive measures on resilience, energy, and comfort (Section 3). Section 4 describes the baseline assumptions, the development of example DAC datasets, the passive measures, and the weather data used in simulation. Section 5 analyzes the simulation results, including the effectiveness of passive measures on improving heat resilience at different scales, as well as their impact on energy consumption. Finally, conclusions are drawn and future studies are proposed (Sections 6 and 7).

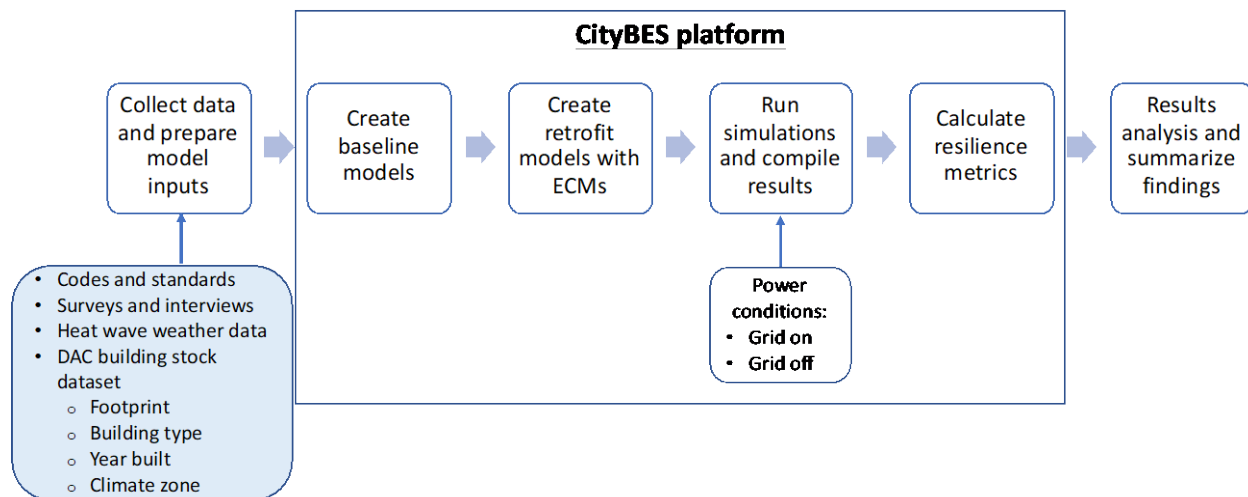
2. Method

Figure 1 illustrates the overall workflow of the modeling approach at the building and district scales. First, modeling inputs are collected from multiple sources, including building energy codes and standards, tax assessor records, site surveys and interviews of residents at the local communities. Specifically, for district-scale analysis, inputs sources also include Google Map API and real estate database, and that the building stock characteristics, such as building footprint, building type, year of construction, and climate zone, are compiled in the DAC building

stock dataset. Second, the baseline models of the prototypes and the DAC buildings are developed based on the modeling inputs. Third, energy conservation measures (ECMs) are applied to the baseline models to evaluate their effectiveness in improving heat resilience in representative prototypes and at the district level under two power scenarios: “grid on” (electric grid power available) and “grid off” (electric grid power unavailable). Fourth, simulation runs are conducted at both the prototype level in EnergyPlus and at district scale in CityBES, and their outputs used to calculate resilience metrics. Lastly, results are analyzed and findings are summarized. We review resilience metrics and select four that are most appropriate and complementary to assess the performance of the ECMs. Each workflow step is detailed in Sections 3 and 4.



(a) Building-level using prototype models



(b) District scale

Figure 1. Overall workflow of the characterization of the building stock and local climate, passive measures modeling, from model input to model development to resilience analysis at (a) building scale and (b) district scale.

The current study focuses on passive measure modeling and analysis; we are preparing a parallel study on active cooling solutions. Passive measures are technologies or design features that can still function during power outages. We scanned a broad set of passive measures and focused on those that are typically effective considering climate and cost for DACs. Eleven

passive measures are selected and modeled in this study. These include envelope improvements, such as adding insulation to ceiling and roofs, installing shading devices, increasing exterior surface reflectance, reducing window thermal transmittance (“U-value”), and reducing window solar heat gain coefficient (SHGC); and natural ventilation, provided by occupants opening windows when the outdoor air is cooler than the indoor air. Passive ECM definitions, modeling assumptions, and methods are detailed in Section 4.3.

Single- and multi-family home prototypes based on prescriptive specifications in California’s Title 24, Part 6 building energy efficiency standards (hereinafter, “Title 24”) [208] are used to model single-building performance, using EnergyPlus version 9.2 as the simulation engine [209]. EnergyPlus has been verified according to ASHRAE Standard 140, Standard Method of Test for Building Energy Simulation Computer Programs [210].

CityBES is used for district-scale modeling and analysis. CityBES is a web-based data and computing platform developed by Lawrence Berkeley National Laboratory [211–213]. It focuses on energy modeling and analysis of a city’s building stock to support district or city-scale efficiency programs. CityBES uses an international open data standard, CityGML, to represent and exchange three-dimensional city models. CityBES employs EnergyPlus to simulate building energy use and savings from energy efficient retrofits. CityBES provides a suite of features for urban planners, city energy managers, building owners, utilities, energy consultants, and researchers.

We added to CityBES a resilience analysis feature that simulates building responses under extreme events such as heat waves. Several predefined building operation conditions, such as loss of grid power or loss of natural gas supply, can be coupled with extreme events. The time span and the weather conditions during the event can also be specified by the user. CityBES will by default begin the simulation one day before the extreme event and end it one day after the event, to reflect not only the building’s response during extreme conditions, but also the variations from normal to extreme conditions and back to normal.

Two power scenarios are considered to cover the full range of vulnerability of DACs to heatwaves. The grid-on scenario assumes that electric grid power is available and the building is under normal operation status during heatwaves. The HVAC systems are sized to cover 99.6% of outdoor weather conditions for cooling, which means the most extreme 0.4% hot summer conditions in a year cannot be met by the HVAC system [214]. In this case, the major concerns are whether the air-conditioning system has adequate cooling capacity to meet the cooling loads during heatwaves, and if not, how many hours the occupants will experience thermal discomfort. The grid-off scenario assumes that electric grid power is not available due to power outage. In this case, the major concerns are indoor temperature rise and how long the occupants will be overheated. Different metrics and thresholds apply in each of the two power scenarios.

3. Resilience, energy, and comfort metrics

We reviewed the literature to identify existing metrics that gauge occupant thermal comfort and heat stress. There are two major types of metrics: simplified biometeorological indices and

those based on heat-budget models [215]. The former is based on air temperature, or a combination of air temperature and humidity; the latter covers a set of meteorological and physiological parameters to describe the physiological heat load, including air temperature, water vapor pressure, wind velocity, and short- and long-wave radiant fluxes [216]. We selected air temperature and heat index from the simplified indices, and standard effective temperature (SET) and predicted mean vote (PMV) from the complex indices, as the fundamental metrics for this study. Air temperature is typically used to calculate unmet hours during building design, while heat index was recommended by National Oceanic and Atmospheric Administration (NOAA) and was used by Sun et al. [142] in a thermal resilience case study of a Florida nursing home. SET is adopted by the Leadership in Energy and Environmental Design (LEED) Passive Survivability pilot credit to define “livable temperatures” [217], and PMV is adopted by ASHRAE Standard 55 to evaluate thermal comfort. We also selected thresholds for resilience quantification based on the literature review, with more details described in Sections 3.1-3.4. The exceedance of the thresholds indicates that the indoor thermal conditions are out of the comfort or safety zone. In the grid-off scenario, the indoor environment could become life-threatening, so the metric thresholds are selected mainly to evaluate the impact of overheating on occupant health. In the grid-on scenario, the indoor environment is less extreme, as air conditioning (AC) systems can provide cooling; therefore, the metric thresholds are selected mainly to evaluate the impact of overheating on occupant thermal comfort. To quantify the impact of passive measures on improving resilience, we time-integrated these fundamental metrics over the portions of the heat wave during which the thresholds are exceeded. The four integrated metrics are unmet degree-hours (UDH), heat index hazard hours (HIHH), standard effective temperature unmet degree-hours (SETUDH), and predicted mean vote exceedance hours (PMVEH). Each of these four metrics has its respective limitations under certain circumstances, as summarized in Table 1. Evaluating all of them can provide a comprehensive understanding of the passive measures to various stakeholders.

Table 1. Four selected resilience metrics and their limitations.

Resilience Metric	Parameters Included in Metric	Limitations	Thresholds
UDH (unmet degree hours)	Air temperature	Neglects relative humidity, mean radiant temperature, air speed, clothing, and metabolic rate. Uses cooling setpoint as threshold, which could vary with different control strategies.	Cooling setpoint
HIHH (heat index hazard hours)	- Air temperature - Relative humidity	Neglects mean radiant temperature of zone surfaces, indoor air speed, occupant clothing, and metabolic rate.	- Caution: 27 °C - Extreme caution: 32 °C - Danger: 39 °C

			- Extreme danger: 52 °C
SETUDH (standard effective temperature unmet degree-hours)	<ul style="list-style-type: none"> - Air temperature - Relative humidity - Mean radiant temperature - Air velocity - Metabolic rate - Clothing insulation 	No comfort zone thresholds given by ISO or ASHRAE standards.	<ul style="list-style-type: none"> - Grid-on: SET 28 °C - Grid-off: SET 30 °C
PMVEH (predicted mean vote exceedance hours)	<ul style="list-style-type: none"> - Air temperature - Relative humidity - Mean radiant temperature - Air velocity - Metabolic rate - Clothing insulation 	Fanger's PMV calculated in EnergyPlus may underestimate the cooling effect of increased air velocity.	<ul style="list-style-type: none"> - Thermal comfort: 0.7 - Unbearable limit: 3

3.1 Unmet degree-hours (UDH)

The concept of UDH is analogous to that of temperature-weighted exceedance hours, a metric defined in Section L.3.2.2(b) of ASHRAE Standard 55-2017 [218]. The difference is that the calculation of UDH is based on indoor cooling setpoint, while the number of temperature-weighted exceedance hours is either derived from discomfort-weighted exceedance hours or calculated based on operative temperature. The UDH metric weights each hour that the temperature of a conditioned zone exceeds a certain threshold by the number of degrees Celsius by which it surpasses that threshold. Compared with average temperature or unmet hours (which would be a simple count of how many hours a temperature threshold is breached), UDH provide a more complete picture of the overall history temperature exceedance.

UDH are calculated as follows:

$$UDH = \int_{t_1}^{t_2} [T(t) - T_{\text{threshold}}]_+ dt \quad (1)$$

where T is the indoor air temperature [°C]; $T_{\text{threshold}}$ is the temperature threshold [°C]; t is time [h]; and $x_+ = x$ if $x > 0$, or 0 otherwise. $T_{\text{threshold}}$ is the indoor cooling setpoint in both the grid-on and grid-off scenarios.

3.2 Heat index hazard hours (HIHH)

The heat index (HI), also known as the apparent temperature, combines air temperature and relative humidity (RH) in shaded areas to reflect what the temperature feels like to the human

body [219]. When the relative humidity is high, the evaporation rate of water is reduced. This means that heat is removed from the body at a lower rate, causing it to retain more heat than it would in dry air. Heat index hazard hours (HIHH) are calculated as follows:

$$HIHH = \int_{t_1}^{t_2} f(HI(t) - HI_{\text{threshold}}) dt \quad (2)$$

where $f(x) = 1$ if $x > 0$, or 0 otherwise; HI is the heat index of the zone [°C]; $HI_{\text{threshold}}$ is the heat index threshold [°C]; and t is time [h]. $HI_{\text{threshold}}$ is 27 °C for caution and 39 °C for danger based on Table 2 provided by NOAA [219], which defines the four levels of heat hazards and their associated heat index ranges. Considering that the DAC neighborhoods tend to contain vulnerable populations, we selected “caution” and “danger” (rather than “extreme caution” and “extreme danger”) as the two thresholds to evaluate the measures’ mitigation effects on relatively lower risks and higher risks.

Table 2. Heat hazard classification and impact on human bodies [220].

Classification	Heat index [°C]	Effect on the human body
Caution	27-32	Fatigue is possible with prolonged exposure and activity. Continuing activity could result in heat cramps.
Extreme Caution	32-39	Heat cramps and heat exhaustion are possible. Continuing activity could result in heatstroke.
Danger	39-51	Heat cramps and heat exhaustion are likely; heatstroke probable with continued activity.
Extreme Danger	Above 52	Heatstroke is imminent.

3.3 Standard effective temperature unmet degree-hours (SETUDH)

Standard effective temperature (SET; symbol may also be written SET*) is a temperature metric that factors in relative humidity, mean radiant temperature, air velocity, and anticipated activity rate and clothing level of the occupants. SET is essentially the dry-bulb temperature of an imaginary environment at 50% RH for occupants wearing clothing that would be standard for the given activity in the real environment [218]. In an experimental study, Gonzalez et al. [221] found that the neutral SET for a number of subjects is 25 °C, and that 28 °C induces slight warm discomfort. In another experimental study, Zhang et al. [222] concluded that the 90% acceptable thermal conditions in a conditioned environment correspond to a SET range of 24.5 to 28.1 °C. Therefore, 28 °C is selected as the threshold for SET in the grid-on scenario.

The Passive Survivability pilot credit in version four of the U.S. Green Building Council's LEED green building program credits resilient design that makes the buildings passively survivable. This credit uses SET to define "livable temperatures". The upper SET limit of "Livable Temperatures" is 30 °C (86 °F) [217]; we adopt that limit as the threshold in the grid-off scenario. The unmet degree hours of standard effective temperature (SETUDH) are calculated as follows:

$$\text{SETUDH} = \int_{t_1}^{t_2} [\text{SET}(t) - \text{SET}_{\text{threshold}}]_+ dt \quad (3)$$

where SET is the standard effective temperature [°C]; $\text{SET}_{\text{threshold}}$ is the standard effective temperature threshold [°C]; t is time [h]; and $x_+ = x$ if $x > 0$, or 0 otherwise. $\text{SET}_{\text{threshold}}$ is set to 28 °C in the grid-on scenario and 30 °C in the grid-off scenario.

3.4 Predicted Mean Vote exceedance hours (PMVEH)

The predicted mean vote (PMV) model from ASHRAE 55, initiated by P.O. Fanger, uses heat-balance principles to relate the six key factors for thermal comfort to the average response of people on a scale of -3 to 3 [218,223]. This metric has been widely used to evaluate human comfort level [224]. According to ISO Standard 7730-2005 [225], the thermal comfort requirement criterion for existing buildings is a PMV value between -0.7 and 0.7. We also selected 3, the upper boundary of the defined thermal comfort scale, as the unbearable limit under hot conditions [218]. PMV exceedance hours (PMVEH) are defined for this study to count the number of hours when the indoor PMV exceeds a threshold of 0.7 (grid-on scenario) or 3 (grid-off scenario). PMV exceedance hours are calculated as follows:

$$\text{PMVEH} = \int_{t_1}^{t_2} f(\text{PMV}(t) - \text{PMV}_{\text{threshold}}) dt \quad (4)$$

where $f(x)$ if $x > 0$, or 0 otherwise; PMV is the predicted mean vote; $\text{PMV}_{\text{threshold}}$ is the predicted mean vote threshold; and t is time [h].

4. Modeling ECMs at two scales

The selected ECMs are first applied to a few representative homes to test their performance. We also evaluate their sensitivities to building characteristics like construction year and position of the multi-family unit (e.g., top floor). The prototypes of the single-family homes and multi-family homes across three construction vintages (1976, 2004, and 2015) are simulated to evaluate the effectiveness of the ECMs by building type and vintage. This provides a basic understanding of the potential benefit of each ECM.

However, on a broader scale, there are thousands of buildings in a district/neighborhood, and their characteristics vary substantially. ECM effectiveness may differ from building to building. It is not sufficient information for the policy makers and local residents to make comprehensive decisions if only results for representative buildings are evaluated. Therefore, the ECMs are also applied to two disadvantaged communities in southwest Fresno to estimate the range of

effectiveness for the ECMs in the districts. The characteristics of the two neighborhoods are described in Section 4.2.

Two power scenarios are considered—grid on and grid off. In the latter scenario, the grid power is assumed to be unavailable during the selected heat-wave period, and the buildings operate normally before and after the heat wave.

4.1. Baseline definition

In the selected DAC neighborhoods, more than 95% of the buildings are single-family homes and low-rise multi-family homes. Therefore, we focus mainly on the modeling of residential buildings in this study.

The prototype models are designed to represent existing buildings, and were calibrated in terms of energy usage based on CBECC-RES¹ (California compliance software for residential buildings) and IECC (International Energy Conservation Code) prototype models. For the district scale modeling, the prototype models were modified to reflect the actual floor area of each building in the building stock and our best estimates of in-place equipment.

There are three major types of residential buildings in the studied neighborhoods: one-story single-family homes, two (or more) story single-family homes, and low-rise multi-family homes. Their geometries are based on the California Title 24 Alternative Calculation Method (ACM) [226], as shown in Figure 2. The one-story and two (or more)-story single-family homes are both assumed to have pitched roofs, an unconditioned attic under the roof, and an unconditioned ground-level garage that is attached to the living zone. Low-rise multi-family buildings have pitched roofs and unconditioned attics, but do not have attached garages.

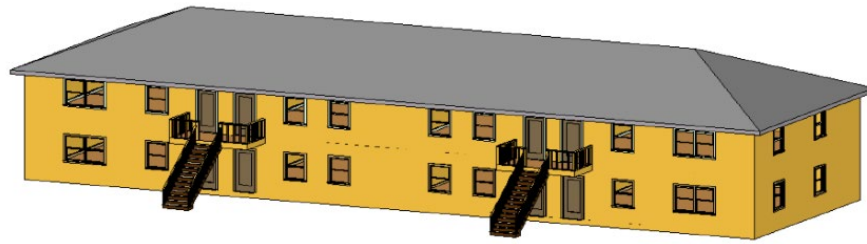


(a) One-story single-family home



(b) Two-story single-family home

¹ CBECC-Res is a free computer program developed by the California Energy Commission for use in demonstrating compliance with the California Residential Building Energy Efficiency Standards [208].



(c) Low-rise multi-family building

Figure 2. Illustrations of three types of residential building defined in the Title 24 ACM: (a) a one-story single-family home, (b) a two-story single-family home, and (c) a low-rise multi-family home [226].

The one-story single family house is modeled as a single conditioned thermal zone. The two-story single family house is modeled as two thermal zones, one for the first (lower) floor and the other for the second (upper) floor. Each apartment unit of the multi-family building is modeled as a thermal zone. The attic and garage are modeled as unconditioned spaces.

The envelope properties, internal loads, and HVAC efficiencies are derived from Title 24 minimum efficiency requirements, as shown in Table 3. Buildings constructed in different years are assumed to comply with Title 24 energy efficiency standards of the corresponding vintages (Title 24 is updated every three years) (e.g., Ref. [227]). For buildings constructed before 1978, when California first building energy codes were developed, it is not uncommon that some buildings have conducted retrofit to improve the thermal performance, such as adding insulation to top-floor ceiling and/or exterior walls. Therefore, two scenarios are considered for the prototype buildings constructed before building codes: (1) no retrofit has been performed, or (2) the building has been retrofitted by adding ceiling and wall insulations. The insulation values in the first scenario are based on 2019 Title 24 Residential Compliance Manual [228], while those in the second scenario are based on energy audits and site surveys to the local communities in Fresno [229–231]. On the district scale, we assume that the fraction of pre-1978 buildings with upgraded ceiling insulation and wall insulation is 10%, and the fraction with only upgraded ceiling insulation is 6%, according to local energy audits and surveys in the Fresno DACs [229–231].

According to the Fresno Economic Opportunities Commission (EOC), which implements energy audits and weatherization in Fresno, the most commonly used types of air conditioning systems in the Fresno DACs are evaporative coolers, window air conditioners, and central air conditioners. Evaporative coolers, sometimes called “swamp” coolers, cool outdoor air by passing it over water-saturated pads, drawing sensible heat from the air to evaporate the water [232]. They are most suitable for areas with low humidity as evaporating water into the air provides a natural and energy-efficient means of cooling. Window air conditioners (mechanical) cool individual rooms rather than the entire home [233]. Central air conditioners (mechanical), comprising an outdoor condenser and compressor, an indoor evaporator coil, and supply fan, circulate cool air through a system of supply and return ducts [234]. In residential buildings constructed before 1978 in the Fresno DACs, our estimates of the proportions of the homes using evaporative coolers, window air conditioners, and central air conditioners are 25%, 50%,

and 25% respectively for single-family homes, and 25%, 25%, and 50% respectively for multi-family homes (one per unit). Nearly all buildings constructed after 1978 are equipped with central air conditioners. We assume that each building uses natural-gas-fired wall furnaces for space heating. These estimates are based on surveys and focus groups conducted by researchers in the authors' project team [229], and inputs from two knowledgeable community stakeholder groups in the Fresno area [230,231].

We assume that refrigerant leakage and coil fouling reduce the capacity and efficiency of each HVAC system over time. To capture these effects, we assume a degradation factor of 2% per year for both the cooling capacity and cooling efficiency (coefficient of performance, abbreviated COP) of the cooling equipment. We chose the average maintenance frequency according to review of the literature [235,236]. Based on a maximum HVAC system service life of 20 years [237,238], buildings constructed over 20 years ago should already have replaced their HVAC systems at least once; therefore, we assign to them an HVAC system age of 10 years.

Otherwise, the HVAC system age is assumed to be the same as the building age. The HVAC degradation may lead to insufficient cooling supply during extreme heat events, which will cause the indoor air temperature to exceed the thermal comfort range.

Per Fresno EOC, the overwhelming majority of homes use natural-gas storage water heaters for service hot water because natural gas is less expensive than electricity in the Fresno area. Each single-family home and each unit in the multi-family building is equipped with its own water heater.

Table 3. Key assumptions of the baseline models of the three studied vintages (single-story single-family home as example).

Property	1976	2004	2015
Gross floor area [m ²]	236		
Conditioned floor area [m ²]	195		
Window-to-wall ratio [-]	Non-north: 0.29; North: 0.20		
Roof area [m ²]	303		
Wall assembly U-factor [W/m ² ·K]	No Retrofit: 2.02 Retrofitted: 0.58	0.42	0.37
Wall cavity insulation [m ² ·K/W]	No Retrofit: RSI-0 Retrofitted: RSI-2.29	RSI-3.35	R2.64 cavity + R0.70 continuous
Top-floor ceiling cavity insulation [m ² ·K/W]	No Retrofit: RSI-1.94 Retrofitted: RSI-5.28	RSI-6.69	RSI-6.69
Window thermal transmittance [W/m ² ·K]	3.69	3.69	1.82
Window SHGC [-]	0.40	0.40	0.25

Cooling equipment efficiency (considering replacement and degradation)			
Central AC: COP [-]	2.63	2.19	2.96
Window AC: COP [-]	2.63	2.19	2.96
Swamp cooler: Cooling saturation efficiency [%]	69.5	61.5	76.8
Gas furnace efficiency [-]	0.78	0.80	0.80
Gas water heater efficiency [-]	0.72	0.80	0.82
Lighting power density [W/m ²]	6.25	3.07	1.95
Plug load power density [W/m ²]	7.91	7.91	7.91

Title 24 requirements for air changes per hour (ACH) at a pressure difference of 50 Pa (ACH₅₀) in residential buildings can be converted to ACH under a natural pressure difference of 4 Pa (ACH₄) via Eq. (5):

$$ACH_4 = ACH_{50} \times \left(\frac{4}{50}\right)^n \quad (5)$$

Here exponent n is based on the characteristic shape of the orifices of the building, and ranges from 0.5 (perfect orifice) to 1.0 (very long and thin crack). We assume $n = 0.75$, yielding the air-change rates shown in Table 4.

Table 4. Infiltration rates (ACH₄) for single- and multi-family homes by year of construction, extrapolated from Title 24 specifications of ACH₅₀.

Year of construction	Air changes per hour at 4 Pa (ACH ₄) in a single-family home	Air changes per hour at 4 Pa (ACH ₄) in a multi-family home
Before 2005	1.29	1.45
2006 to 2013	1.00	1.12
2014 to present	0.75	1.05

The cooling setpoint adopts the assumption from the Title 24 residential ACM [226]. It is set to a constant value of 25.6 °C during the weekend. The cooling setpoint schedule on the weekdays is shown in Figure 3(a), assuming the occupants are not at home during the daytime. The heating setpoint affects the annual energy usage; its schedule on the weekdays is shown in Figure 3(b).

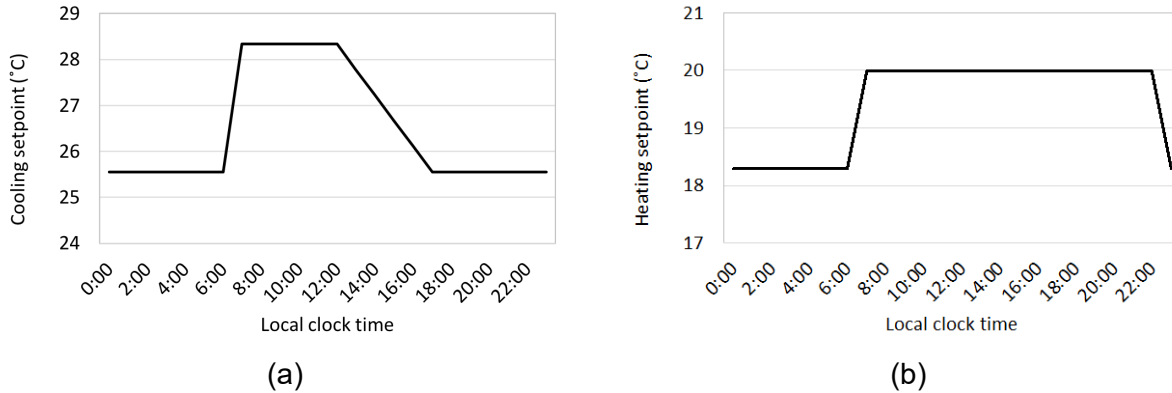


Figure 3. Residential cooling setpoint schedule on weekdays.

For schedules related to internal loads, the lighting schedule and the plug load schedule are each calculated from the 2019 Title 24 prototype model in CBECC-RES, while the occupancy schedule is calculated based on the BEopt default for residential buildings. BEopt (Building Energy Optimization Tool) is free software developed by the National Renewable Energy Laboratory that provides capabilities to evaluate residential building designs and identify cost-optimal efficiency packages at various levels of whole-house energy savings along the path to zero net energy [239]. The number of occupants is projected from the number of bedrooms based on the BEopt default settings, and the number of bedrooms is estimated based on the floor area of the home referring to the Residential Energy Consumption Survey (RECS) 2015 data [240]. RECS is a multi-year effort led by the U.S. Energy Information Administration that includes household surveys, data collection from household energy suppliers, and end-use consumption and expenditures estimation [241].

4.2. DAC dataset development

The King and Kirk neighborhoods in the southwest Fresno are selected as the study districts (Figure 4).

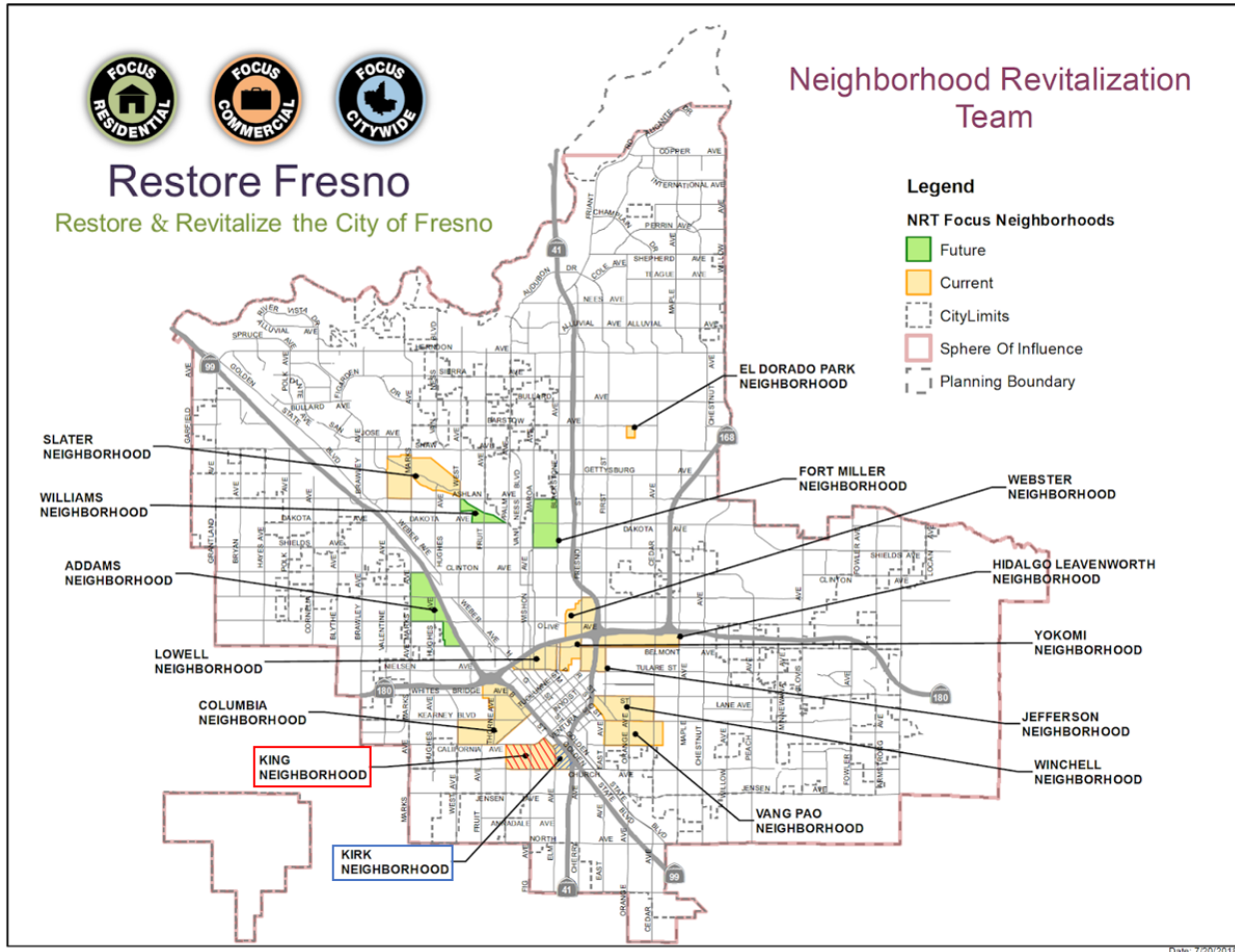
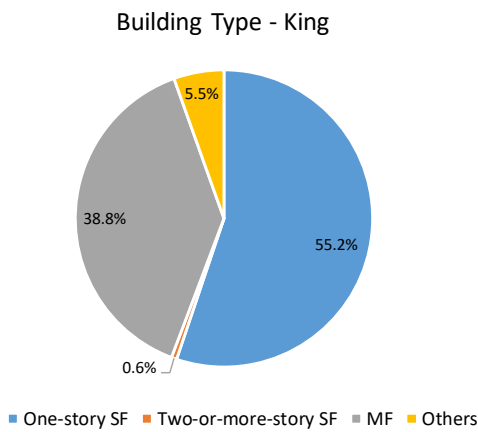


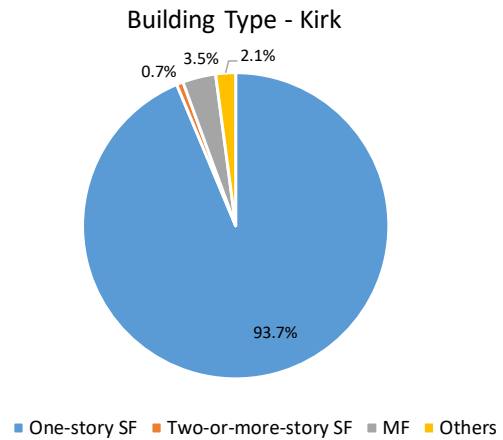
Figure 4. Map of neighborhoods in Fresno [242], including King and Kirk at lower left.

To create the dataset to be used in CityBES, building properties from several sources are collected, including building footprint, use type, height, number of stories, and year built. The building footprints are extracted from multiple sources, including the Microsoft building footprint database [243], Google Maps API [244], Zillow Real Estate API [245], and ATTOM Property Data API [246]. The year of built, use type, and number of stories are mainly from query results using the ATTOM Property Data API [246]. We did not locate a valid data source for the height of the buildings, so we assumed a height of three meters per story for all buildings.

There are 814 residential buildings in the King neighborhood and 280 residential buildings in Kirk. The type, construction year, and size distributions of those buildings are illustrated in Figure 5, Figure 6, and Figure 7. Each building has one or two stories, and over 90% of them are single-family homes in King and Kirk neighborhoods. The King neighborhood is slightly newer than the Kirk neighborhood. The majority of the homes in King were built from 1950 to 1990, while in Kirk most were built between 1910 and 1960.

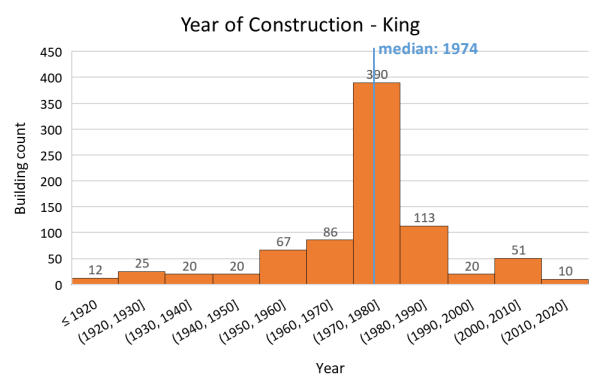


(a)

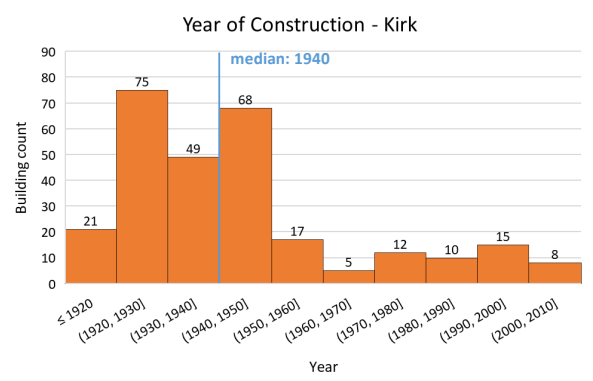


(b)

Figure 5. The distribution of building types for (a) the King neighborhood and (b) the Kirk neighborhood, including single-family (SF) homes, multi-family (MF) homes, and several retail buildings.

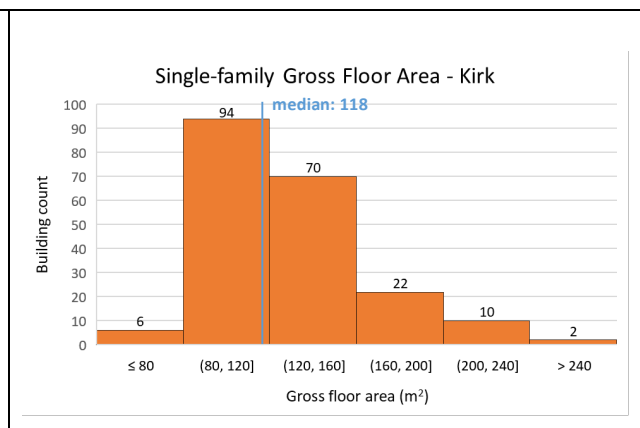
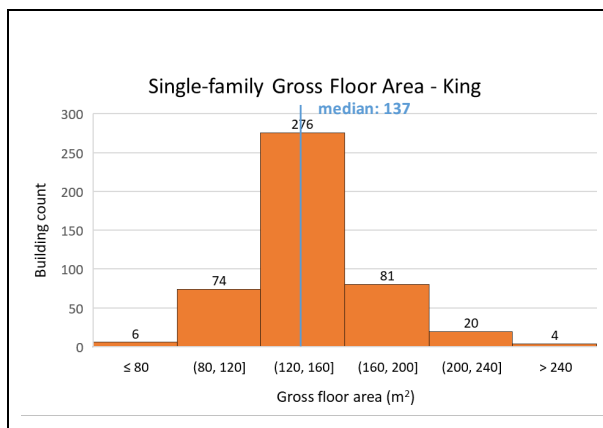


(a)



(b)

Figure 6. The distribution of construction year for the residential homes in (a) the King neighborhood and (b) the Kirk neighborhood.



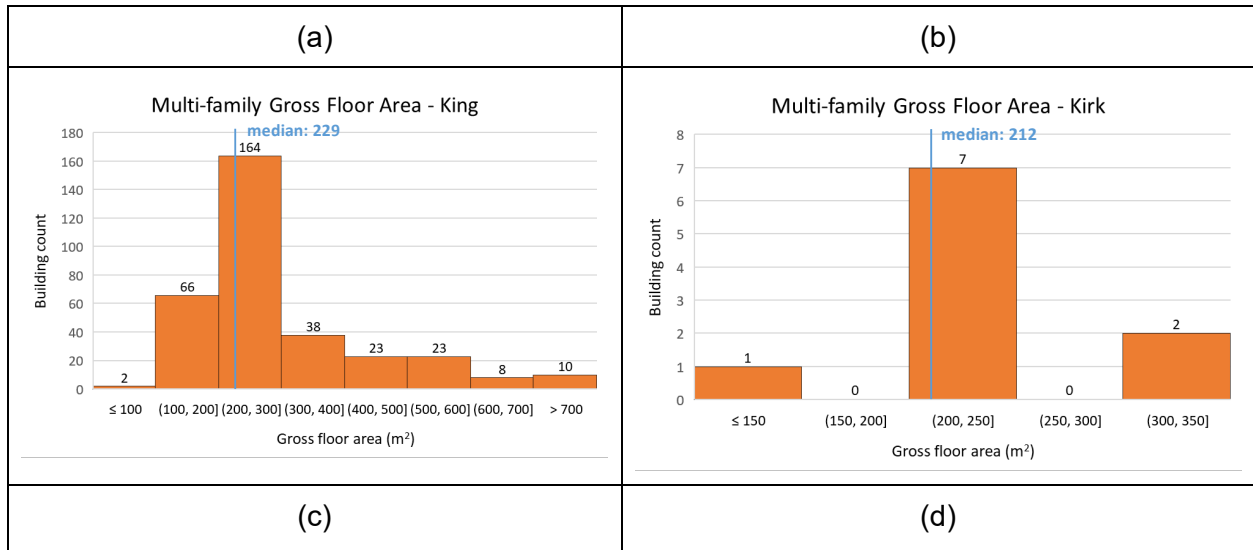


Figure 7. The distribution of building gross floor area for (a) single-family homes in the King neighborhood, (b) single-family homes in the Kirk neighborhood, (c) multi-family homes in the King neighborhood, and (d) multi-family homes in the Kirk neighborhood.

Pre-1978 homes are randomly assigned one of the three cooling systems—central AC, evaporative cooler, or window AC—to match the estimated distributions of the cooling equipment type in each DAC. They are also sampled according to the ceiling and wall insulation percentages in Section 4.1.

Results and analysis are presented for the King neighborhood; those for Kirk are very similar. The King neighborhood, located in southwest Fresno, has 461 single-family buildings and 410 multi-family buildings. Figure 8 illustrates its building stock created in CityBES.



Figure 8. (a) CityBES representation of King district's building stock; (b) GIS location of the King district in southwest Fresno.

4.3. ECMs description

To evaluate the ability of each ECM to improve heat resilience, 11 passive measures were selected based on their potential influence on indoor environment and energy consumption,

their investment cost, and ease of implementation and maintenance. This is not an exhaustive list of measures, but they cover the most representative types of measures. They include envelope improvements, such as adding insulation to ceiling and roofs, installing shading devices, increasing exterior surface reflectance, reducing window thermal transmittance (“U-value”), and reducing window solar heat gain coefficient (SHGC); and natural ventilation, provided by occupants opening windows when the outdoor air is cooler than the indoor air. This section describes the basic assumptions, key inputs, and modeling methods of each passive ECM. The key assumptions related to each ECM are summarized in Table 5.

Table 5. Summary of baseline and ECM assumptions.

Measure name	Measure description	Baseline assumption	ECM assumption
Roof insulation	Reroof and add roof insulation	Roof has no insulation layer	Add RSI-4.37 ^a insulation layer to roof
Ceiling insulation	Add insulation to top-floor ceiling	Mostly applicable for buildings built before 1978: No Retrofit: RSI-1.94 ^a Retrofitted: RSI-5.28 ^a	Improve the insulation layer to RSI-6.69 ^a
Cool roof	Increase roof solar reflectance by applying a reflective asphalt shingle product	Exterior layer material properties (pitched roof ^b): solar reflectance 0.10 thermal emittance 0.90	Exterior layer material properties (pitched roof ^b): solar reflectance 0.40 thermal emittance 0.90
Cool wall	Increase wall solar reflectance by painting	Exterior layer material properties: solar reflectance 0.25 thermal emittance 0.90	Exterior layer material properties: solar reflectance 0.60 thermal emittance 0.90
Interior blinds	Install and use window blinds	No window blinds	Add interior blinds to windows
Exterior overhang	Add exterior overhang shades	No exterior overhang shades	Add overhang shades with depth of 0.76 m (2.5 ft) and offset of 0.55 m (1.8 ft) from window upper edge
Exterior storm window	Add exterior storm window layer	No storm window	Add an exterior storm window layer, which is assumed to be 3 mm thick low-E glass
Interior storm window	Add interior storm window layer	No storm window	Add an interior storm window layer, which is assumed as a 3 mm low-E glass

Window film	Add solar-control window film	No window film (refer to Table 3 for SHGC values of different vintages)	Apply solar-control window film to the interior surface of the existing window (refer to element (9) in text below)
Natural ventilation	Enable natural ventilation for rooms with windows	No natural ventilation	Enable natural ventilation for each window, controlled by indoor and outdoor temperature difference
Radiant barrier	Add radiant barrier	No radiant barrier	Reduce the material's thermal emittance on the bottom of the roof to 0.10

^a Thermal insulances reported as “RSI-X” have units of $m^2 \cdot K/W$. To convert between SI thermal insulance (RSI-X) and inch-pound insulance (R-X), note that $RSI-1 (1 m^2 \cdot K/W) = R-5.678 (5.678 ft^2 \cdot ^\circ F \cdot h/BTU)$.

^b We assume the single-family and low-rise multi-family homes have pitched roofs. These homes comprise 95% of the buildings in the studied neighborhoods.

(1) Roof insulation

As roof insulation was not prescribed in California low-rise residential buildings until the 2016 edition of Title 24, we assume that was not included in buildings that were built before 2016. This measure installs an R-24.8 (RSI-4.37) insulation layer under the roof deck during a roof retrofit to reduce unwanted heat gain or loss. This measure is most applicable to older roofs. It is modeled by adding an extra layer of R-24.8 insulation to the roof construction (underneath the deck) in the building prototype.

(2) Ceiling insulation

This measure installs an R-38 (RSI-6.69) insulation layer above the ceiling of the top floor. Per Section 4.1, we assume two scenarios for buildings constructed before 1978: (1) no retrofit has been done, (2) building has been retrofitted with ceiling and/or wall insulations added. The ceiling insulation is R-11 (RSI-1.94) [228] without retrofit and R-30 (RSI-5.28) with retrofit [229–231]. After 1980, the ceiling insulation prescription is R-38 in California climate zone 13, which Fresno belongs to. Therefore, this measure is mostly applicable for older buildings, and also for newer buildings in certain climate zones. This is simulated by upgrading the existing insulation layer to R-38 in the ceiling construction on the top floor.

(3) Cool roof

This measure increases the roof solar reflectance by applying a reflective asphalt shingle product to pitched roofs or applying white single-ply membrane to flat roofs. Such a reflective layer can deliver a high solar reflectance ($SR=0.40$ for pitched roofs and 0.60 for flat roofs) and high thermal emittance ($TE=0.90$). An existing dark roof ($SR 0.10$, $TE 0.90$ for a pitched roof; $SR 0.20$, $TE 0.90$ for a flat roof [37]) is a prerequisite for applying the measure.

(4) Cool wall

The concept of this measure is similar to the cool roof measure. It applies a cool exterior wall paint, which can deliver a high solar reflectance (0.60) and high thermal emittance (0.90), commonly associated with a dull-white, off-white, or other light-colored wall. An existing dark-to-medium colored wall (SR 0.25, TE 0.90 [37]) is a prerequisite for applying the measure. In simulation, the thermal resistance of the cool wall coating (i.e., the paint) is neglected, and the high solar reflectance and high thermal emittance are directly applied to the outside layer of the exterior wall construction.

(5) Interior blinds

This measure adds interior blinds with white horizontal slats to the windows and pulls them down to block direct sunshine, as shown in Figure 9(a). When completely closed and lowered on a sunny window, highly reflective blinds can reduce solar heat gain moderately. More importantly, blinds improve occupants' thermal sensation by blocking direct sunshine. The solar reflectance of the blinds is assumed to be 0.70. This measure is simulated by attaching an interior blind object to the windows in the EnergyPlus model.

Figure 9 illustrates all the window-related ECMs included in this study.



(a) Window blinds



(b) Exterior overhang



(c) Exterior storm window



(d) Window film

Figure 9. Window-related ECMs: (a) window blinds, (b) exterior overhang, (c) exterior storm window, (d) window film. Image credits: (a) SelectBlinds.com [247], (b) Pinterest [248], (c) Hatch Homes [249], (d) Ideaing.com [250]

(6) Exterior overhang

This measure adds exterior overhang shades to the upper edge of the windows, as shown in Figure 9(b). They can help block the sun's heat energy when it is not desired. According to Sustainable By Design [251], the recommended overhang dimension for Fresno's climate and latitude is 0.76 m (2.5 ft) in depth and 0.55 m (1.8 ft) in height. Height refers to the offset distance from the upper edge of the windows. The dimension applies to the horizontal shading surface of the overhang structure. In EnergyPlus modeling, overhang shades are implemented as detailed shading objects, and attached to each window.

(7) Exterior storm window layer

Storm windows are an extra layer added to the existing windows, intended to improve comfort and reduce heating and cooling costs by increasing thermal resistance and reducing air movement through existing windows. Storm windows can produce similar savings to the measure of replacing single-pane windows with double-pane windows [252]. This measure adds an exterior storm window layer to each existing window. The storm window layer is assumed to be a 3 mm-thick low-E glass.

The existing windows are simulated in EnergyPlus using the SimpleGlazing object, which inputs the overall thermal transmittance, SHGC, and visible transmittance (VT). In EnergyPlus, the SimpleGlazing object cannot be combined directly with another material layer. An extra layer like a storm window can only be added to an existing window object that is defined using layer-by-layer structure. Therefore, a methodology developed by Lawrence Berkeley National Laboratory is adopted to translate the SimpleGlazing object with simple input properties (thermal transmittance, SHGC, and VT) into a representative layer defined with detailed properties, such as glass thickness, thermal conductivity, and solar transmittance [253]. The

extra storm window layer is attached to the representative layer, and updated thermal transmittance, SHGC, and VT values of the new composite window are calculated.

(8) Interior storm window layer

This measure adds an interior storm window layer to the existing windows. The storm window properties and simulation method are basically identical to those of the exterior storm window; the only difference is that this measure adds the storm window layer to the interior side of the window.

(9) Window film

Solar-control window films help reduce solar heat gain and protect against glare and ultraviolet exposure. They are best used in climates with long cooling seasons, because they also block the sun's heat in the winter. The properties of the window film refer to the solar control film products by LLumar Spectrally Selective Series [254]: thermal transmittance $4.94 \text{ W/m}^2\cdot\text{K}$, solar transmittance 0.34, SHGC 0.45, visible transmittance 0.66. For the three sample vintages listed in Table 3, the baseline SHGC are 0.40, 0.40, and 0.25, and will be reduced to 0.13, 0.13, and 0.07 with window film added.

The simulation method is similar to that used for the interior storm window: (a) the simple input properties of the existing windows are translated into detailed properties for a representative layer, (b) the window film layer is attached to the interior side of the representative layer, and (c) updated properties are calculated.

(10) Natural ventilation

Natural ventilation can provide free cooling when the outdoor environment is cooler than the occupied space. This measure assumes that the windows in the building are operable, and that the occupants can and will open and close windows. The windows are assumed to be opened only when the outdoor air temperature is lower than indoor air temperature, and the temperature difference should be big enough to be noticeable by the occupants, which is assumed to be $2 \text{ }^\circ\text{C}$ in the study. Meanwhile, the windows will be closed to avoid over-cooling when the outdoor air temperature drops below a certain threshold. When grid power is available, the windows and air conditioners are operated in “concurrent mixed-mode”, referring to the research of Wang et al. [255]. Natural ventilation has a higher priority to provide cooling, and air conditioners provide supplementary cooling when natural ventilation alone is not enough to meet cooling load. In other words, if natural ventilation can meet cooling loads, the air conditioners will be turned off. We did not consider door opening while modeling natural ventilation due to security concerns, because free cooling is available mostly in the evening, night and early morning.

The “ZoneVentilation:WindandStackOpenArea” object in EnergyPlus is used to simulate natural ventilation. The ventilation air flow rate is a function of wind speed and thermal stack effect, along with the area of the opening being modeled. The effective opening area fraction (i.e., the area fraction of the windows that can be open for ventilation) can be specified by the user. It varies with type of window, such as single or double-hung, sliding, awning, or casement, each of which has its own effective opening area fractions. By default, the effective opening area fraction is set to 0.4, the lower threshold of outdoor temperature for opening the window is set to

20 °C to avoid over-cooling, and the air temperature difference across the envelope (indoor minus outdoor) should be at least 2 °C to enable natural ventilation.

(11) Radiant barrier

Radiant barriers consist of a highly reflective material that reflects radiant heat rather than absorbing it [256]. The material also has low thermal emittance, which will reduce the radiant heat transfer from the roof surface to other surfaces in the attic zone. They do not, however, reduce heat conduction like bulk insulation. In EnergyPlus, radiant barriers can be modeled by specifying a very low thermal emittance (e.g., 0.10) for the roof's innermost material layer.

4.4. Weather data

Extreme weather event (heat wave) data are used to evaluate the effect of passive measures on building thermal resilience. A heat wave can be characterized by three metrics: duration, intensity, and severity [257]. The intensity is measured by the average elevation of outside air temperature above a reference temperature. The severity is the time integral of the elevation of outside air temperature above a reference temperature over the whole heat-wave period. Previous studies showed that risk of mortality is highly correlated with heat waves with high intensity [258]. Thus we selected a heat wave based on intensity using the historical weather data. The weather data of Fresno for the past 29 years (1989–2017) at the station CA_FRESNO-YOSEMITE-IAP_723890S were purchased from White Box Technologies, a private company specialized in weather data for energy calculations. A reference temperature of 40 °C (104 °F) is selected, as the peak temperature of extreme heat waves in Fresno is usually higher than 40 °C. The most intense heat wave occurred on July 19 to July 27, 2006. It included five consecutive days (July 22–26) when the daily maximum outdoor air temperature was always above 44 °C (Figure 10). These five days are selected as the heat wave days for simulating the resilience performance of the passive measures. The grid-off scenario is only applied to the heat-wave periods; all other times are under normal operation.

The impact of passive measures on the annual energy consumption of homes is also investigated. Their EnergyPlus simulations are run for a whole year using Typical Meteorological Year 3 (TMY3) (TMY3 user manual) weather data. TMY3 data are derived from a 1991-2005 period of record to represent the weather of a typical year.

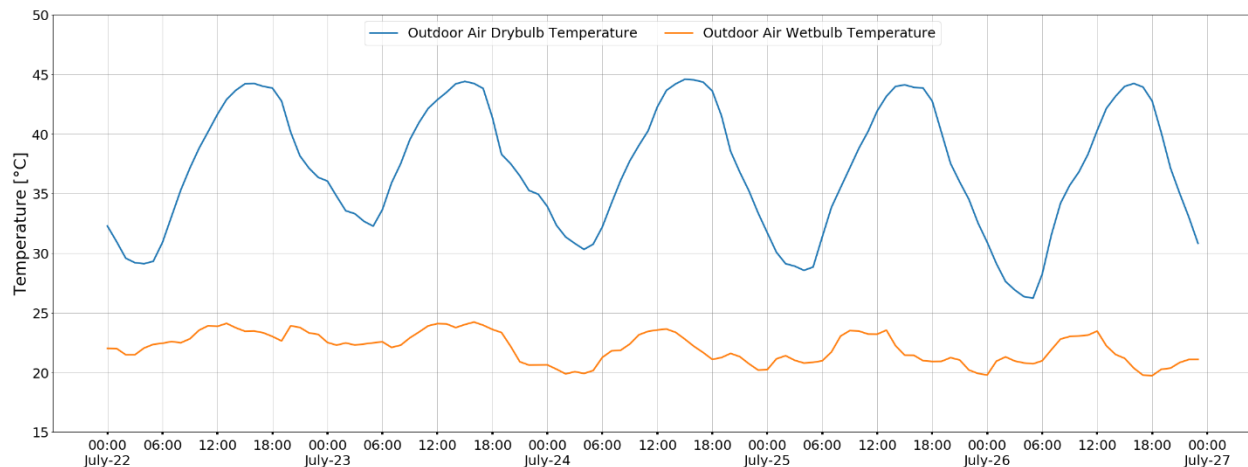


Figure 10. The temperature profile of the selected heat wave spanning July 22-26, 2006.

5. Results and analysis

The individual building simulations are first analyzed to explore the effectiveness of each ECM for different building types, building vintages, and power supply scenarios. A one-story single-family home and a multi-family home are selected as the representative building types for this analysis, based on the building type distribution in Figure 5.

Next, the district-scale results show the overall influence on the selected DACs. Finally, the energy impacts of the ECMs under typical weather conditions are analyzed to make up a comprehensive evaluation.

5.1. Resilience analysis for prototype houses

5.1.1 Single-family homes

Figure 11 shows the indoor air temperatures of the single-family homes built in 1967, 2004, and 2015 during the 2006 heat wave, in the grid-on and grid-off scenarios. The heat wave lasted for five days from Jul 22 to Jul 26, as highlighted in the figure. The grayed-out periods are one day before and one day after the heat wave under normal operation to illustrate the impact of the heat wave. Even when the grid is on, the indoor temperature in the afternoon cannot be cooled to the setpoint, because the outdoor temperature during the heat wave is in the 0.4% of the warmest cases that are not covered by the sizing of the air conditioner, and the capacity of the air conditioner has degraded over the years. When the grid is off, the air temperature of the home built in 1976 without retrofit can exceed 40 °C. With better envelope constructions, newer buildings have relatively cooler indoor air temperature. For example, the indoor air temperature in the home built in 2015 can be 4 °C cooler than that of the home built in 1976 when grid power is unavailable. On the other hand, when power is available, the indoor environment is affected comprehensively by multiple factors like envelope properties, internal heat gains, and AC equipment capacity. For example, the home built in 2004 performs worse than the home built in 1976 mainly because: (1) the home built in 2004 has a smaller cooling load due to the better envelope construction and lower internal heat gains, so its air conditioning equipment was sized to be smaller; and (2) per Section 4.1, the AC equipment in the 2004 home is assumed to be as old as the house, i.e., 16 years old (current year is 2020), while that in the 1976 home is 10 years old (replaced at least once)—therefore, the AC equipment in the 2004 home has more severe degradation, leading to less available capacity.

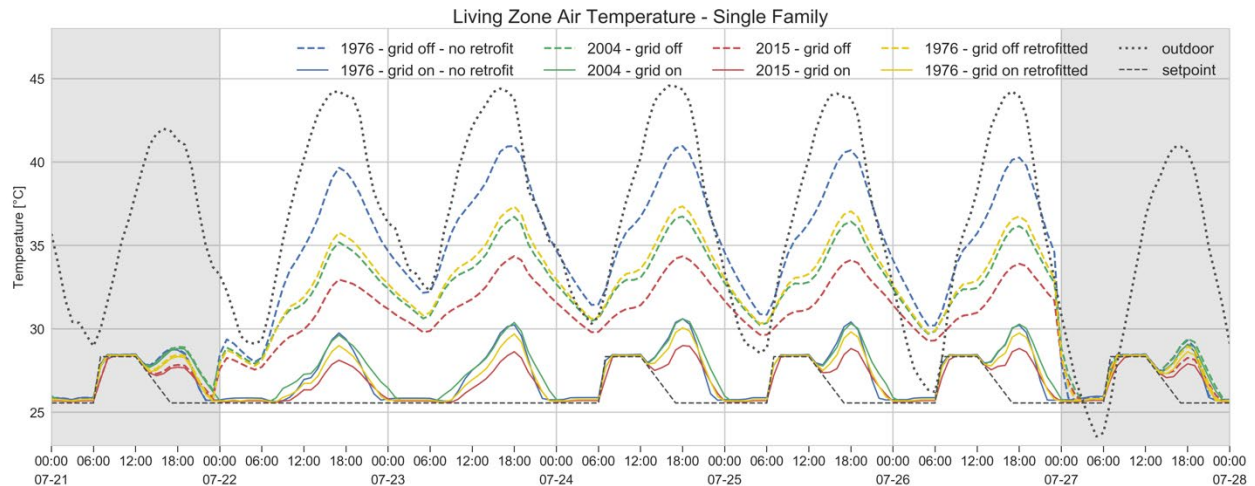


Figure 11. Comparison of the air temperature of the living zone in the single-story single-family home with different vintages, with and without grid power.

Figure 12 through Figure 15 illustrate the reductions in UDH and SETUDH compared to the baseline for the three vintages simulated under two power scenarios. The ECMs are sorted by the percentage reduction of UDH for the home built in 1976 and kept the same order for all figures to facilitate comparison. The columns represent the absolute values of the metric and the dots represent the percentage improvement of each ECM compared with the baseline value of that metric. The figures for other metrics such as PMVEH and HHH are included in the Supporting Information (SI) Section A.

Adding window film and adding roof insulation are generally the most effective ECMs for all vintages in terms of reducing UDH and SETUDH. Taking the representative home built in 1976 as an example, these two measures can reduce UDH by 11.7% and 10.6% with grid power unavailable, or 28.2% and 37.4% with grid power available. Adding window film lowers SHGC and thus reduces the heat gain from windows. As shown in SI Figure A-1, adding roof insulation dramatically lowers the attic air temperature, which reduces the heat transfer from the attic to the living zone. Without roof insulation, the air temperature in the attic can reach almost 70 °C; this can be lowered by more than 20 °C via adding roof insulation.

Since baseline UDH or SETDH of the newer home is lower, the percentage of improvement tends to be higher for the home built in 2015. However, depending on the baseline settings, some measures, such as adding ceiling insulation, have no effect on newer buildings because the baseline ceiling insulation is already good enough in buildings built in 2004 or 2015. For single-story single-family homes, there is limited time when indoor air temperature exceeds outdoor air temperature due to heat transfer from the cool ground. As a result, natural ventilation is not an effective measure for these homes.

The influence of adding interior window blinds is more complex. On one hand, the interior blinds can reflect part of the solar radiation, a small fraction of which will be transmitted through the windows to the outside. Therefore, the blinds can slightly reduce the solar heat gain from windows. On the other hand, the blinds absorb the solar radiation transmitted from exterior windows, and gradually re-distribute the heat to the zone air and surfaces via convection and radiation. This redistribution process shifts the heat gain to later in the afternoon, which further

increases the temperature during peak hours. Therefore, the overall effect of the interior blinds depends on the combines result of these two factors. Generally, blinds have a marginal effect on reducing the indoor air temperature. However, interior blinds help block direct solar radiation, so they have more evident influence on metrics that incorporate mean radiant temperature, such as SET and PMV.

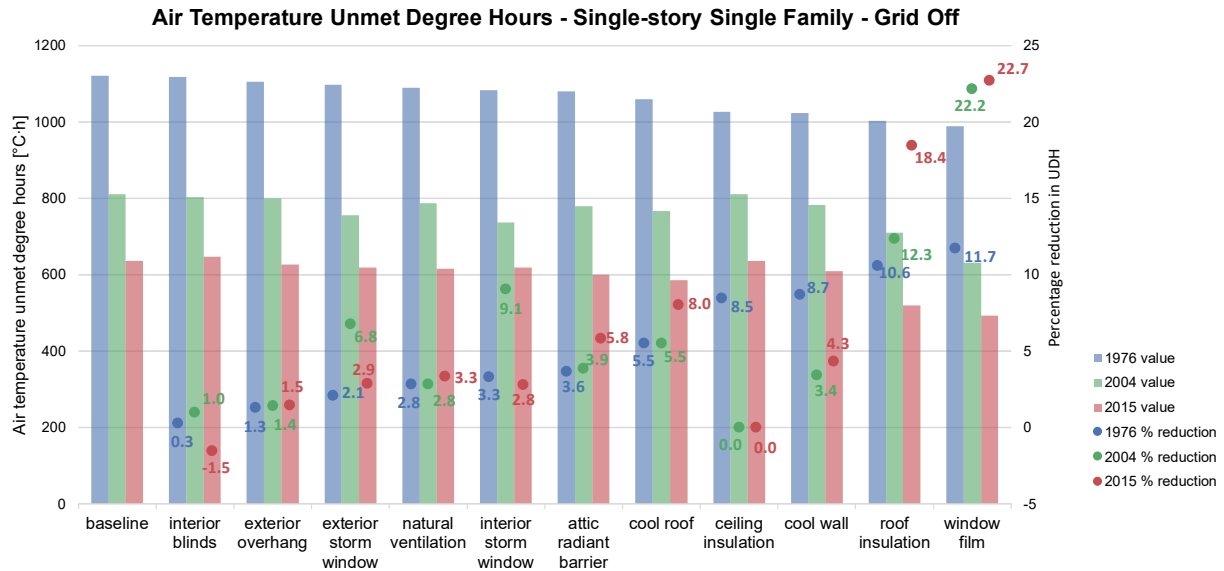


Figure 12. Air temperature unmet degree hours during the heat wave in the baseline case and after applying each ECM, show for single-family homes of different vintages in the grid-off scenario. Columns represent absolute values and the dots mark percentage reduction.

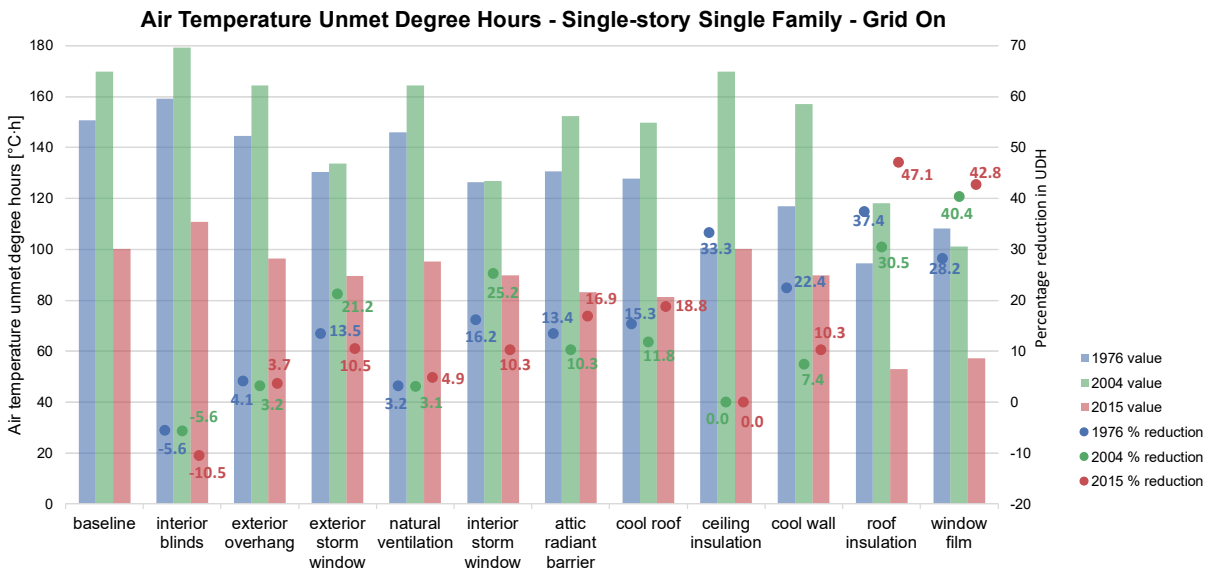


Figure 13. Air temperature unmet degree hours during the heat wave in the baseline case and after applying each ECM, show for single-family homes of different vintages in the grid-on scenario. Columns represent absolute values and the dots mark percentage reduction.

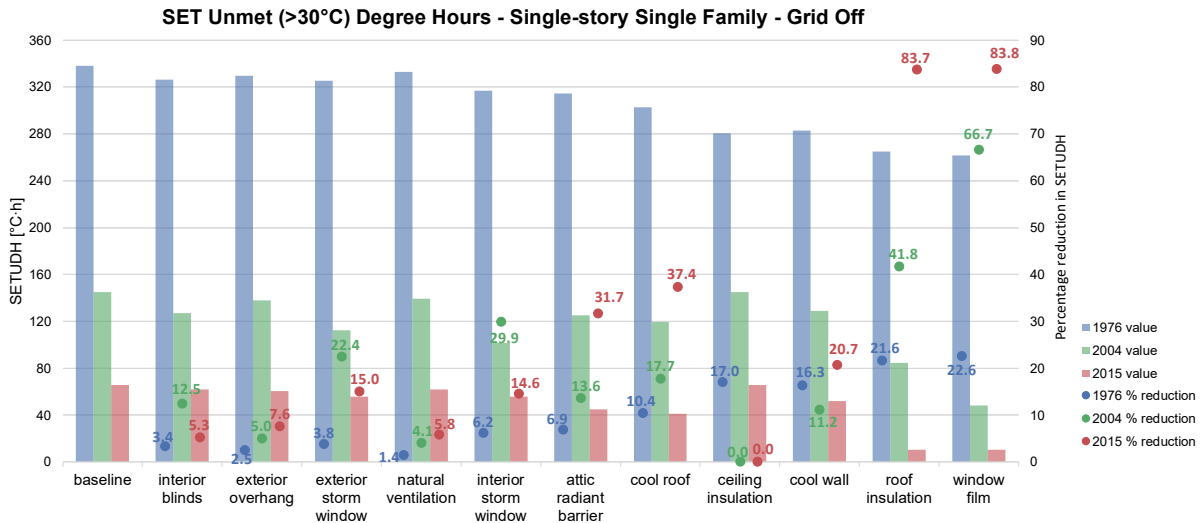


Figure 14. Standard effective temperature unmet degree hours during the heat wave in the baseline case and after applying each ECM, show for single-family homes of different vintages in the grid-off scenario. Columns represent absolute values and the dots mark percentage reduction.

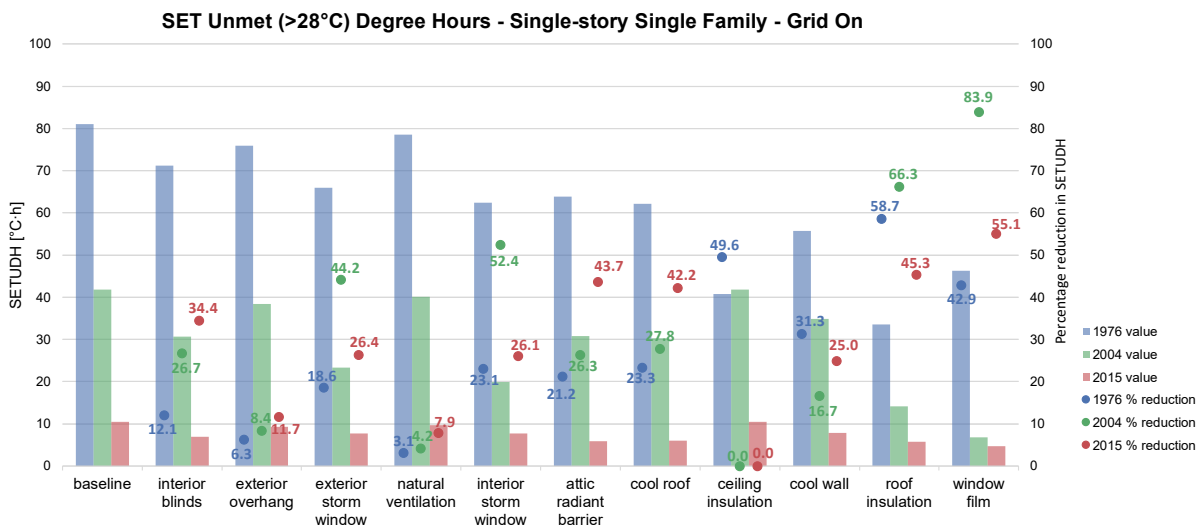


Figure 15. Standard effective temperature unmet degree hours during the heat wave in the baseline case and after applying each ECM, show for single-family homes of different vintages in the grid-on scenario. Columns represent absolute values and the dots mark percentage reduction.

Figure 16 and Figure 17 compare the home built in 1976 with or without retrofit under two power scenarios. For both power scenarios, UDH of the retrofitted home is lower than the non-retrofitted home for baseline and almost all ECMs because the retrofitted home has a better ceiling and wall performance. The ECM of adding ceiling insulation under the grid-on scenario is an exception, because by applying this ECM, both retrofitted and non-retrofitted homes will have the same ceiling construction, but the air conditioner in the retrofitted home was sized to be smaller since the original cooling load was lower. . Thus, the smaller-size air conditioner will result in a higher indoor air temperature during the heat wave when grid power is available.

Regardless of power scenario, the UDH reduction percentages for all the window-related ECMs (window film, exterior storm window, and interior storm window) are lower in the non-retrofitted home than in the retrofitted home. This is because the retrofitted home has better ceilings and walls, so the heat gain through windows accounts for a smaller proportion in total cooling load.

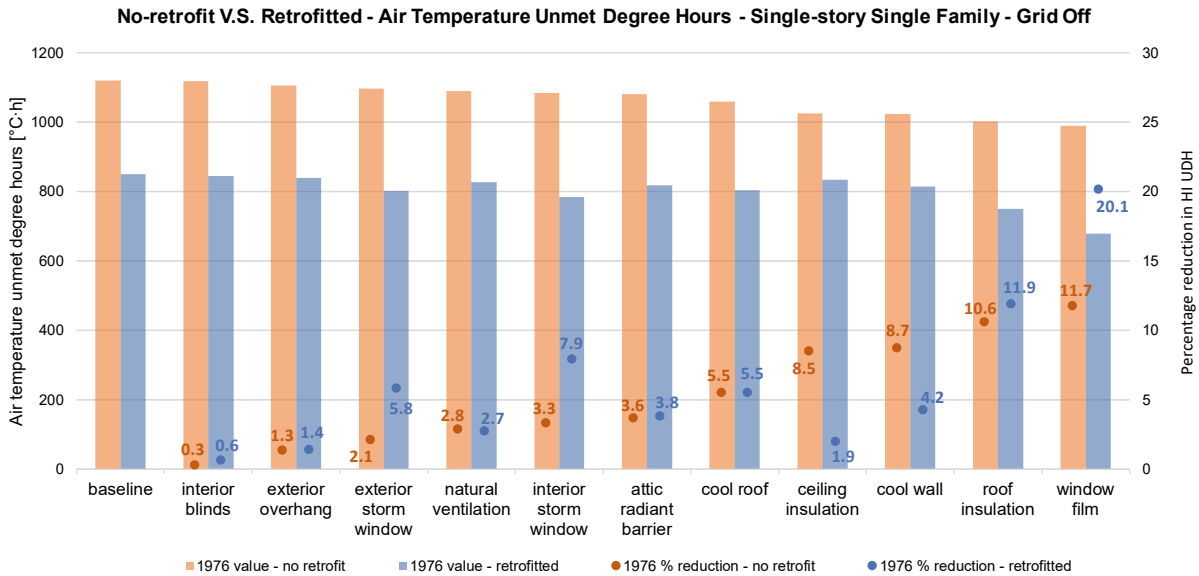


Figure 16. Air temperature unmet degree hours during the heat wave in the baseline case and after applying each ECM, show for single-family homes of 1976 with or without retrofit in the grid-off scenario. Columns represent absolute values and the dots mark percentage reduction.

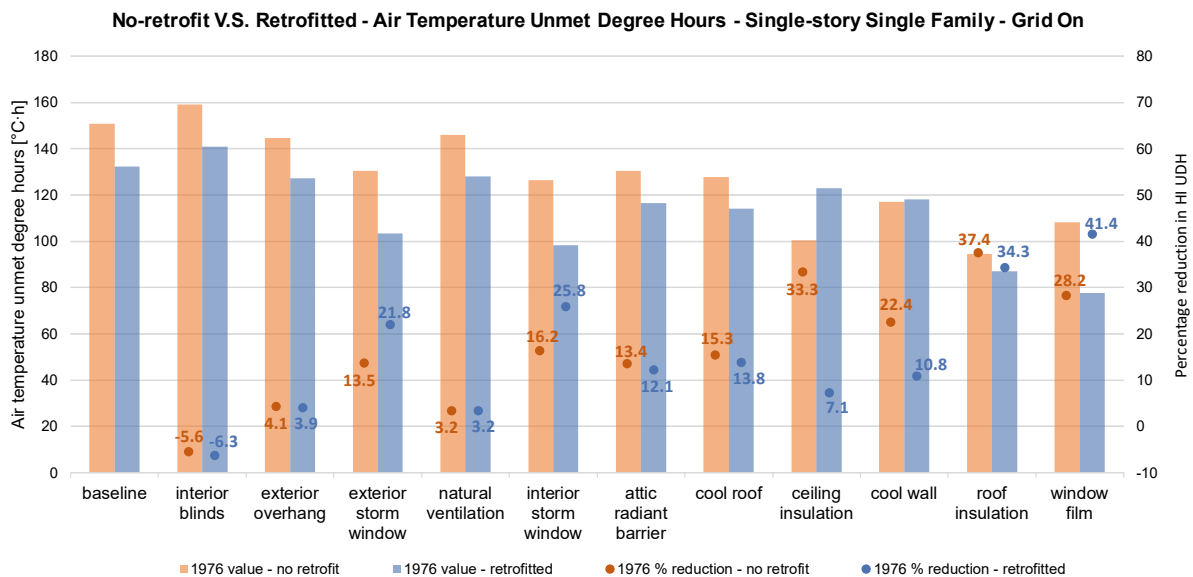


Figure 17. Air temperature unmet degree hours during the heat wave in the baseline case and after applying each ECM, show for single-family homes of 1976 with or without retrofit in the grid-on scenario. Columns represent absolute values and the dots mark percentage reduction.

5.1.2 Multi-family homes

The prototype multi-family building has eight units in total, four on each of the two floors. The conditions of different units vary substantially. For example, Figure 18 shows that the temperatures of units on the second floor are much higher than those on the first floor under the grid-off scenario, sometimes even higher than the outdoor air temperature. There is a variance among the units on the first floor as well, depending on the location of the unit. The coolest unit has an indoor temperature lower than the single-family living zone of the same vintage.

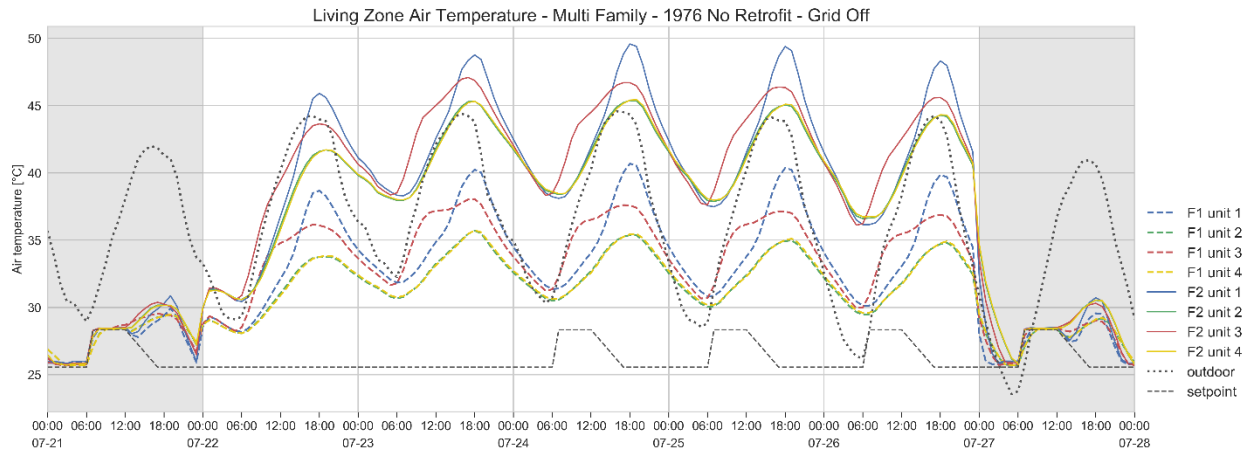


Figure 18. Baseline air temperature of each unit of the multi-family home built in 1978 in the grid-off scenario. Labels “F1” and “F2” in the legend refer to units on the first and second floor, respectively. The temperatures for “unit 2” and “unit 4” are the same.

Figure 19 illustrates the effects of different ECMs on SET under grid-off scenario (see Figure A-2 for grid-on result), where each box represents the distribution of the results for all units on the floor. The ECMs show varying performance in units located on different floors as well as under different power scenarios. For example, exterior storm windows and interior storm windows can help reduce SET for both floors when the power is available, but may raise SET in second-floor units when the grid is off. This is mainly because the indoor air temperature of the second-floor units can exceed the outdoor temperature when grid power is unavailable, while the indoor temperature of the first-floor units is lower than the outdoor temperature for most of the time. As shown in Figure 20, the indoor air temperature exceeds the outdoor temperature during the nights and mornings in the heat wave. Adding an exterior storm window adds an extra low-e glass layer, which increases the window assembly’s thermal resistance and impedes heat

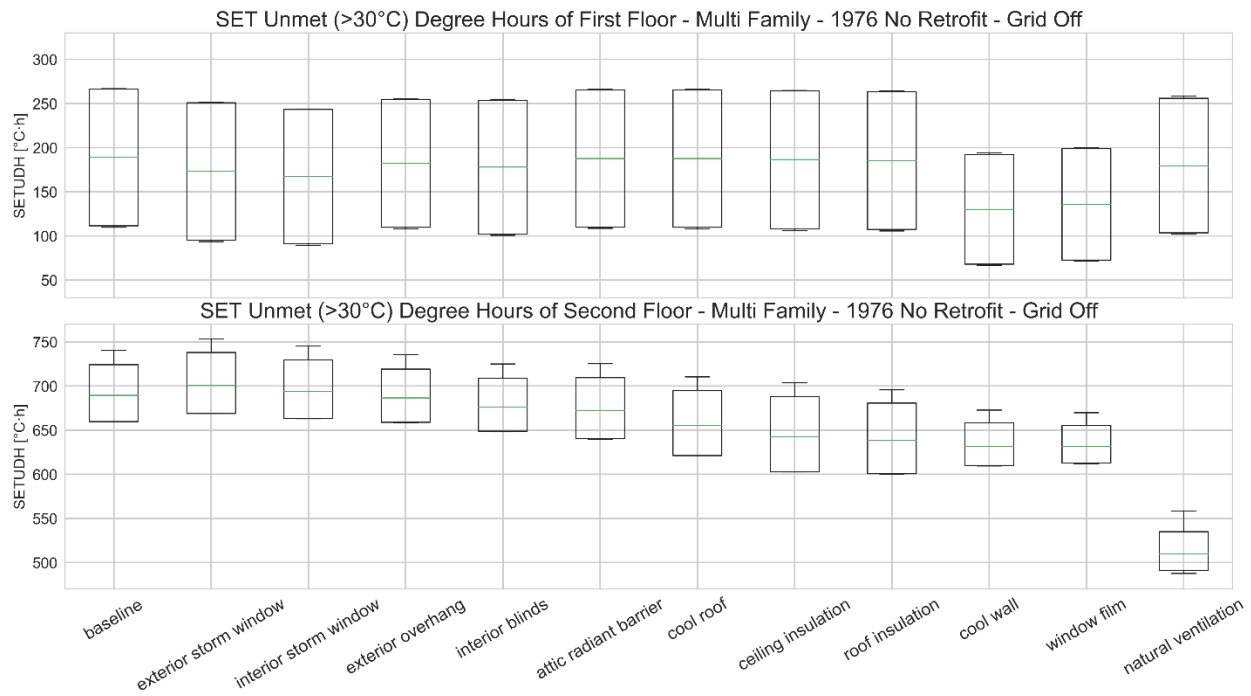


Figure 19. Standard effective temperature unmet degree hours during the heat wave in the baseline case and after applying each ECM, shown for the multi-family home built in 1976 in the grid-off scenario. Each box shows the distribution of different apartments within the multi-family home.

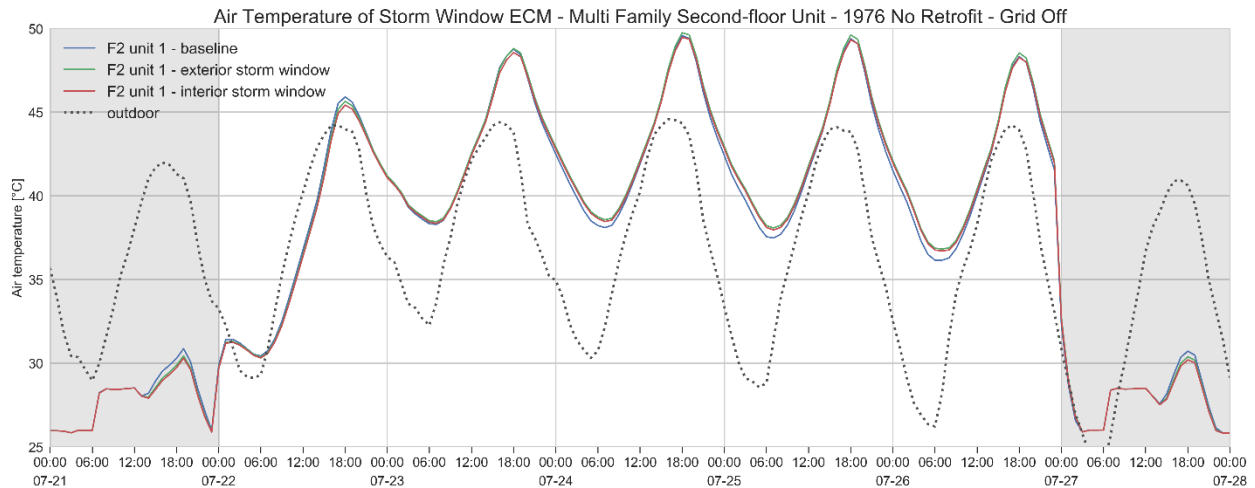


Figure 20. Indoor air temperature of the F2 unit 1 in the multi-family home built in 1976 in the grid-off scenario by adding exterior or interior storm windows, compared with baseline.

As shown in Figure 20, during the second half of the heat wave, the interior storm window also increases the indoor air temperature, but not as much as the exterior storm window—mainly because the overall SHGC after adding an interior storm window is lower than that after adding an exterior storm window. The following equation describes how the SHGC of a two-layer window is calculated [259].

$$\text{SHGC}_{2\text{-layer}} = T_{s_{2\text{-layer}}} + \alpha_o \frac{V}{h_o} + \alpha_i V \left(\frac{1}{h_s} + \frac{1}{h_o} \right) \quad \text{with} \quad \frac{1}{V} = \frac{1}{h_i} + \frac{1}{h_s} + \frac{1}{h_o} \quad (6)$$

where T_s is the solar transmittance of the two-layer window, α_o is the solar absorptance of the outer layer; α_i is the solar absorptance of the inner layer; h_o is the exterior surface heat transfer coefficient; h_i is the interior surface heat transfer coefficient; h_s is the thermal conductance of the gap between the two layers; and V is the total thermal resistance of the window assembly. All the heat transfer coefficients are invariant to the order of the window layers, so putting the layer with a lower absorptance at the outer layer will result in a higher overall SHGC than putting it at the inner layer. Since the additional storm window layer has a lower solar absorptance than the original window pane, adding it to the interior side will have less solar heat gain.

For the natural ventilation ECM, the occupants are assumed to open the windows only when the outdoor temperature is notably lower than the indoor temperature (difference ≥ 2 °C). The measure is found to be the most effective for the second-floor units in multi-family homes during the power outage as they experience the highest indoor temperature. Figure 21

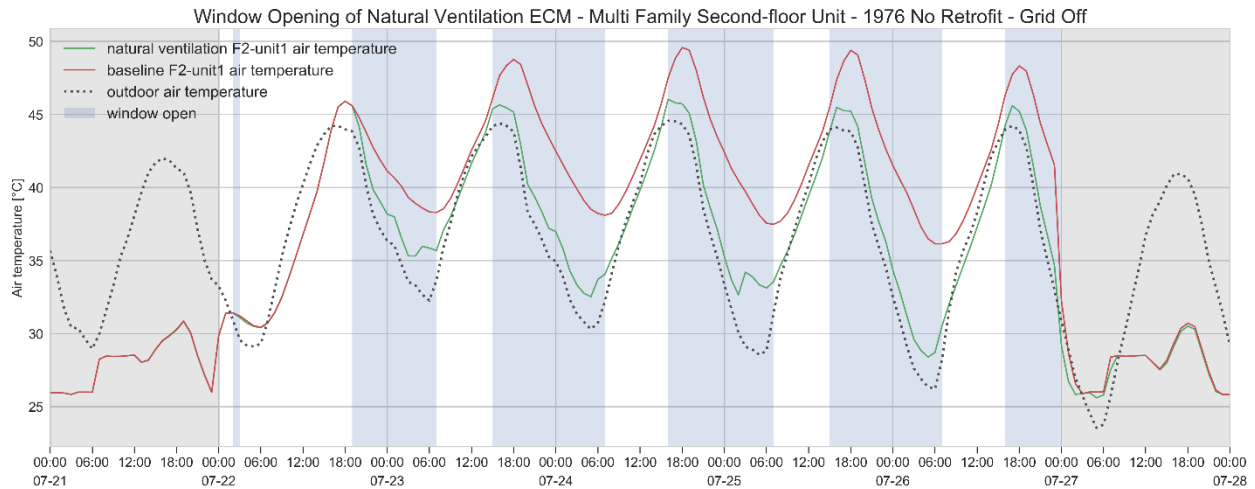


Figure 21. The window opening of the natural ventilation ECM for the core unit on the second floor of the multi-family home built in 1976 in the grid-off scenario. The blue areas represent the time periods when natural ventilation is on.

The results for multi-family homes of different vintages generally exhibit the same trends as the single-family homes, as shown in SI Figure A-14 to SI Figure A-17.

5.2. Resilience analysis on district-scale

5.2.1. Baseline models results

The indoor temperature profiles of all the homes in King district are shown in Figure 22. For single-family homes, each curve represents the temperature of one floor, while for multi-family homes, each curve represents the temperature of one unit. The profiles of single-family homes and multi-family homes are plotted in separate panels to avoid overlapping. There are three clusters of curves, corresponding to all-floor grid on, lower-floor grid off, and top-floor grid off. We can see that the temperature in the grid-off scenario is significantly higher than that in the grid-on scenario, and that when the grid is off, top-floor zones perform much worse than lower floor ones due to the extra heat gain through the roof and no free cooling via the cool ground.

When the grid is on, the curves are also divided into two clusters because the buildings are equipped with different types of air conditioners (central AC system, window air conditioner, or evaporative cooler). Those buildings equipped with evaporative coolers have notably higher temperatures than others because evaporative coolers only use the evaporation of water to cool the air so its capacity is limited to the outdoor air humidity. Even for buildings equipped with central AC systems or window air conditioners, there are still many unmet hours in which the indoor temperature is notably higher than the cooling setpoint because the cooling systems are sized for normal weather and cannot satisfy cooling needs under extreme heat waves. Therefore, measures should be taken to improve the indoor thermal conditions during heat waves.

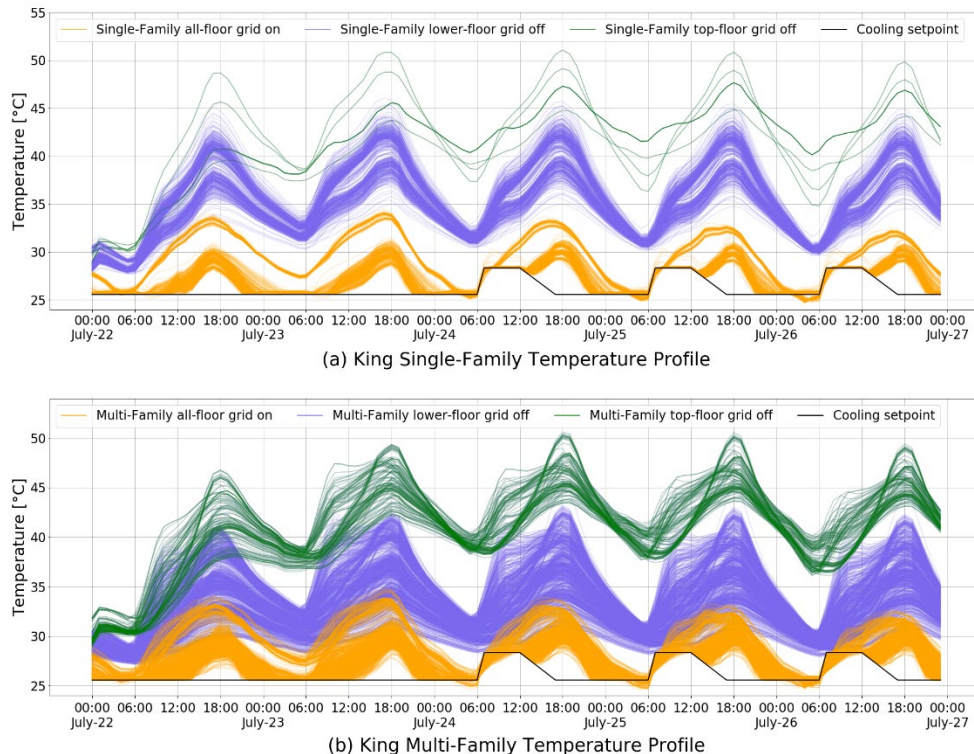


Figure 22. Indoor temperature profiles of homes in King district.

5.2.2. Passive measures

Due to limited space, only UDH and SETUDH will be discussed here. The results of HHH and PMVEH are presented in SI Section B.

5.2.2.1. UDH

(1) Grid-off scenario

Figure 23 shows the UDH during the heat wave in the baseline case and after applying each ECM for the grid-off scenario for King district. It contains three panels. The first shows the boxplot of the UDH of each passive measure. The second and the third show the absolute and relative reductions, respectively, of the UDH of each passive measure compared with the baseline.

Results are presented by zone. The top-floor zones are shown separately because their UDH are prominently higher than those of lower-floor zones when there is no active cooling. Window film provides the highest reduction for lower-floor zones (interquartile range 8%-18% for single- and multi-family homes) and the second highest reduction for top-floor zones (interquartile range 8%-20% for single- and multi-family homes). Natural ventilation is the most effective measure for top-floor zones (interquartile range 21%-26% for single- and multi-family homes) but has little effect on the UDH for lower-floor zones. This is because the indoor temperature of top-floor zones exceeds the outdoor temperature by 2 °C (the criterion for opening windows) for a substantial portion of the time during the heat wave, while the temperature of lower-floor zones seldom meets the criterion. Cool walls, ceiling insulation, and roof insulation are also good performers in terms of reducing UDH when the grid is off. The overall trend is consistent with the results from prototype homes.

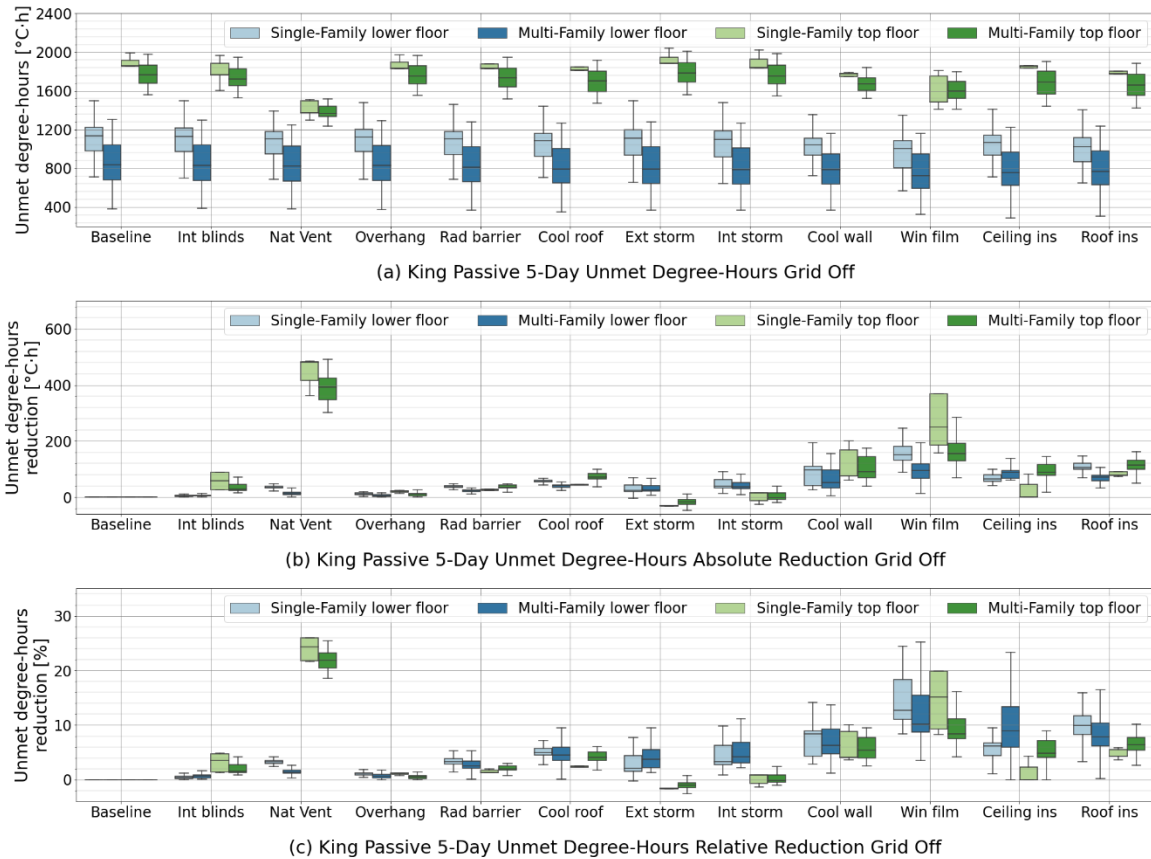


Figure 23. Unmet degree hours during the heat wave in the baseline case and after applying each ECM for the grid-off scenario .

The exterior storm window has a negative impact on the resilience of top-floor zones. This is probably because the exterior storm window decreases the U-value of the baseline window but does not change its SHGC, which reduces the convective heat gain or loss through the window but does not influence the solar heat gain. The lower-floor zones can typically maintain lower indoor air temperature than the outdoor air temperature most of the time because they are ground-contacting and can release heat to the cool ground. In contrast, the top-floor zones get lots of heat from the attic, per Section 5.1.1, making the top-floor zone air warmer than the outdoor air temperature most of the time. Thus, the exterior storm window diminishes the convective heat loss through windows, as shown in Figure 20. The interior storm window is favorable for top-floor zones, because its equivalent SHGC drops slightly to 0.37, which is moderately lower than that of the baseline window.

(2) Grid-on scenario

Figure 24 shows the UDH during the heat wave in the baseline case and after applying each ECM for the grid-on scenario. All passive measures except interior blinds can reduce the UDH. Roof insulation, ceiling insulation, and window film are the most effective passive measures. Roof insulation is more effective in reducing the UDH for single-family homes (median reduction is 37%) than for multi-family homes (median reduction is 24%). Adopting interior blinds increases the UDH, the reason for which has been explained in Section 5.1.1.

Natural ventilation slightly reduces the UDH of single-family homes and has almost no effect on multi-family homes when the grid is on. This is because the criterion for opening the windows is that the indoor air temperature is 2 °C higher than the outdoor air temperature. With the cooling system running, the indoor air temperature of single-family homes meets this criterion for only a few hours during the heat wave, leading to a small reduction of the UDH. On the other hand, when the grid is off, the indoor air temperature is much higher, which leads to longer hours of effective natural ventilation.

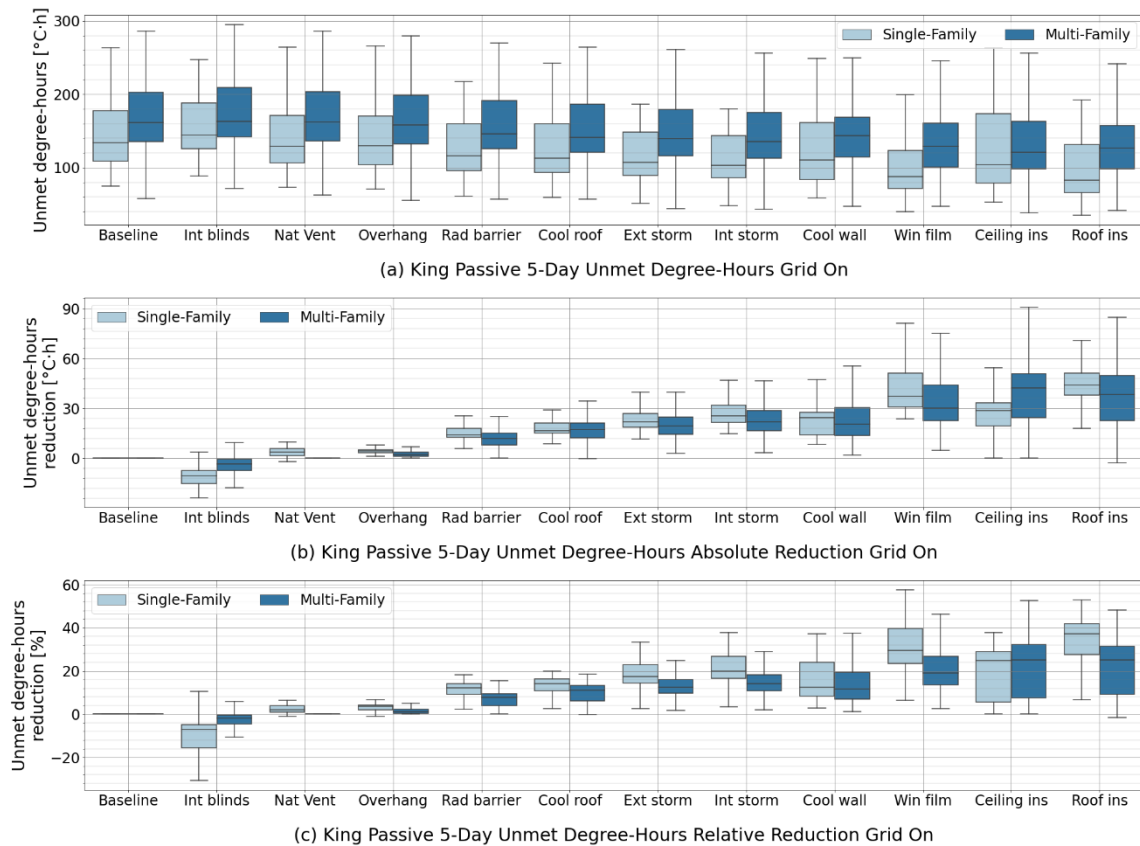
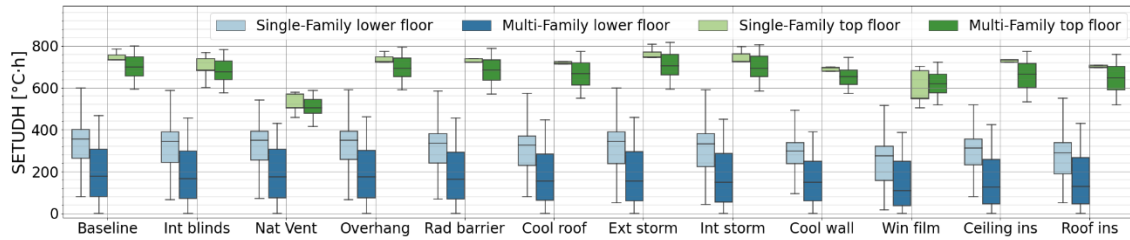


Figure 24. Unmet degree hours during the heat wave in the baseline case and after applying each ECM for the grid-on scenario.

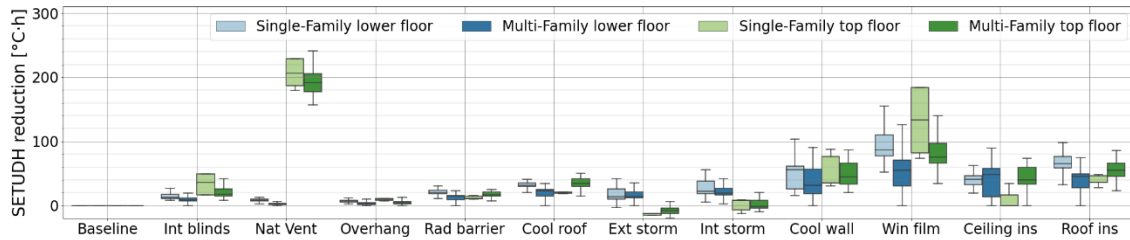
5.2.2.2. SETUDH

(1) Grid-off scenario

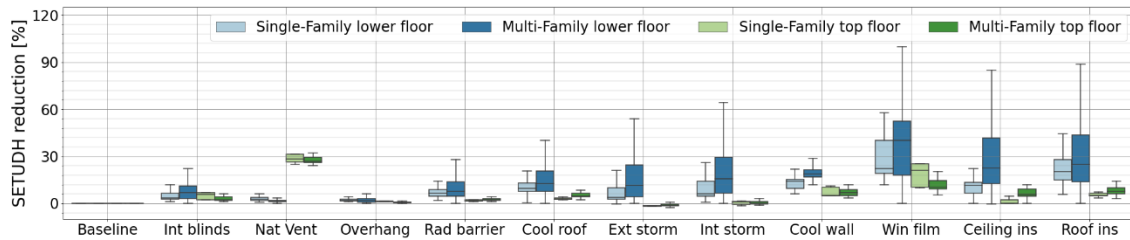
The SETUDH during the heat wave in the baseline case and after applying each ECM for the grid-off scenario for King district are shown in Figure 25. Similar to the results of UDH, window film has the best performance overall and natural ventilation has the best performance in top-floor zones.



(a) King Passive 5-Day SETUDH Grid Off



(b) King Passive 5-Day SETUDH Absolute Reduction Grid Off

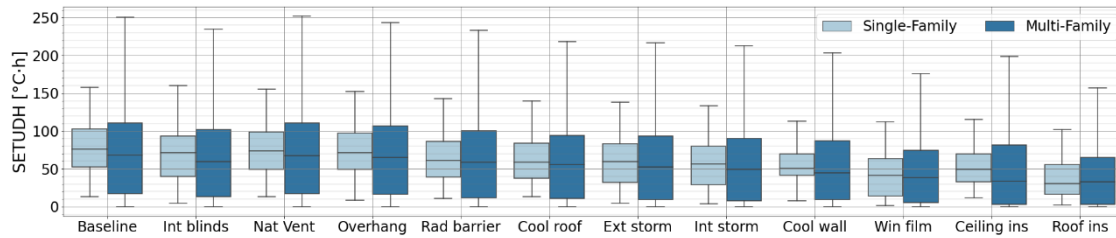


(c) King Passive 5-Day SETUDH Relative Reduction Grid Off

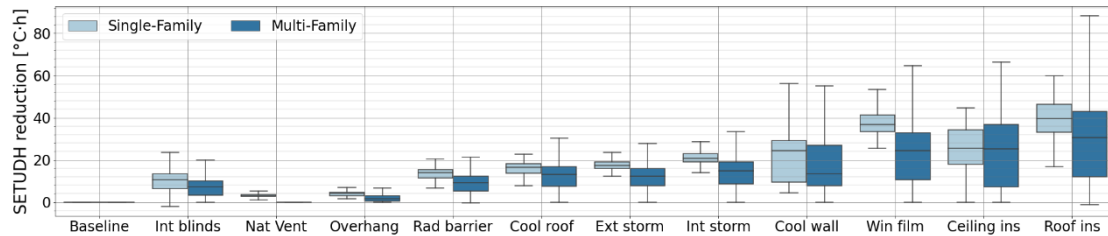
Figure 25. Standard effective temperature unmet degree hours during the heat wave in the baseline case and after applying each ECM for the grid-off scenario.

(2) Grid-on scenario

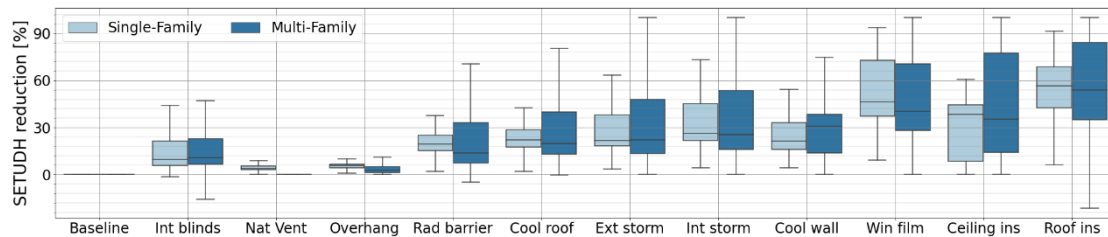
The SETUDH during the heat wave in the baseline case and after applying each ECM for the grid-on scenario are shown in Figure 26. We can see that roof insulation, ceiling insulation, and window film are the most effective measures. Different from UDH, interior blinds can moderately reduce SETUDH, because SETUDH include the effect of mean radiant temperature and interior blinds can block solar radiation transmitted through the window and the thermal radiation emitted by the window.



(a) King Passive 5-Day SETUDH Grid On



(b) King Passive 5-Day SETUDH Absolute Reduction Grid On



(c) King Passive 5-Day SETUDH Relative Reduction Grid On

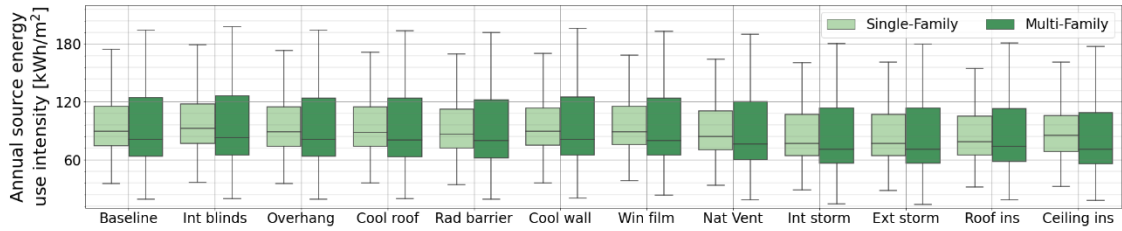
Figure 26. Standard effective temperature unmet degree hours during the heat wave in the baseline case and after applying each ECM for the grid-on scenario.

6. Discussion

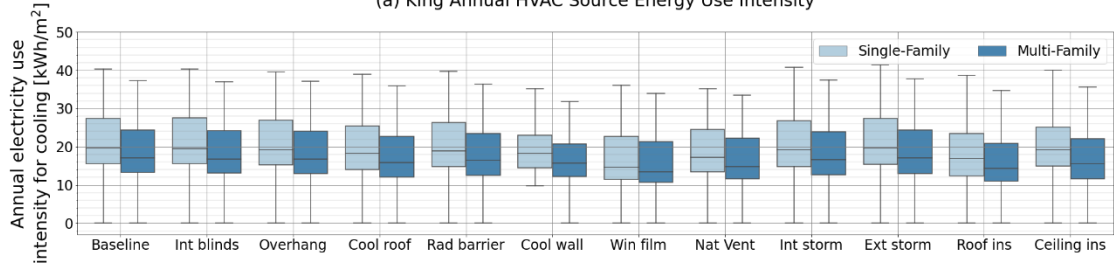
6.1. Effect on annual energy consumption

Figure 27 shows the annual HVAC source energy use intensity, annual electricity use intensity for cooling, and annual natural gas use intensity for heating in the baseline case and after applying each ECM; Figure 28 shows the percentage reduction (savings) provided by each ECM. The HVAC source energy use is calculated as the sum of source energy from electricity use (cooling + fans) with a site-to-source factor of 1.97, and from natural gas use with a site-to-source factor of 1.09. These factors are based on the eGRID 2018 plant level database for all plants in California, with a 100% conversion efficiency for renewable energy [260].

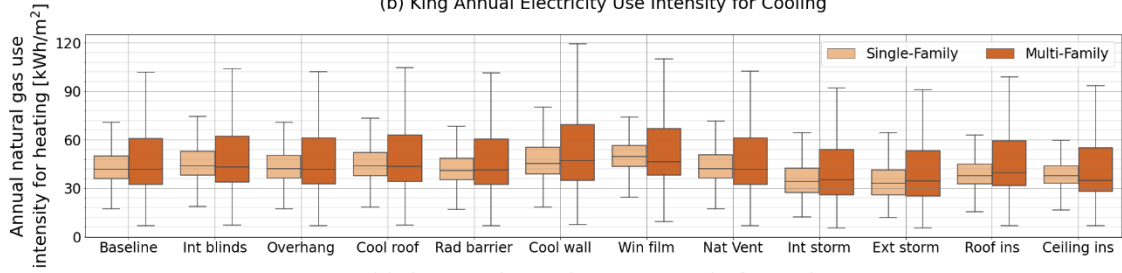
In terms of reducing the annual HVAC source energy use, increasing the insulation of the envelope is more effective than controlling solar heat gain. This is supported by the fact that improving ceiling insulation, improving roof insulation, adding exterior storm windows, and adding interior storm windows are the four most effective measures in terms of saving energy. The reason is that better envelope insulation can reduce both heat gain in the summer and heat loss in the winter. On the contrary, while controlling solar heat gain reduces the cooling energy use in the summer, it tends to increase the heating energy use in the winter.



(a) King Annual HVAC Source Energy Use Intensity



(b) King Annual Electricity Use Intensity for Cooling



(c) King Annual Natural Gas Use Intensity for Heating

Figure 27. Annual energy use intensities in the baseline case and after applying each ECM

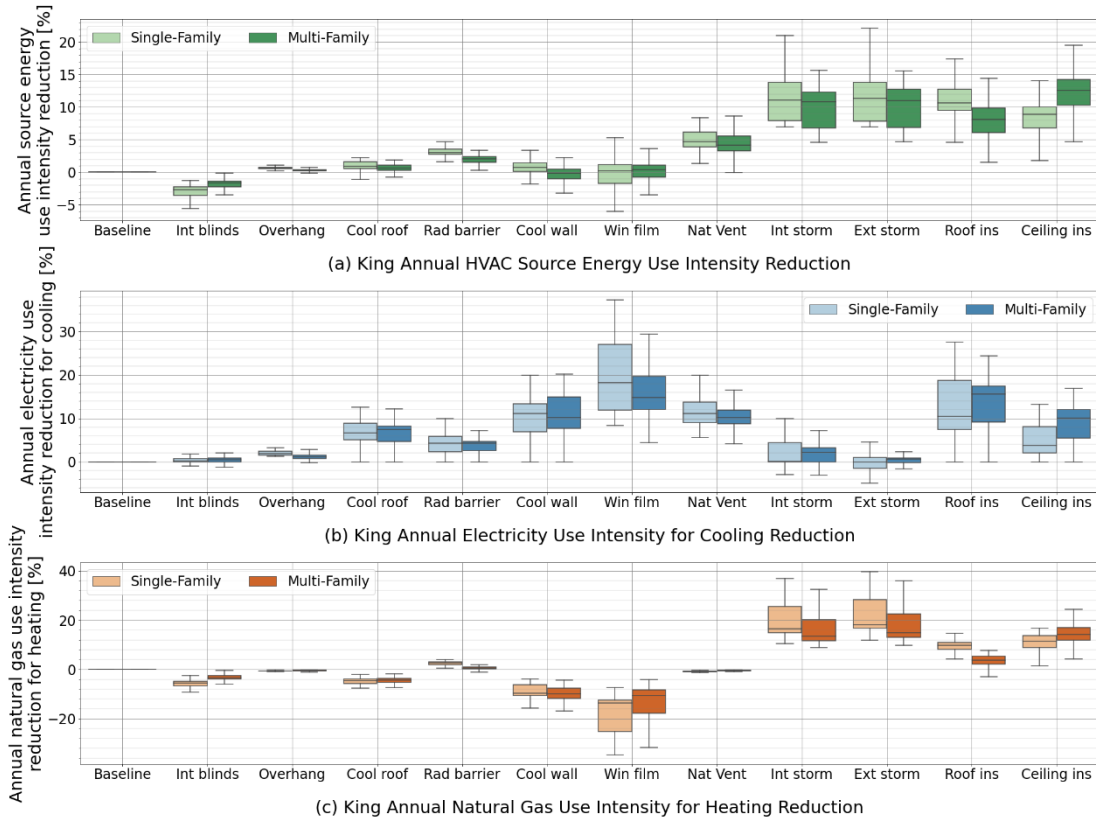


Figure 28. Annual energy use intensity reduction in the baseline case and after applying each ECM.

6.2. Implications

Current building energy codes do not provide regulations for heat resilience, although the LEED voluntary performance rating systems gives pilot credit to passive survivability for green building certifications. We recommend that new building energy codes or retrofit guides for existing buildings incorporate provisions to improve the heat resilience of buildings. A holistic life cycle analysis of benefits and costs of measures, covering energy supply, demand, storage, and human behavior, should be required in the design process. This is an important area of follow up research in future projects.

Although effective, adding roof insulation is an expensive major retrofit, so should only happen when the roof needs replacement. Window film was found to be not widely used in our survey due to concerns about its durability and difficulty to remove. However, with the advancement of window film technology and deployment technique, this can be a promising and low-cost retrofit option. Cool walls and cool roofs can also provide resilience benefits with little to no incremental cost to non-cool walls and roofs, and should be prioritized when homes are re-painted or re-roofed.

6.3 Limitations and future research

This study has some limitations described below.

Details of building characteristics are limited for the buildings studied and must be based on limited surveys, city's public data, and assumptions in California building energy efficiency standards. Utility bills are not available for calibrating the developed energy models. This is partly due to the 2020 pandemic that limits on-site audit or other data collection efforts.

Due to lack of information, we were not able to model detailed zoning in each home, so could not capture the variations of indoor environment among different zones within a home. As a side effect, we could not consider any possible variations in the health hazard thresholds of different room functions—e.g., living room vs. sleeping room. For single-family homes, indoor environment is analyzed for each floor; for multi-family homes, indoor environment is analyzed for each apartment unit.

The performance of some passive design measures depends on occupant behavior. For instance, the natural ventilation measure assumes that the occupants would monitor the indoor and outdoor environment and would operate windows for more efficient natural ventilation. Our analysis is aimed to illustrate the potential of the measures, the effects of these measures in real practice may differ from the simulation results. Without occupants' active engagement, the natural ventilation measure would be less effective; on the other hand, if the occupants engage even more aggressively than our assumption—e.g., control windows by closely monitoring the indoor and outdoor temperature with thermometers—the measure could be even more effective than predicted by our simulation results. Also, when we simulate natural ventilation assuming windows are open, EnergyPlus doesn't take into consideration the changes of window positions and still calculates solar heat gains as normal. This is a limitation of the EnergyPlus engine.

Costs - limitation

We do not include costs or cost benefit analysis in this study. Costs are tricky to estimate due to wide ranges and variations. They become even more trickier when considering the non-energy benefits such as thermal resilience and health. More work is needed in the future to perform a comprehensive analysis to account for the non-energy benefits.

Future work can include collecting more extensive data to improve the modeling, as well as considering other measures like spraying water on roof or walls that might be effective to reduce indoor temperature during heat waves or power outages. Human behavior is another essential aspect to improve heat resilience—wearing lightweight clothing, engaging in calm or less-energetic activities, use of manual fans, and taking baths or showers are potential examples that can help reduce heat hazards during heat waves especially coupled with power outages. Modeling the worst-case heat waves in future climate scenarios is another follow up, as well as modeling the coupling of passive measures with active measures for optimal heat resilience.

7. Conclusions

This paper presents the methodology, data, tools, workflow, results, and analysis of passive measures to improve heat resilience of single- and multi-family homes at individual representative buildings and district scales in disadvantaged communities under two power scenarios in Fresno. The two most effective measures for both grid-on and grid-off scenarios are adding roof insulation and adding solar-control window films; these reduce heat gains

through the building envelope, decreasing cooling loads and indoor air temperature. It should be noted that roof insulation is expensive and should only happen when the roof needs replacement. Window film has not been widely adopted by the DACs but can be a promising and low-cost solution.

When grid power is not available, the top floors of a multi-story single-family home or multi-family building can have higher risk for unsafe conditions during heat waves due to their greater exposure to solar heat gains (through roofs, walls, and windows) with less shading. Operable windows can enable natural ventilation for top floors when the indoor temperature is higher than the outdoor temperature, which can be very effective in mitigating extreme heat hazards.

Although most passive measures can improve heat resilience, some show varying performance that depends on building characteristics and external conditions, such as interior blinds (grid on vs. grid off), exterior storm windows (ground floor vs. top floor), and natural ventilation (grid on vs. grid off; ground floor vs. top floor). Also, passive measures may not be sufficient to fully guarantee thermal comfort when power is available but are helpful since cooling is constrained at maximal capacity during heat waves, especially for cooling systems whose performance is highly dependent on outdoor environment—e.g., evaporative coolers. Under such situations, active measures such as ceiling and portable fans as well as energy efficient air-conditioning can be integrated with passive measures to provide adequate cooling to vulnerable occupants to reduce risks during extended heat waves. Passive measures can also help protect residents' health and safety from overheating during a power outage when there is no active cooling available.

The methodology and workflow developed in this work are applicable to studies to improve heat resilience of individual houses or residential communities during heat waves in other urban areas with hot climate. Although the recommended passive measures are based on simulation results and can benefit from further field validation, they can inform cities, communities, and utilities in developing effective and targeted strategies to ensure heat resilience for residents during increasingly frequent heat waves.

Acknowledgments

This search was supported by the California Strategic Growth Council under Contract CCR0047, and by the U.S. Department of Energy's Building Technology Office and Office of Energy Efficiency and Renewable Energy under Contract No. DE-AC02-05CH11231. We thank the Fresno Economic Opportunities Commission and Fresno Housing Authority for providing feedback and sharing insights. We thank the CAL-THRIVES project team (University of Southern California, Indicia Consulting, and West Fresno Family Resource Center) for providing feedback on this task. We also thank Steven Selkowitz for guidance about past window and shading technology research.

References

- [1] National Oceanic and Atmospheric Administration, Weather Related Fatality and Injury Statistics, (2018). <https://www.weather.gov/hazstat/>.
- [2] U.S. Environmental Protection Agency, Heat-Related Deaths, 2016. https://www.epa.gov/sites/production/files/2016-08/documents/print_heat-deaths-2016.pdf.
- [3] G. Luber, M. McGeehin, Climate Change and Extreme Heat Events, *American Journal of Preventive Medicine*. 35 (2008) 429–435. <https://doi.org/10.1016/j.amepre.2008.08.021>.
- [4] K. Knowlton, M. Rotkin-Ellman, G. King, H.G. Margolis, D. Smith, G. Solomon, R. Trent, P. English, The 2006 California heat wave: Impacts on hospitalizations and emergency department visits, *Environmental Health Perspectives*. 117 (2009) 61–67. <https://doi.org/10.1289/ehp.11594>.
- [5] R. Salonga, Six heat-related deaths reported in San Mateo County, San Francisco, 2017. <https://www.mercurynews.com/2017/09/07/six-heat-related-deaths-reported-in-san-mateo-county-san-francisco>.
- [6] California State Government, California’s Fourth Climate Change Assessment, (2020). <https://www.climateassessment.ca.gov/about/>.
- [7] A. Seville, N. Steinberg, R. Dickinson, N. Maizlish, C. Quiner, L. Rudolph, E. Mazzacurati, California heat and health project: A decision support tool, 2016. http://427mt.com/wp-content/uploads/2017/01/427_CA_HeatHealth_DecisionTool_UserNeedsAssessment-1.pdf.
- [8] U.S. Environmental Protection Agency, Centers for Disease Control and Prevention, Climate Change and Extreme Heat: What You Can Do to Prepare, 2016. <https://www.cdc.gov/climateandhealth/pubs/extreme-heat-guidebook.pdf>.
- [9] M. Auffhammer, A. Aroonruengsawat, Simulating the impacts of climate change, prices and population on California’s residential electricity consumption, *Climatic Change*. 109 (2011) 191–210. <https://doi.org/10.1007/s10584-011-0299-y>.
- [10] J. Huang, K.R. Gurney, Impact of climate change on U.S. building energy demand: sensitivity to spatiotemporal scales, balance point temperature, and population distribution, *Climatic Change*. 137 (2016) 171–185. <https://doi.org/10.1007/s10584-016-1681-6>.
- [11] M. Davis, S. Clemmer, Power Failure: How Climate Change Puts Our Electricity at Risk - and What We Can Do, 2014. <https://doi.org/10.37419/lr.v1.i1.8>.
- [12] J. McNamara, S. Clemmer, K. Dahl, E. Spanger-Siegfried, Lights Out? Storm Surge, Blackouts, and How Clean Energy Can Help, Union of Concerned Scientists, 2015.
- [13] D.T. Ton, W.-T.P. Wang, A More Resilient Grid: The U.S. Department of Energy Joins with Stakeholders in an R&D Plan, *IEEE Power and Energy Magazine*. 13 (2015) 26–34. <http://ieeexplore.ieee.org/document/7091092/> (accessed December 31, 2020).
- [14] Pacific Gas and Electric Company, Learn about Public Safety Power Shutoff (PSPS) events, (2021). https://www.pge.com/en_US/residential/outages/public-safety-power-shutoff/learn-about-psps.page.

- [15] Julie Cart, Answers to 7 burning questions about California's rolling blackouts, CALMatters. (2020). <https://calmatters.org/environment/2020/08/california-2020-rolling-blackouts-explainer/>.
- [16] ASHRAE, ANSI/ASHRAE Standard 169-2020: Climatic Data for Building Design Standards, ASHRAE, 2020.
- [17] K. Camero, These California cities are among the worst for air pollution in the US, The Sacramento Bee. (2020). <https://www.sacbee.com/news/california/article242169741.html>.
- [18] R.R. Rockzsfforde, M. Zafar, Comparative Analysis of Utility Services & Rates in California, California Public Utilities Commission Policy & Planning Division, n.d. https://www.cpuc.ca.gov/uploadedFiles/CPUC_Public_Website/Content/About_Us/Organization/Divisions/Policy_and_Planning/PPDComparativeAnalysisofUtilityServicesRatesinCAFinal.pdf.
- [19] N. Thomas, S. Mukhtyar, B. Galey, S. Wilhelm, M. Kelly, Cal-Adapt: A Cloud Optimized Web Application for Linking Climate Science to Practitioner Need, in: 2019 AGU Fall Meeting Abstracts: IN22A-03, 2019.
- [20] California Office of Environmental Health Hazard Assessment, CalEnviroScreen 3.0, CA.GOV. (2018). <https://oehha.ca.gov/calenviroscreen/report/calenviroscreen-30>.
- [21] S. Sarihi, F. Mehdizadeh Saradj, M. Faizi, A Critical Review of Façade Retrofit Measures for Minimizing Heating and Cooling Demand in Existing Buildings, Sustainable Cities and Society. 64 (2021) 102525. <https://doi.org/10.1016/j.scs.2020.102525>.
- [22] R. Kumar A, K. Vijayakumar, P. Srinivasan, A Review on Passive Cooling Practices in Residential Buildings, International Journal of Mathematical Sciences and Engineering (IJMSE). 1 (2014) 1–6. https://www.researchgate.net/publication/290061695_A_Review_on_Passive_Cooling_Practices_in_Residential_Buildings.
- [23] F. Amirifard, S.A. Sharif, F. Nasiri, Application of passive measures for energy conservation in buildings – a review, Advances in Building Energy Research. 13 (2019) 282–315. <https://doi.org/10.1080/17512549.2018.1488617>.
- [24] N. Gupta, Exploring passive cooling potentials in Indian vernacular architecture, Journal of Buildings and Sustainability. 2 (2017) 11. <http://www.insightcore.com/journal/exploring-passive-cooling-potentials-indian-vernacular-architecture-gupta-2017.html>.
- [25] S. Stevanović, Optimization of passive solar design strategies: A review, Renewable and Sustainable Energy Reviews. 25 (2013) 177–196. <https://doi.org/10.1016/j.rser.2013.04.028>.
- [26] A. Prieto, U. Knaack, T. Auer, T. Klein, Passive cooling & climate responsive façade design: Exploring the limits of passive cooling strategies to improve the performance of commercial buildings in warm climates, Energy and Buildings. 175 (2018) 30–47. <https://doi.org/10.1016/j.enbuild.2018.06.016>.
- [27] D.K. Bhamare, M.K. Rathod, J. Banerjee, Passive cooling techniques for building and their applicability in different climatic zones—The state of art, Energy and Buildings. 198 (2019) 467–490. <https://doi.org/10.1016/j.enbuild.2019.06.023>.
- [28] V. Chetan, K. Nagaraj, P.S. Kulkarni, S.K. Modi, U.N. Kempaiah, Review of Passive Cooling Methods for Buildings, J. Phys.: Conf. Ser. 1473 (2020) 012054. <https://doi.org/10.1088/1742-6596/1473/1/012054>.

- [29] N. Gupta, G.N. Tiwari, Review of passive heating/cooling systems of buildings, *Energy Science & Engineering*. 4 (2016) 305–333. <https://doi.org/10.1002/ese3.129>.
- [30] I. Oropeza-Perez, P.A. Østergaard, Active and passive cooling methods for dwellings: A review, *Renewable and Sustainable Energy Reviews*. 82 (2018) 531–544. <https://doi.org/10.1016/j.rser.2017.09.059>.
- [31] M. Alam, J. Sanjayan, P.X.W. Zou, Chapter Eleven - Balancing Energy Efficiency and Heat Wave Resilience in Building Design, in: E. Bastidas-Arteaga, M.G. Stewar (Eds.), *Climate Adaptation Engineering*, Butterworth-Heinemann, 2019: pp. 329–349. <https://doi.org/10.1016/B978-0-12-816782-3.00011-5>.
- [32] B. Givoni, Indoor temperature reduction by passive cooling systems, *Solar Energy*. 85 (2011) 1692–1726. <https://doi.org/10.1016/j.solener.2009.10.003>.
- [33] J. Testa, M. Krarti, A review of benefits and limitations of static and switchable cool roof systems, *Renewable and Sustainable Energy Reviews*. 77 (2017) 451–460. <https://doi.org/10.1016/j.rser.2017.04.030>.
- [34] R. Levinson, H. Akbari, S. Konopacki, S. Bretz, Inclusion of cool roofs in nonresidential Title 24 prescriptive requirements, *Energy Policy*. 33 (2005) 151–170. [https://doi.org/10.1016/S0301-4215\(03\)00206-4](https://doi.org/10.1016/S0301-4215(03)00206-4).
- [35] Global Cool Cities Alliance, *A Practical Guide to Cool Roofs and Cool Pavements*, 2012. <https://CoolRoofToolkit.org>.
- [36] M. Santamouris, A. Synnefa, T. Karlessi, Using advanced cool materials in the urban built environment to mitigate heat islands and improve thermal comfort conditions, *Solar Energy*. 85 (2011) 3085–3102. <https://doi.org/10.1016/j.solener.2010.12.023>.
- [37] R. Levinson, G. Ban-Weiss, P. Berdahl, S. Chen, H. Destailats, N. Dumas, H. Gilbert, H. Goudey, S. Houzé de l'Aulnoit, J. Kleissl, B. Kurtz, Y. Li, Y. Long, A. Mohegh, N. Nazarian, M. Pizzicotti, P. Rosado, M. Russell, J. Slack, X. Tang, J. Zhang, W. Zhang, *Solar-Reflective “Cool” Walls: Benefits, Technologies, and Implementation*, California Energy Commission, Sacramento, CA, 2019. <http://dx.doi.org/10.20357/B7SP4H>.
- [38] R. Levinson, P. Berdahl, H. Akbari, W. Miller, I. Joedicke, J. Reilly, Y. Suzuki, M. Vondran, Methods of creating solar-reflective nonwhite surfaces and their application to residential roofing materials, *Solar Energy Materials and Solar Cells*. 91 (2007) 304–314. <https://doi.org/10.1016/j.solmat.2006.06.062>.
- [39] R. Levinson, P. Berdahl, H. Akbari, Solar spectral optical properties of pigments - Part I: Model for deriving scattering and absorption coefficients from transmittance and reflectance measurements, *Solar Energy Materials and Solar Cells*. 89 (2005) 319–349. <https://doi.org/10.1016/j.solmat.2004.11.012>.
- [40] R. Levinson, P. Berdahl, H. Akbari, Lawrence Berkeley National Laboratory Pigment Database, (2005). <http://pigments.lbl.gov>.
- [41] R.F. Brady, L.V. Wake, Principles and formulations for organic coatings with tailored infrared properties, *Progress in Organic Coatings*. 20 (1992) 1–25. [https://doi.org/10.1016/0033-0655\(92\)85001-C](https://doi.org/10.1016/0033-0655(92)85001-C).
- [42] R. Levinson, H. Akbari, P. Berdahl, K. Wood, W. Skilton, J. Petersheim, A novel technique for the production of cool colored concrete tile and asphalt shingle roofing products, *Solar Energy Materials and Solar Cells*. 94 (2010) 946–954. <https://doi.org/10.1016/j.solmat.2009.12.012>.

- [43] A. Synnefa, M. Santamouris, K. Apostolakis, On the development, optical properties and thermal performance of cool colored coatings for the urban environment, *Solar Energy*. 81 (2007) 488–497. <https://doi.org/10.1016/j.solener.2006.08.005>.
- [44] P. Berdahl, S.S. Chen, H. Destailats, T.W. Kirchstetter, R. Levinson, M.A. Zalich, Fluorescent cooling of objects exposed to sunlight - The ruby example, *Solar Energy Materials and Solar Cells*. 157 (2016) 312–317. <https://doi.org/10.1016/j.solmat.2016.05.058>.
- [45] P. Berdahl, S.K. Boocock, G.C.-Y. Chan, S.S. Chen, R.M. Levinson, M.A. Zalich, High quantum yield of the Egyptian blue family of infrared phosphors (MCuSi₄O₁₀, M = Ca, Sr, Ba), *Journal of Applied Physics*. 123 (2018) 193103. <https://doi.org/10.1063/1.5019808>.
- [46] S. Garshasbi, M. Santamouris, Using advanced thermochromic technologies in the built environment: Recent development and potential to decrease the energy consumption and fight urban overheating, *Solar Energy Materials and Solar Cells*. 191 (2019) 21–32. <https://doi.org/10.1016/j.solmat.2018.10.023>.
- [47] J. Testa, M. Krarti, Evaluation of energy savings potential of variable reflective roofing systems for US buildings, *Sustainable Cities and Society*. 31 (2017) 62–73. <https://doi.org/10.1016/j.scs.2017.01.016>.
- [48] T. Karlessi, M. Santamouris, K. Apostolakis, A. Synnefa, I. Livada, Development and testing of thermochromic coatings for buildings and urban structures, *Solar Energy*. 83 (2009) 538–551. <https://doi.org/10.1016/j.solener.2008.10.005>.
- [49] H. Akbari, D. Kolokotsa, Three decades of urban heat islands and mitigation technologies research, *Energy and Buildings*. 133 (2016) 834–842. <https://doi.org/10.1016/j.enbuild.2016.09.067>.
- [50] K.M. Bailey, CoolAngle shingles, (2020). <http://coolangle.com/coolangle-shingles>.
- [51] K.M. Bailey, M.E. Ewing, Roofing material with directionally dependent properties, US20110183112A1, 2011. <https://patents.google.com/patent/US20110183112A1/en> (accessed March 15, 2020).
- [52] J. Yuan, K. Emura, C. Farnham, Potential for application of retroreflective materials instead of highly reflective materials for urban heat island mitigation, *Urban Studies Research*. 2016 (2016) 1–10. <https://doi.org/10.1155/2016/3626294>.
- [53] R. Levinson, S. Chen, J. Slack, H. Goudey, T. Harima, P. Berdahl, Design, characterization, and fabrication of solar-retroreflective cool-wall materials, *Solar Energy Materials and Solar Cells*. 206 (2020) 110117. <https://doi.org/10.1016/j.solmat.2019.110117>.
- [54] M. Santamouris, J. Feng, Recent Progress in Daytime Radiative Cooling: Is It the Air Conditioner of the Future?, *Buildings*. 8 (2018) 168. <https://doi.org/10.3390/buildings8120168>.
- [55] D. Zhao, A. Aili, Y. Zhai, S. Xu, G. Tan, X. Yin, R. Yang, Radiative sky cooling: Fundamental principles, materials, and applications, *Applied Physics Reviews*. 6 (2019) 021306. <https://doi.org/10.1063/1.5087281>.
- [56] S. Catalanotti, V. Cuomo, G. Piro, D. Ruggi, V. Silvestrini, G. Troise, The radiative cooling of selective surfaces, *Solar Energy*. 17 (1975) 83–89. [https://doi.org/10.1016/0038-092X\(75\)90062-6](https://doi.org/10.1016/0038-092X(75)90062-6).

- [57] M. Casini, Active dynamic windows for buildings: A review, *Renewable Energy*. 119 (2018) 923–934. <https://doi.org/10.1016/j.renene.2017.12.049>.
- [58] IGDB | Windows and Daylighting, (2020). <https://windows.lbl.gov/software/igdb> (accessed May 14, 2020).
- [59] B.P. Jelle, A. Hynd, A. Gustavsen, D. Arasteh, H. Goudey, R. Hart, Fenestration of today and tomorrow: A state-of-the-art review and future research opportunities, *Solar Energy Materials and Solar Cells*. 96 (2012) 1–28.
- [60] C. Kocer, The Past, Present, and Future of the Vacuum Insulated Glazing Technology, in: *Glassonweb.Com*, 2019. <https://www.glassonweb.com/article/past-present-and-future-vacuum-insulated-glazing-technology> (accessed June 1, 2020).
- [61] E.S. Lee, Innovative Glazing Materials, in: *Handbook of Energy Efficiency in Buildings*, Butterworth Heinemann, 2019: pp. 358–372.
- [62] C.K. Leung, L. Lu, Y. Liu, H.S. Cheng, J.H. Tse, Optical and thermal performance analysis of aerogel glazing technology in a commercial building of Hong Kong, *Energy and Built Environment*. 1 (2020) 215–223. <https://doi.org/10.1016/j.enbenv.2020.02.001>.
- [63] M. Rubin, K. von Rottkay, R. Powles, Window optics, *Solar Energy*. 62 (1998) 149–161. [https://doi.org/10.1016/S0038-092X\(98\)00010-3](https://doi.org/10.1016/S0038-092X(98)00010-3).
- [64] C. Schaefer, G. Bräuer, J. Szczyrbowski, Low emissivity coatings on architectural glass, *Surface and Coatings Technology*. 93 (1997) 37–45. [https://doi.org/10.1016/S0257-8972\(97\)00034-0](https://doi.org/10.1016/S0257-8972(97)00034-0).
- [65] S.E. Selkowitz, M. Rubin, E.S. Lee, R. Sullivan, Electrochromic window performance factors, in: *Optical Materials Technology for Energy Efficiency and Solar Energy Conversion XIII*, International Society for Optics and Photonics, 1994: pp. 226–248. <https://doi.org/10.1117/12.185373>.
- [66] Attachment Energy Rating Council, AERC - Attachments Energy Rating Council, AERC. (2020). <https://aercnet.org/> (accessed May 17, 2020).
- [67] S. Attia, S. Bilir, T. Safy, C. Struck, R. Loonen, F. Goia, Current trends and future challenges in the performance assessment of adaptive façade systems, *Energy and Buildings*. 179 (2018) 165–182. <https://doi.org/10.1016/j.enbuild.2018.09.017>.
- [68] ES-SO, European Solar Shading Organization, (2020). <https://www.es-so.com/> (accessed May 17, 2020).
- [69] S. Hoffmann, E. Lee, Potential energy savings with exterior shades in large office buildings and the impact of discomfort glare, 2015. <https://doi.org/10.2172/1248922>.
- [70] E.S. Lee, D.L. DiBartolomeo, S.E. Selkowitz, Thermal and daylighting performance of an automated venetian blind and lighting system in a full-scale private office, *Energy and Buildings*. 29 (1998) 47–63.
- [71] A.I. Palmero-Marrero, A.C. Oliveira, Effect of louver shading devices on building energy requirements, *Applied Energy*. 87 (2010) 2040–2049. <https://doi.org/10.1016/j.apenergy.2009.11.020>.
- [72] Y.-H. Perng, Y.-Y. Huang, Investigation of technological trends in shading devices through patent analysis, *Journal of Civil Engineering and Management*. 22 (2016) 818–830. <https://doi.org/10.3846/13923730.2014.914091>.

- [73] A. Sherif, A. El-Zafarany, R. Arafa, External perforated window Solar Screens: The effect of screen depth and perforation ratio on energy performance in extreme desert environments, *Energy and Buildings*. 52 (2012) 1–10.
<https://doi.org/10.1016/j.enbuild.2012.05.025>.
- [74] Y. Sun, Y. Wu, R. Wilson, S. Lu, Experimental measurement and numerical simulation of the thermal performance of a double glazing system with an interstitial Venetian blind, *Building and Environment*. 103 (2016) 111–122.
<https://doi.org/10.1016/j.buildenv.2016.03.028>.
- [75] A. Tzempelikos, A Review of Optical Properties of Shading Devices, *Advances in Building Energy Research*. 2 (2008) 211–239. <https://doi.org/10.3763/aber.2008.0207>.
- [76] K.V.D. Wymelenberg, Patterns of occupant interaction with window blinds: A literature review, *Energy and Buildings*. 51 (2012) 165–176.
<https://doi.org/10.1016/j.enbuild.2012.05.008>.
- [77] Z. Ioannidis, A. Buonomano, A.K. Athienitis, T. Stathopoulos, Modeling of double skin façades integrating photovoltaic panels and automated roller shades: Analysis of the thermal and electrical performance, *Energy and Buildings*. 154 (2017) 618–632.
<https://doi.org/10.1016/j.enbuild.2017.08.046>.
- [78] R.R. Lunt, V. Bulovic, Transparent, near-infrared organic photovoltaic solar cells for window and energy-scavenging applications, *Applied Physics Letters*. 98 (2011) 113305.
<https://doi.org/10.1063/1.3567516>.
- [79] J. Peng, D.C. Curcija, L. Lu, S.E. Selkowitz, H. Yang, R. Mitchell, Developing a method and simulation model for evaluating the overall energy performance of a ventilated semi-transparent photovoltaic double-skin facade, *Progress in Photovoltaics: Research and Applications*. 24 (2016) 781–799. <https://doi.org/10.1002/pip.2727>.
- [80] X. Zhang, S.-K. Lau, S.S.Y. Lau, Y. Zhao, Photovoltaic integrated shading devices (PVSDs): A review, *Solar Energy*. 170 (2018) 947–968.
<https://doi.org/10.1016/j.solener.2018.05.067>.
- [81] A.L. Pisello, F. Rosso, Natural Materials for Thermal Insulation and Passive Cooling Application, *Key Engineering Materials*. 666 (2016) 1–16.
<https://doi.org/10.4028/www.scientific.net/KEM.666.1>.
- [82] L. Aditya, T.M.I. Mahlia, B. Rismanchi, H.M. Ng, M.H. Hasan, H.S.C. Metselaar, O. Muraza, H.B. Aditya, A review on insulation materials for energy conservation in buildings, *Renewable and Sustainable Energy Reviews*. 73 (2017) 1352–1365.
<https://doi.org/10.1016/j.rser.2017.02.034>.
- [83] C. Silva, M.S. Chandra, Study on suitable wall thermal insulation methods for dwellings under tropical climatic conditions: a review, in: *Galle, Sri Lanka, 2019*.
- [84] Dr.M.S. Al-Homoud, Performance characteristics and practical applications of common building thermal insulation materials, *Building and Environment*. 40 (2005) 353–366.
<https://doi.org/10.1016/j.buildenv.2004.05.013>.
- [85] M.A. Medina, A Comprehensive Review of Radiant Barrier Research Including Laboratory and Field Experiments, *ASHRAE Transactions*. 118 (2012) 400–407.
<https://libproxy.berkeley.edu/login?qurl=https%3a%2f%2fsearch.ebscohost.com%2flogin.aspx%3fdirect%3dtrue%26db%3da9h%26AN%3d77709093%26site%3ded-live> (accessed December 19, 2020).

- [86] H. Sghiouri, M. Charai, A. Mezrhab, M. Karkri, Comparison of passive cooling techniques in reducing overheating of clay-straw building in semi-arid climate, *Build. Simul.* 13 (2020) 65–88. <https://doi.org/10.1007/s12273-019-0562-0>.
- [87] S.W. Lee, C.H. Lim, E.@ I.B. Salleh, Reflective thermal insulation systems in building: A review on radiant barrier and reflective insulation, *Renewable and Sustainable Energy Reviews.* 65 (2016) 643–661. <https://doi.org/10.1016/j.rser.2016.07.002>.
- [88] NREL, Cooling your home naturally, National Renewable Energy Lab., Golden, CO (United States), 1994. <https://doi.org/10.2172/34351>.
- [89] B. Raji, M.J. Tenpierik, A. Dobbelsteen, The impact of greening systems on building energy performance: A literature review, *Renewable and Sustainable Energy Reviews.* 45 (2015) 610–623. <https://doi.org/10/gcv7ks>.
- [90] G. Pérez, J. Coma, I. Martorell, L.F. Cabeza, Vertical Greenery Systems (VGS) for energy saving in buildings: A review, *Renewable and Sustainable Energy Reviews.* 39 (2014) 139–165. <https://doi.org/10.1016/j.rser.2014.07.055>.
- [91] A. Sharifi, Y. Yamagata, Roof ponds as passive heating and cooling systems: A systematic review, *Applied Energy.* 160 (2015) 336–357. <https://doi.org/10.1016/j.apenergy.2015.09.061>.
- [92] A. Spanaki, T. Tsoutsos, D. Kolokotsa, On the selection and design of the proper roof pond variant for passive cooling purposes, *Renewable and Sustainable Energy Reviews.* 15 (2011) 3523–3533. <https://doi.org/10.1016/j.rser.2011.05.007>.
- [93] E. Erell, S. Yannas, J. L. Molina, Roof Cooling Techniques, in: *The 23rd Conference on Passive and Low Energy Architecture*, Geneva, Switzerland, 2006: pp. 571–576. https://www.researchgate.net/publication/267771767_Roof_Cooling_Techniques.
- [94] L. Liu, Z. Yu, H. Zhang, Simulation study of an innovative ventilated facade utilizing indoor exhaust air, *Energy Procedia.* 121 (2017) 126–133. <https://doi.org/10.1016/j.egypro.2017.08.009>.
- [95] S. Fantucci, V. Serra, M. Perino, Dynamic Insulation Systems: Experimental Analysis on a Parietodynamic Wall, *Energy Procedia.* 78 (2015) 549–554. <https://doi.org/10.1016/j.egypro.2015.11.734>.
- [96] T. Başaran, T. İnan, Experimental investigation of the pressure loss through a double skin facade by using perforated plates, *Energy and Buildings.* 133 (2016) 628–639. <https://doi.org/10.1016/j.enbuild.2016.10.020>.
- [97] E. Osterman, V.V. Tyagi, V. Butala, N.A. Rahim, U. Stritih, Review of PCM based cooling technologies for buildings, *Energy and Buildings.* 49 (2012) 37–49. <https://doi.org/10.1016/j.enbuild.2012.03.022>.
- [98] L.F. Cabeza, A. Castell, C. Barreneche, A.D. Gracia, A.I. Fernández, Materials used as PCM in thermal energy storage in buildings : A review, *Renewable and Sustainable Energy Reviews.* 15 (2011) 1675–1695. <https://doi.org/10.1016/j.rser.2010.11.018>.
- [99] D. Zhou, C.Y. Zhao, Y. Tian, Review on thermal energy storage with phase change materials (PCMs) in building applications, *Applied Energy.* 92 (2012) 593–605. <https://doi.org/10.1016/j.apenergy.2011.08.025>.
- [100] B. Zalba, J.M. Marín, L.F. Cabeza, H. Mehling, Review on thermal energy storage with phase change: Materials, heat transfer analysis and applications, 2003. [https://doi.org/10.1016/S1359-4311\(02\)00192-8](https://doi.org/10.1016/S1359-4311(02)00192-8).

- [101] F. Souayfane, F. Fardoun, P.H. Biwole, Phase change materials (PCM) for cooling applications in buildings: A review, *Energy and Buildings*. 129 (2016) 396–431. <https://doi.org/10.1016/j.enbuild.2016.04.006>.
- [102] A.-S.F. Ahmed, K.-M.M.K. Khan, A.-A. Maung Than Oo, R.-M.G. Rasul, Selection of suitable passive cooling strategy for a subtropical climate, *International Journal of Mechanical and Materials Engineering*. 9 (2014) 14. <https://doi.org/10.1186/s40712-014-0014-7>.
- [103] A. Aflaki, N. Mahyuddin, Z. Al-Cheikh Mahmoud, M.R. Baharum, A review on natural ventilation applications through building façade components and ventilation openings in tropical climates, *Energy and Buildings*. 101 (2015) 153–162. <https://doi.org/10.1016/j.enbuild.2015.04.033>.
- [104] F. Jomehzadeh, P. Nejat, J.K. Calautit, M.B.M. Yusof, S.A. Zaki, B.R. Hughes, M.N.A.W.M. Yazid, A review on windcatcher for passive cooling and natural ventilation in buildings, Part 1: Indoor air quality and thermal comfort assessment, *Renewable and Sustainable Energy Reviews*. 70 (2017) 736–756. <https://doi.org/10.1016/j.rser.2016.11.254>.
- [105] E.M. Okba, Building envelope design as a passive cooling technique, in: *Passive and Low Energy Cooling for the Built Environment*, Santorini, Greece, 2005. <http://citeseerx.ist.psu.edu/viewdoc/download?doi=10.1.1.496.3526&rep=rep1&type=pdf>.
- [106] M.S. Hatamipour, A. Abedi, Passive cooling systems in buildings: Some useful experiences from ancient architecture for natural cooling in a hot and humid region, *Energy Conversion and Management*. 49 (2008) 2317–2323. <https://doi.org/10.1016/j.enconman.2008.01.018>.
- [107] F. Donegan, A Guide to Passive House Renovations, Sweeten Blog. (2018). <https://sweeten.com/renovation-101/a-guide-to-passive-house-renovations/> (accessed December 12, 2020).
- [108] P. Burkholder, C. Anderson, Be cool: natural systems to beat the heat, *Home Power*. 108 (2005) 20–25. <https://www.homepower.com/>.
- [109] D. Hansmann, Beat the Heat without AC: Passive Cooling and You, Moss Design. (2014). <http://moss-design.com/passive-cooling/> (accessed December 12, 2020).
- [110] C. Anderson, Cooling your home efficiently, *Home Power*. 154 (2013) 84–88. <https://www.homepower.com/>.
- [111] J. Grove-Smith, F. Bosenick, How do Passive House buildings stay comfortable in summer?, IPHA Blog. (2018). <https://blog.passivehouse-international.org/summer-comfort-passive-house/> (accessed December 12, 2020).
- [112] D. Thorpe, How to Save Millions on Air Conditioning by Designing Passively Cooled Buildings | Smart Cities Dive, (n.d.). <https://www.smartcitiesdive.com/ex/sustainablecitiescollective/hoe-save-millions-air-conditioning-designing-passively-cooled-buildings/1029451/> (accessed December 12, 2020).
- [113] C. Reardon, D. Clarke, Passive cooling, *YourHome: Australia's Guide to Environmentally Sustainable Homes*. (2013). <https://www.yourhome.gov.au/passive-design/passive-cooling> (accessed December 12, 2020).
- [114] Ministry of Business, Innovation and Employment, Passive cooling - Smarter Homes Practical advice on smarter home essentials, *Smarter Homes*. (2017).

- <https://www.smarterhomes.org.nz/smart-guides/design/passive-cooling/> (accessed December 12, 2020).
- [115] M. Pelletier, E. Varmecky, *Passive Cooling Design: The Natural Way to Air Condition Your Home, Distinctly Montana*. (2018). <https://www.distinctlymontana.com/passive-cooling-design> (accessed December 12, 2020).
- [116] D. Miles, *Passive cooling for low-energy buildings*, (n.d.). <https://www.atamate.com/atamate-blog/passive-cooling-for-low-energy-buildings> (accessed December 12, 2020).
- [117] AIA Research Corporation, *Passive Cooling: Designing natural solutions to summer cooling loads, Research & Design*. 2 (1979). https://www.briqbase.org/sites/default/files/researchdesign_journal_1979_fall_passcool.pdf.
- [118] D. Thorpe, *Ways to keep cool without costing the planet Part 1: Passive cooling, The Fifth Estate*. (2019). <https://www.thefifthestate.com.au/housing-2/ways-to-keep-cool-without-costing-the-planet-part-1-passive-cooling/> (accessed December 12, 2020).
- [119] D. Chiras, *What Is Passive Cooling and What Can You Do to Make It Work for You?*, *Mother Earth News*. (2016). <https://www.motherearthnews.com/green-homes/passive-cooling-ze0z1604znsp> (accessed December 12, 2020).
- [120] Dan Sandink, *Reducing heat-wave risk through active and passive measures, Municipal World*. (2013). https://www.iclr.org/april_2013_muni_world_sandink-2/ (accessed December 25, 2020).
- [121] National Renewable Energy Lab, *Cooling Your Home Naturally, Technical Information Program, Energy Efficiency & Renewable Energy Clearinghouse, U.S. Department of Energy*, 1994. <https://doi.org/10.2172/34351>.
- [122] S. Boddy, *Cooling Your Home with Fans and Ventilation, Technical Information Program, Energy Efficiency & Renewable Energy Clearinghouse, U.S. Department of Energy*, 2001. <https://www.osti.gov/biblio/783410-cooling-your-home-fans-ventilation> (accessed January 12, 2021).
- [123] C. Zografos, I. Anguelovski, M. Grigorova, *When exposure to climate change is not enough: Exploring heatwave adaptive capacity of a multi-ethnic, low-income urban community in Australia, Urban Climate*. 17 (2016) 248–265. <https://doi.org/10.1016/j.uclim.2016.06.003>.
- [124] A. Laouadi, M. Bartko, M.A. Lacasse, *A new methodology of evaluation of overheating in buildings, Energy and Buildings*. 226 (2020). <https://doi.org/10.1016/j.enbuild.2020.110360>.
- [125] F. Encinas, A. De Herde, *Sensitivity analysis in building performance simulation for summer comfort assessment of apartments from the real estate market, Energy and Buildings*. 65 (2013) 55–65. <https://doi.org/10.1016/j.enbuild.2013.05.047>.
- [126] S. Porritt, L. Shao, P. Cropper, C. Goodier, *Adapting dwellings for heat waves, Sustainable Cities and Society*. 1 (2011) 81–90. <https://doi.org/10.1016/j.scs.2011.02.004>.
- [127] P.F.G. Banfill, D.P. Jenkins, S. Patidar, M. Gul, G.F. Menzies, G.J. Gibson, *Towards an overheating risk tool for building design, Structural Survey*. 31 (2013) 253–266. <https://doi.org/10.1108/SS-01-2013-0004>.

- [128] Y. Ji, R. Fitton, W. Swan, P. Webster, Assessing overheating of the UK existing dwellings – A case study of replica Victorian end terrace house, *Building and Environment*. 77 (2014) 1–11. <https://doi.org/10.1016/j.buildenv.2014.03.012>.
- [129] C. Liu, T. Kershaw, D. Fosas, A.P. Ramallo Gonzalez, S. Natarajan, D.A. Coley, High resolution mapping of overheating and mortality risk, *Building and Environment*. 122 (2017) 1–14. <https://doi.org/10.1016/j.buildenv.2017.05.028>.
- [130] J. Morey, A. Beizaee, A. Wright, An investigation into overheating in social housing dwellings in central England, *Building and Environment*. 176 (2020) 106814. <https://doi.org/10.1016/j.buildenv.2020.106814>.
- [131] N. Murtagh, B. Gatersleben, C. Fife-Schaw, Occupants' motivation to protect residential building stock from climate-related overheating: A study in southern England, *Journal of Cleaner Production*. 226 (2019) 186–194. <https://doi.org/10.1016/j.jclepro.2019.04.080>.
- [132] A. Pathan, A. Mavrogianni, A. Summerfield, T. Oreszczyn, M. Davies, Monitoring summer indoor overheating in the London housing stock, *Energy and Buildings*. 141 (2017) 361–378. <https://doi.org/10.1016/j.enbuild.2017.02.049>.
- [133] M. Vellei, A.P. Ramallo-González, D. Coley, J. Lee, E. Gabe-Thomas, T. Lovett, S. Natarajan, Overheating in vulnerable and non-vulnerable households, *Building Research & Information*. 45 (2017) 102–118. <https://doi.org/10.1080/09613218.2016.1222190>.
- [134] D. Coley, T. Kershaw, Changes in internal temperatures within the built environment as a response to a changing climate, *Building and Environment*. 45 (2010) 89–93. <https://doi.org/10.1016/j.buildenv.2009.05.009>.
- [135] A. Sakka, M. Santamouris, I. Livada, F. Nicol, M. Wilson, On the thermal performance of low income housing during heat waves, *Energy and Buildings*. 49 (2012) 69–77. <https://doi.org/10.1016/j.enbuild.2012.01.023>.
- [136] Z. Tian, B.D. Hrynyszyn, Overheating risk of a typical Norwegian residential building retrofitted to higher energy standards under future climate conditions, *E3S Web Conf.* 172 (2020) 02007. <https://doi.org/10.1051/e3sconf/202017202007>.
- [137] A. Monge-Barrio, A. Sánchez-Ostiz Gutiérrez, Facing Heatwaves and Warming Conditions in the Mediterranean Region, in: A. Monge-Barrio, A. Sánchez-Ostiz Gutiérrez (Eds.), *Passive Energy Strategies for Mediterranean Residential Buildings: Facing the Challenges of Climate Change and Vulnerable Populations*, Springer International Publishing, Cham, 2018: pp. 167–204. https://doi.org/10.1007/978-3-319-69883-0_7.
- [138] R.-L. Hwang, C.-Y. Lin, K.-T. Huang, Spatial and temporal analysis of urban heat island and global warming on residential thermal comfort and cooling energy in Taiwan, *Energy and Buildings*. 152 (2017) 804–812. <https://doi.org/10.1016/j.enbuild.2016.11.016>.
- [139] A. Baniassadi, D.J. Sailor, E.S. Krayenhoff, A.M. Broadbent, M. Georgescu, Passive survivability of buildings under changing urban climates across eight US cities, *Environ. Res. Lett.* 14 (2019) 074028. <https://doi.org/10.1088/1748-9326/ab28ba>.
- [140] S.H. Holmes, T. Phillips, A. Wilson, Overheating and passive habitability: indoor health and heat indices, *Building Research & Information*. 44 (2016) 1–19. <https://doi.org/10.1080/09613218.2015.1033875>.
- [141] T. Aduralere, J. Isaacs, D. Fannon, Passive Survivability in Residential Buildings during Heat Waves under Dynamic Exterior Conditions, *International Building Physics Conference*. (2018). <https://surface.syr.edu/ibpc/2018/MS1/6>.

- [142] K. Sun, M. Specian, T. Hong, Nexus of Thermal Resilience and Energy Efficiency in Buildings: A case study of a nursing home, *Building and Environment*. 177 (2020) 106842. <https://doi.org/10.1016/j.buildenv.2020.106842>.
- [143] W. Endlicher, G. Jendritzky, J. Fischer, J.-P. Redlich, Heat Waves, Urban Climate and Human Health, in: J.M. Marzluff, E. Shulenberger, W. Endlicher, M. Alberti, G. Bradley, C. Ryan, U. Simon, C. ZumBrunnen (Eds.), *Urban Ecology*, Springer US, Boston, MA, 2008: pp. 269–278. https://doi.org/10.1007/978-0-387-73412-5_16.
- [144] S.M. Porritt, P.C. Cropper, L. Shao, C.I. Goodier, Ranking of interventions to reduce dwelling overheating during heat waves, *Energy and Buildings*. 55 (2012) 16–27. <https://doi.org/10.1016/j.enbuild.2012.01.043>.
- [145] M.G.M. Van Der Heijden, B. Blocken, J.L.M. Hensen, Heat wave vulnerability classification of residential buildings, in: 2012.
- [146] J. Zuo, S. Pullen, J. Palmer, H. Bennetts, N. Chileshe, T. Ma, Impacts of heat waves and corresponding measures: a review, *Journal of Cleaner Production*. 92 (2015) 1–12. <https://doi.org/10.1016/j.jclepro.2014.12.078>.
- [147] M. Santamouris, K. Pavlou, A. Synnefa, K. Niachou, D. Kolokotsa, Recent progress on passive cooling techniques: Advanced technological developments to improve survivability levels in low-income households, *Energy and Buildings*. 39 (2007) 859–866. <https://doi.org/10.1016/j.enbuild.2007.02.008>.
- [148] I. Tsoulou, C.J. Andrews, R. He, G. Mainelis, J. Senick, Summertime thermal conditions and senior resident behaviors in public housing: A case study in Elizabeth, NJ, USA, *Building and Environment*. 168 (2020) 106411. <https://doi.org/10.1016/j.buildenv.2019.106411>.
- [149] K. Imessad, L. Derradji, N.A. Messaoudene, F. Mokhtari, A. Chenak, R. Kharchi, Impact of passive cooling techniques on energy demand for residential buildings in a Mediterranean climate, *Renewable Energy*. 71 (2014) 589–597. <https://doi.org/10.1016/j.renene.2014.06.005>.
- [150] L. Kuiru, Retrofitting Passive Cooling Strategies to a Brisbane School: A Case Study of the Physical and Social Aspects, MPhil Thesis, The University of Queensland, 2016. <https://doi.org/10.14264/uql.2016.1124>.
- [151] G. Hatvani-Kovacs, M. Belusko, N. Skinner, J. Pockett, J. Boland, Heat stress risk and resilience in the urban environment, *Sustainable Cities and Society*. 26 (2016) 278–288. <https://doi.org/10.1016/j.scs.2016.06.019>.
- [152] Morrison Hershfield, *Passive Cooling Measures for Multi-Unit Residential Buildings*, Vancouver, BC, 2017. <https://vancouver.ca/files/cov/passive-cooling-measures-for-murbs.pdf>.
- [153] Y. Wang, E. Long, S. Deng, Applying passive cooling measures to a temporary disaster-relief prefabricated house to improve its indoor thermal environment in summer in the subtropics, *Energy and Buildings*. 139 (2017) 456–464. <https://doi.org/10.1016/j.enbuild.2016.12.081>.
- [154] F. Yang, F. Yuan, F. Qian, Z. Zhuang, J. Yao, Summertime thermal and energy performance of a double-skin green facade: A case study in Shanghai, *Sustainable Cities and Society*. 39 (2018) 43–51. <https://doi.org/10.1016/j.scs.2018.01.049>.
- [155] R. Yao, V. Costanzo, X. Li, Q. Zhang, B. Li, The effect of passive measures on thermal comfort and energy conservation. A case study of the hot summer and cold winter climate

- in the Yangtze River region, *Journal of Building Engineering*. 15 (2018) 298–310. <https://doi.org/10.1016/j.jobbe.2017.11.012>.
- [156] M. Zinzi, S. Agnoli, Cool and green roofs. An energy and comfort comparison between passive cooling and mitigation urban heat island techniques for residential buildings in the Mediterranean region, *Energy and Buildings*. 55 (2012) 66–76. <https://doi.org/10.1016/j.enbuild.2011.09.024>.
- [157] S. Attia, A. De Herde, Impact and potential of community scale low-energy retrofit: case study in Cairo, (2009). <https://orbi.uliege.be/handle/2268/167596> (accessed December 12, 2020).
- [158] M. Dabaieh, O. Wanas, M.A. Hegazy, E. Johansson, Reducing cooling demands in a hot dry climate: A simulation study for non-insulated passive cool roof thermal performance in residential buildings, *Energy and Buildings*. 89 (2015) 142–152. <https://doi.org/10.1016/j.enbuild.2014.12.034>.
- [159] Z.D. Grussa, D. Andrews, G. Lowry, E.J. Newton, K. Yiakoumetti, A. Chalk, D. Bush, A London residential retrofit case study: Evaluating passive mitigation methods of reducing risk to overheating through the use of solar shading combined with night-time ventilation, *Building Services Engineering Research and Technology*. 40 (2019) 389–408. <https://doi.org/10.1177/0143624419840768>.
- [160] A. Mavrogianni, P. Wilkinson, M. Davies, P. Biddulph, E. Oikonomou, Building characteristics as determinants of propensity to high indoor summer temperatures in London dwellings, *Building and Environment*. 55 (2012) 117–130. <https://doi.org/10.1016/j.buildenv.2011.12.003>.
- [161] A. Paipai, Computational Assessment of Passive Cooling Methods in Buildings, M.S. Thesis, Technical University of Vienna, 2006. https://publik.tuwien.ac.at/files/pub-ar_7964.pdf.
- [162] S. Liu, Y.T. Kwok, K.K.-L. Lau, W. Ouyang, E. Ng, Effectiveness of passive design strategies in responding to future climate change for residential buildings in hot and humid Hong Kong, *Energy and Buildings*. 228 (2020) 110469. <https://doi.org/10.1016/j.enbuild.2020.110469>.
- [163] C.-R. Yu, H.-S. Guo, Q.-C. Wang, R.-D. Chang, Revealing the Impacts of Passive Cooling Techniques on Building Energy Performance: A Residential Case in Hong Kong, *Applied Sciences*. 10 (2020) 4188. <https://doi.org/10.3390/app10124188>.
- [164] P. Samani, V. Leal, A. Mendes, N. Correia, Comparison of passive cooling techniques in improving thermal comfort of occupants of a pre-fabricated building, *Energy and Buildings*. 120 (2016) 30–44. <https://doi.org/10.1016/j.enbuild.2016.03.055>.
- [165] K. Panchabikesan, K. Vellaisamy, V. Ramalingam, Passive cooling potential in buildings under various climatic conditions in India, *Renewable and Sustainable Energy Reviews*. 78 (2017) 1236–1252. <https://doi.org/10.1016/j.rser.2017.05.030>.
- [166] G.N. Tiwari, M. Upadhyay, S.N. Rai, A comparison of passive cooling techniques, *Building and Environment*. 29 (1994) 21–31. [https://doi.org/10.1016/0360-1323\(94\)90049-3](https://doi.org/10.1016/0360-1323(94)90049-3).
- [167] R. Lapisa, A. Karudin, F. Rizal, Krismadinata, Nasruddin, Passive cooling strategies in roof design to improve the residential building thermal performance in tropical region, *Asian J Civ Eng*. 20 (2019) 571–580. <https://doi.org/10.1007/s42107-019-00125-1>.

- [168] R. Suárez, J. Fernández-Agüera, Passive energy strategies in the retrofitting of the residential sector: A practical case study in dry hot climate, *Build. Simul.* 8 (2015) 593–602. <https://doi.org/10.1007/s12273-015-0234-7>.
- [169] M.S. Hatamipour, H. Mahiyar, M. Taheri, Evaluation of existing cooling systems for reducing cooling power consumption, *Energy and Buildings.* 39 (2007) 105–112. <https://doi.org/10.1016/j.enbuild.2006.05.007>.
- [170] M.A. Del Rio, T. Asawa, Y. Hirayama, R. Sato, I. Ohta, Evaluation of passive cooling methods to improve microclimate for natural ventilation of a house during summer, *Building and Environment.* 149 (2019) 275–287. <https://doi.org/10.1016/j.buildenv.2018.12.027>.
- [171] D.H.C. Toe, T. Kubota, Comparative assessment of vernacular passive cooling techniques for improving indoor thermal comfort of modern terraced houses in hot–humid climate of Malaysia, *Solar Energy.* 114 (2015) 229–258. <https://doi.org/10.1016/j.solener.2015.01.035>.
- [172] V.K. Venkiteswaran, J. Liman, S.A. Alkaff, Comparative Study of Passive Methods for Reducing Cooling Load, *Energy Procedia.* 142 (2017) 2689–2697. <https://doi.org/10.1016/j.egypro.2017.12.212>.
- [173] E.-H. Drissi Lamrhari, B. Benhamou, Thermal behavior and energy saving analysis of a flat with different energy efficiency measures in six climates, *Build. Simul.* 11 (2018) 1123–1144. <https://doi.org/10.1007/s12273-018-0467-3>.
- [174] L. Metibogun, G. Baird, Rethinking Architectural Passive Cooling Strategies in New Zealand's Non-residential Building Stock, in: Hong Kong, Hong Kong, 2017: p. 6.
- [175] S.N.J. Al-Saadi, J. Al-Hajri, M.A. Sayari, Energy-Efficient Retrofitting Strategies for Residential Buildings in hot climate of Oman, *Energy Procedia.* 142 (2017) 2009–2014. <https://doi.org/10.1016/j.egypro.2017.12.403>.
- [176] K. Grygierek, I. Sarna, Impact of Passive Cooling on Thermal Comfort in a Single-Family Building for Current and Future Climate Conditions, *Energies.* 13 (2020) 5332. <https://doi.org/10.3390/en13205332>.
- [177] A. Alaidroos, M. Krarti, Evaluation of Passive Cooling Systems for Residential Buildings in the Kingdom of Saudi Arabia, *Journal of Solar Energy Engineering.* 138 (2016). <https://doi.org/10.1115/1.4033112>.
- [178] D. Kimemia, A. Van Niekerk, H. Annegarn, M. Seedat, Passive cooling for thermal comfort in informal housing, *Journal of Energy in Southern Africa.* 31 (2020) 28–39. <https://doi.org/10.17159/2413-3051/2020/v31i1a7689>.
- [179] M. Macias, J.A. Gaona, J.M. Luxan, G. Gomez, Low cost passive cooling system for social housing in dry hot climate, *Energy and Buildings.* 41 (2009) 915–921. <https://doi.org/10.1016/j.enbuild.2009.03.013>.
- [180] S. Pathirana, A. Rodrigo, R. Halwatura, Effect of building shape, orientation, window to wall ratios and zones on energy efficiency and thermal comfort of naturally ventilated houses in tropical climate, *Int J Energy Environ Eng.* 10 (2019) 107–120. <https://doi.org/10.1007/s40095-018-0295-3>.
- [181] K. Saafi, N. Daouas, A life-cycle cost analysis for an optimum combination of cool coating and thermal insulation of residential building roofs in Tunisia, *Energy.* 152 (2018) 925–938. <https://doi.org/10.1016/j.energy.2018.04.010>.

- [182] H.M. Taleb, Using passive cooling strategies to improve thermal performance and reduce energy consumption of residential buildings in U.A.E. buildings, *Frontiers of Architectural Research*. 3 (2014) 154–165. <https://doi.org/10.1016/j.foar.2014.01.002>.
- [183] I. Hernández-Pérez, G. Álvarez, J. Xamán, I. Zavala-Guillén, J. Arce, E. Simá, Thermal performance of reflective materials applied to exterior building components—A review, *Energy and Buildings*. 80 (2014) 81–105. <https://doi.org/10.1016/j.enbuild.2014.05.008>.
- [184] R. Levinson, H. Akbari, Potential benefits of cool roofs on commercial buildings: Conserving energy, saving money, and reducing emission of greenhouse gases and air pollutants, *Energy Efficiency*. 3 (2010) 53–109. <https://doi.org/10.1007/s12053-008-9038-2>.
- [185] P.J. Rosado, R. Levinson, Potential benefits of cool walls on residential and commercial buildings across California and the United States: conserving energy, saving money, and reducing emission of greenhouse gases and air pollutants, *Energy and Buildings*. 199 (2019) 588–607. <https://doi.org/10.1016/j.enbuild.2019.02.028>.
- [186] S. Konopacki, H. Akbari, M. Pomerantz, S. Gabersek, L. Gartland, Cooling energy savings potential of light-colored roofs for residential and commercial buildings in 11 US metropolitan areas, 1997. <https://doi.org/10.2172/510556>.
- [187] S. Kriner, W.A. Miller, A.O. Desjarlais, The Trade-off between Solar Reflectance and Above-Sheathing Ventilation for Metal Roofs on Residential and Commercial Buildings, in: *Thermal VII: Thermal Performance of the Exterior Envelopes of Buildings VII*, Oak Ridge National Lab. (ORNL), Oak Ridge, TN (United States); Building Technologies Research and Integration Center, Clearwater, FL, 2013. <https://www.osti.gov/biblio/1110888-trade-off-between-solar-reflectance-above-sheathing-ventilation-metal-roofs-residential-commercial-buildings> (accessed March 1, 2020).
- [188] P.J. Rosado, D. Faulkner, D.P. Sullivan, R. Levinson, Measured temperature reductions and energy savings from a cool tile roof on a central California home, *Energy and Buildings*. 80 (2014) 57–71. <https://doi.org/10.1016/j.enbuild.2014.04.024>.
- [189] M.A.M. Ahrab, H. Akbari, Hygrothermal behaviour of flat cool and standard roofs on residential and commercial buildings in North America, *Building and Environment*. 60 (2013) 1–11. <https://doi.org/10.1016/j.buildenv.2012.11.003>.
- [190] H. Akbari, S. Bretz, D.M. Kurn, J. Hanford, Peak power and cooling energy savings of high-albedo roofs, *Energy and Buildings*. 25 (1997) 117–126. [https://doi.org/10.1016/S0378-7788\(96\)01001-8](https://doi.org/10.1016/S0378-7788(96)01001-8).
- [191] H. Akbari, S. Konopacki, M. Pomerantz, Cooling energy savings potential of reflective roofs for residential and commercial buildings in the United States, *Energy*. 24 (1999) 391–407. [https://doi.org/10.1016/S0360-5442\(98\)00105-4](https://doi.org/10.1016/S0360-5442(98)00105-4).
- [192] H. Akbari, R. Levinson, L. Rainer, Monitoring the energy-use effects of cool roofs on California commercial buildings, *Energy and Buildings*. 37 (2005) 1007–1016. <https://doi.org/10.1016/j.enbuild.2004.11.013>.
- [193] H. Akbari, P. Berdahl, R. Levinson, S. Wiel, W. Miller, A. Desjarlais, *Cool-Color Roofing Material*, California Energy Commission, Sacramento, CA, 2006. <https://ww2.energy.ca.gov/2006publications/CEC-500-2006-067/CEC-500-2006-067-ALL.PDF>.

- [194] H. Akbari, S. Konopacki, Streamlined energy-savings calculations for heat-island reduction strategies, Lawrence Berkeley National Laboratory, Berkeley, CA, 2003. <https://www.osti.gov/servlets/purl/816531>.
- [195] R. Levinson, Using solar availability factors to adjust cool-wall energy savings for shading and reflection by neighboring buildings, *Solar Energy*. 180 (2019) 717–734. <https://doi.org/10.1016/j.solener.2019.01.023>.
- [196] T.W. Petrie, J.A. Atchley, P.W. Childs, A.O. Desjarlais, Energy savings for stucco walls coated with cool colors, in: *Thermal Performance of Exterior Envelopes of Whole Buildings X*, Clearwater, FL, 2007. <https://www.coolrooftoolkit.org/wp-content/uploads/2012/05/Energy-Savings-for-Stucco-Walls.pdf>.
- [197] T. Hong, S. Selkowitz, M. Yazdani, Assessment of Energy Impact of Window Technologies for Commercial Buildings, 2009. <https://doi.org/10.2172/1168734>.
- [198] N. DeForest, A. Shehabi, G. Garcia, J. Greenblatt, E. Masanet, E.S. Lee, S. Selkowitz, D.J. Milliron, Regional performance targets for transparent near-infrared switching electrochromic window glazings, *Building and Environment*. 61 (2013) 160–168. <https://doi.org/10.1016/j.buildenv.2012.12.004>.
- [199] U.S. Environmental Protection Agency, Community-based Adaptation to a Changing Climate, (2015). https://www.epa.gov/sites/production/files/2016-09/documents/community-based-adaptation_handout.pdf.
- [200] Public Health England, Department of Health and Social Care, NHS England, Heatwave Plan for England, 2020. https://assets.publishing.service.gov.uk/government/uploads/system/uploads/attachment_data/file/888668/Heatwave_plan_for_England_2020.pdf.
- [201] P. Berry, G.R.A. Richardson, Approaches for Building Community Resilience to Extreme Heat - Extreme Weather, Health, and Communities: Interdisciplinary Engagement Strategies, in: S.L. Steinberg, W.A. Sprigg (Eds.), Springer International Publishing, Cham, 2016: pp. 351–388. https://doi.org/10.1007/978-3-319-30626-1_15.
- [202] G. Hatvani-Kovacs, J. Bush, E. Sharifi, J. Boland, Policy recommendations to increase urban heat stress resilience, *Urban Climate*. 25 (2018) 51–63. <https://doi.org/10.1016/j.uclim.2018.05.001>.
- [203] Y.T. Maru, M. Stafford Smith, A. Sparrow, P.F. Pinho, O.P. Dube, A linked vulnerability and resilience framework for adaptation pathways in remote disadvantaged communities, *Global Environmental Change*. 28 (2014) 337–350. <https://doi.org/10.1016/j.gloenvcha.2013.12.007>.
- [204] A. Katal, M. Mortezaadeh, L. (Leon) Wang, Modeling building resilience against extreme weather by integrated CityFFD and CityBEM simulations, *Applied Energy*. 250 (2019) 1402–1417. <https://doi.org/10.1016/j.apenergy.2019.04.192>.
- [205] C.A. Short, K.J. Lomas, R. Giridharan, A.J. Fair, Building resilience to overheating into 1960's UK hospital buildings within the constraint of the national carbon reduction target: Adaptive strategies, *Building and Environment*. 55 (2012) 73–95. <https://doi.org/10.1016/j.buildenv.2012.02.031>.
- [206] S. Flores-Larsen, C. Filippin, Energy efficiency, thermal resilience, and health during extreme heat events in low-income housing in Argentina, *Energy and Buildings*. 231 (2021) 110576. <https://doi.org/10.1016/j.enbuild.2020.110576>.

- [207] J.J. Hess, L.M. Sathish, K. Knowlton, S. Saha, P. Dutta, P. Ganguly, A. Tiwari, A. Jaiswal, P. Sheffield, J. Sarkar, S.C. Bhan, A. Begda, T. Shah, B. Solanki, D. Mavalankar, Building resilience to climate change: Pilot evaluation of the impact of India's first heat action plan on all-cause mortality, *Journal of Environmental and Public Health*. 2018 (2018). <https://doi.org/10.1155/2018/7973519>.
- [208] California Energy Commission, 2019 Building Energy Efficiency Standards for Residential and Nonresidential Buildings (Title 24, Part 6), Sacramento, CA, 2018. <https://ww2.energy.ca.gov/2018publications/CEC-400-2018-020/CEC-400-2018-020-CMF.pdf>.
- [209] D.B. Crawley, L.K. Lawrie, F.C. Winkelmann, W.F. Buhl, Y.J. Huang, C.O. Pedersen, R.K. Strand, R.J. Liesen, D.E. Fisher, M.J. Witte, J. Glazer, EnergyPlus: Creating a new-generation building energy simulation program, *Energy and Buildings*. 33 (2001) 319–331. [https://doi.org/10.1016/S0378-7788\(00\)00114-6](https://doi.org/10.1016/S0378-7788(00)00114-6).
- [210] R.H. Henninger, M.J. Witte, EnergyPlus testing with ANSI/ASHRAE standard 140-2001 (BESTEST), Lawrence Berkely National Laboratory, Prepared for U.S. Department of Energy. https://Simulationresearch.Lbl.Gov/Dirpubs/Epl_bestest_ash.Pdf. (2004). https://simulationresearch.lbl.gov/dirpubs/epl_bestest_ash.pdf.
- [211] Y. Chen, T. Hong, M.A. Piette, Automatic generation and simulation of urban building energy models based on city datasets for city-scale building retrofit analysis, *Applied Energy*. 205 (2017) 323–335. <https://doi.org/10.1016/j.apenergy.2017.07.128>.
- [212] T. Hong, Y. Chen, S.H. Lee, M.A. Piette, CityBES : A Web-based Platform to Support City-Scale Building Energy Efficiency, *Urban Computing*. (2016). <https://doi.org/10.1145/12345.67890>.
- [213] Y. Chen, Z. Deng, T. Hong, Automatic and rapid calibration of urban building energy models by learning from energy performance database, *Applied Energy*. 277 (2020) 115584. <https://doi.org/10.1016/j.apenergy.2020.115584>.
- [214] ASHRAE—American Society of Heating, Ventilating and Air-Conditioning Engineers, ASHRAE Handbook—Fundamentals, ASHRAE, 2017. <https://www.ashrae.org/technical-resources/ashrae-handbook/description-2017-ashrae-handbook-fundamentals>.
- [215] World Meteorological Organization, World Health Organization, Heatwaves and Health: Guidance on Warning-System Development, 2015.
- [216] C. Koppe, S. Kovats, G. Jendritzky, B. Menne, Heat-waves: risks and responses, 2004.
- [217] A. Wilson, LEED Pilot Credits on Resilient Design Adopted!, 2015. <https://www.resilientdesign.org/leed-pilot-credits-on-resilient-design-adopted/>.
- [218] ASHRAE, ASHRAE Standard 55-2017: Thermal Environmental Conditions for Human Occupancy, 2017.
- [219] National Oceanic and Atmospheric Administration, Heat Index, 2018. <https://www.weather.gov/safety/heat-index>.
- [220] National Oceanic and Atmospheric Administration, Heat Safety, 2019. <https://www.weather.gov/grb/heat>.
- [221] R.R. Gonzalez, Y. Nishi, A.P. Gagge, Experimental evaluation of standard effective temperature a new biometeorological index of man's thermal discomfort, *International Journal of Biometeorology*. 18 (1974) 1–15. <https://doi.org/10.1007/BF01450660>.

- [222] Y. Zhang, H. Chen, J. Wang, Q. Meng, Thermal comfort of people in the hot and humid area of China—impacts of season, climate, and thermal history, *Indoor Air*. 26 (2016) 820–830. <https://doi.org/10.1111/ina.12256>.
- [223] P.O. Fanger, *Thermal Comfort: Analysis and Application in Environment Engineering*, 1970.
- [224] S.I.U.H. Gilani, M.H. Khan, W. Pao, Thermal Comfort Analysis of PMV Model Prediction in Air Conditioned and Naturally Ventilated Buildings, *Energy Procedia*. 75 (2015) 1373–1379. <https://doi.org/10.1016/j.egypro.2015.07.218>.
- [225] International Organization Standardization, ISO 7730:2005 - Ergonomics of the thermal environment — Analytical determination and interpretation of thermal comfort using calculation of the PMV and PPD indices and local thermal comfort criteria, 2005. <https://www.iso.org/standard/39155.html>.
- [226] California Energy Commission, 2016 Residential Alternative Calculation Method Reference Manual for the 2016 Building Energy Efficiency Standards, (2016). http://www.bwilcox.com/BEES/docs/2016_Res_ACM_Reference_Manual_Sept%2020162.pdf.
- [227] California Energy Commission, 2016 Building Energy Efficiency Standards for Residential and Nonresidential Buildings, (2016). <https://ww2.energy.ca.gov/2015publications/CEC-400-2015-037/CEC-400-2015-037-CMF.pdf>.
- [228] California Energy Commission, 2019 Residential Compliance Manual for the 2019 Building Energy Efficiency Standards, (2018). https://www.energy.ca.gov/sites/default/files/2020-06/Compliance_Manual-Complete_without_forms_ada.pdf.
- [229] S. Mazur-Stommen, H. Gilbert, Personal Communications: surveys and focus groups with residents at the neighborhoods in Southwest Fresno, (2020).
- [230] Fresno Economic Opportunities Commission, Weatherization programs at disadvantaged communities in Fresno, (2020). <https://fresnoeoc.org/energy/>.
- [231] Fresno Housing Authority, Interview with Fresno Housing Authority, (2020).
- [232] U.S. Department of Energy, Evaporative Coolers, 2020. <https://www.energy.gov/energysaver/home-cooling-systems/evaporative-coolers>.
- [233] U.S. Department of Energy, Room Air Conditioners, 2020. <https://www.energy.gov/energysaver/room-air-conditioners>.
- [234] U.S. Department of Energy, Central Air Conditioning, 2020. <https://www.energy.gov/energysaver/central-air-conditioning>.
- [235] K. Fenaughty, D. Parker, Evaluation of Air Conditioning Performance Degradation: Opportunities from Diagnostic Methods, in: 2018 ACEEE Summer Study on Energy Efficiency in Buildings. [Http://Publications.Energyresearch.Ucf.Edu/Wp-Content/Uploads/2018/09/FSEC-PF-474-18.Pdf](http://Publications.Energyresearch.Ucf.Edu/Wp-Content/Uploads/2018/09/FSEC-PF-474-18.Pdf), 2018. <http://publications.energyresearch.ucf.edu/wp-content/uploads/2018/09/FSEC-PF-474-18.pdf>.
- [236] R. Hendron, *Building America Performance Analysis Procedures for Existing Homes*, 2006. <http://www.nrel.gov/buildings/pdfs/38238.pdf>.
- [237] M. Althoff, 5, 15 or 20? Your Commercial HVAC Life Expectancy, 2020. <https://www.althoffind.com/blog/5-15-or-20-your-commercial-hvac-life-expectancy>.

- [238] Princeton Air, What is the Average Life Expectancy of an HVAC System?, 2019. <https://www.princetonair.com/blog/what-average-life-expectancy-hvac-system>.
- [239] National Renewable Energy Laboratory, BEopt: Building Energy Optimization Tool, (2018). beopt.nrel.gov/home.
- [240] U.S. Energy Information Administration, Residential Energy Consumption Survey: Table HC10.14 Average square footage of single-family homes, 2015, (2015). <https://www.eia.gov/consumption/residential/data/2015/hc/php/hc10.14.php>.
- [241] U.S. Energy Information Administration, Residential Energy Consumption Survey (RECS), (2020). <https://www.eia.gov/consumption/residential/index.php>.
- [242] Neighborhood Revitalization Team, Restore & Revitalize the City of Fresno, (2017). <https://www.fresno.gov/darm/wp-content/uploads/sites/10/2018/02/Future-and-Current-NRT-Neighborhoods-Update-12-14-17-.pdf>.
- [243] Microsoft, Building Footprints - Bing Maps, 2019. <https://www.microsoft.com/en-us/maps/building-footprints>.
- [244] Google, Google Maps Platform, (2021). <https://developers.google.com/maps>.
- [245] Zillow, Zillow Real Estate and Mortgage Data, (2021). <https://www.zillow.com/howto/api/APIOverview.htm>.
- [246] Attom Data Solutions, Attom Property Data API, (2020). <https://www.attomdata.com/solutions/property-data-api/>.
- [247] SelectBlinds.com, 2" Luxe Modern Faux Wood Blinds, (2021). <https://www.selectblinds.com/fauxwoodblinds/2-inch-premium-faux-wood-blinds.html>.
- [248] Alecia Klinner, Metal awnings for windows, (2021). <https://www.pinterest.com/klinneralecia/metal-awnings-for-windows/>.
- [249] Hatch Homes, Storm Windows, (2021). <https://www.hatchyourhome.com/storm-windows/>.
- [250] Ideaing.com, Gila LES361 Heat Control Residential Window Film, (2021). <https://ideaing.com/product/gila-les361-heat-control-residential-window-film>.
- [251] C. Gronbeck, Sustainable By Design: Overhang Recommendations, 2009. https://susdesign.com/overhang_recs/index.php.
- [252] U.S. Department of Energy, Storm Windows, (2020). <https://www.energy.gov/energysaver/storm-windows>.
- [253] D. Arasteh, C. Kohler, B. Griffith, Modeling Windows in Energy Plus with Simple Performance Indices, 2009. <https://doi.org/10.2172/975375>.
- [254] LLumar, LLumar Vista Window Films, LLumar. (2020). <https://northamerica.llumar.com/vista-window-films>.
- [255] L. Wang, S. Greenberg, Window operation and impacts on building energy consumption, Energy and Buildings. 92 (2015) 313–321. <https://doi.org/10.1016/j.enbuild.2015.01.060>.
- [256] U.S. Department of Energy, Radiant Barriers, (2020). <https://www.energy.gov/energysaver/weatherize/insulation/radiant-barriers>.
- [257] A. Laouadi, A. Gaur, M.A. Lacasse, M. Bartko, M. Armstrong, Development of reference summer weather years for analysis of overheating risk in buildings, Journal of Building Performance Simulation. 13 (2020) 301–319. <https://doi.org/10.1080/19401493.2020.1727954>.

- [258] G.B. Anderson, M.L. Bell, Heat Waves in the United States: Mortality Risk during Heat Waves and Effect Modification by Heat Wave Characteristics in 43 U.S. Communities, *Environ Health Perspect.* 119 (2011) 210–218. <https://doi.org/10.1289/ehp.1002313>.
- [259] J.F. Kreider, P.S. Curtiss, A. Rabl, *Heating and Cooling of Buildings: Design for Efficiency*, CRC Press, 2009.
- [260] Gas Technology Institute, *Source Energy and Emissions Analysis Tool*, (2021). <http://seeatcalc.gastechnology.org/>.

Supporting Information

Section A

This section shows the figures for metrics and scenarios of prototype houses that are not listed in Chapter 5.1.

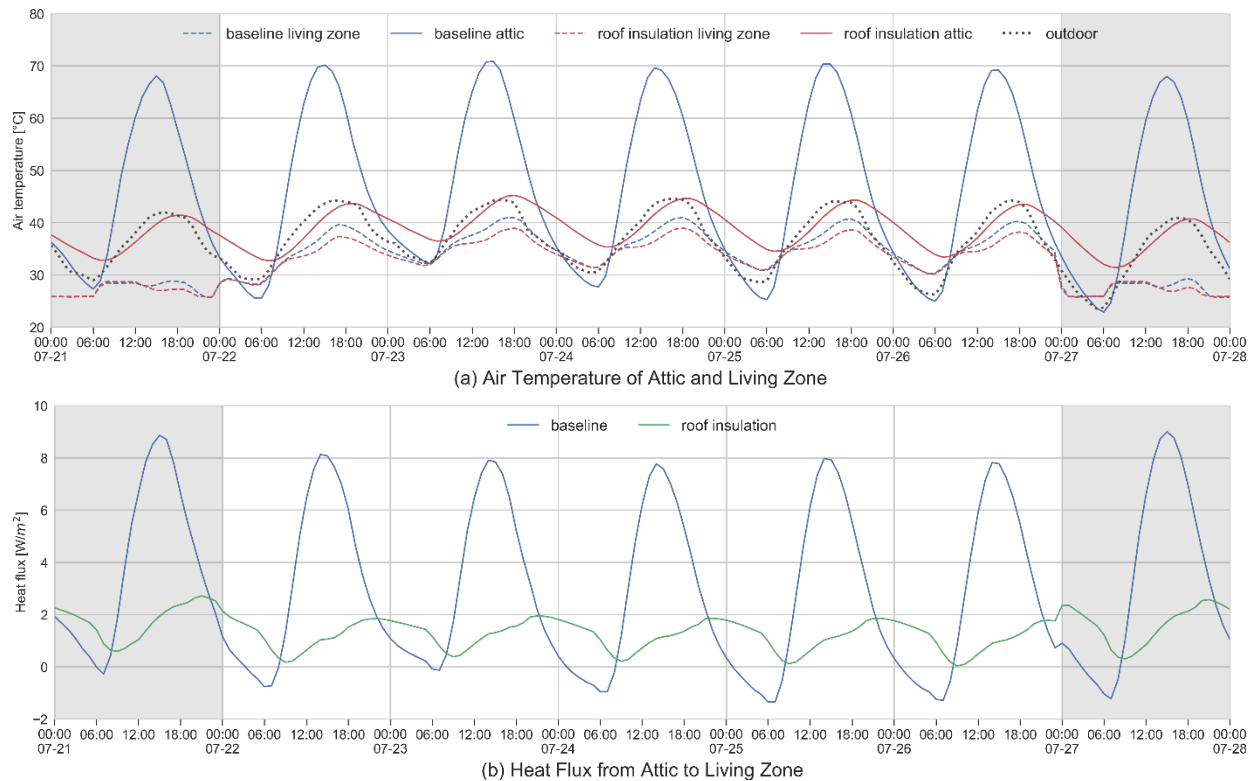


Figure A-1. (a) Attic and living zone air temperature and (b) heat flux from attic to living zone during a heat wave of the single-family home built in 1976 after adding roof insulation compared with baseline in the grid-off scenario.

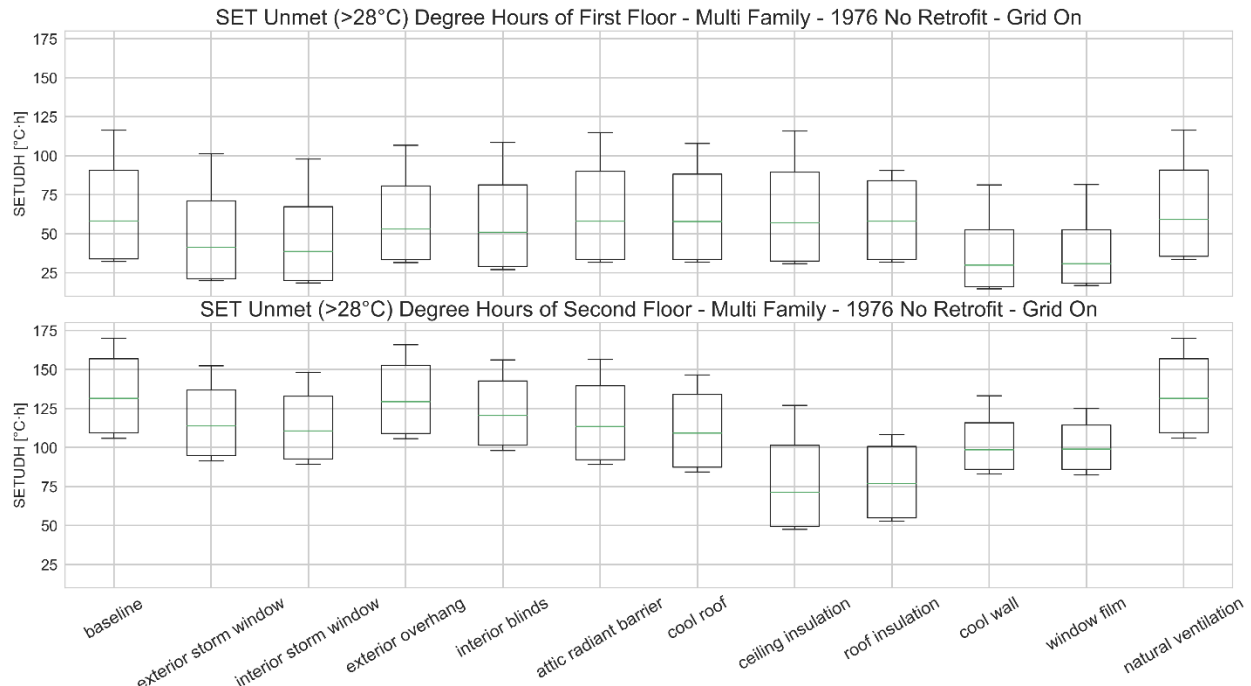


Figure A-2. Standard effective temperature unmet degree hours during the heat wave in the baseline case and after applying each ECM, shown for the multi-family home built in 1976 in the grid-on scenario. Each box shows the distribution of different apartments within the multi-family home.

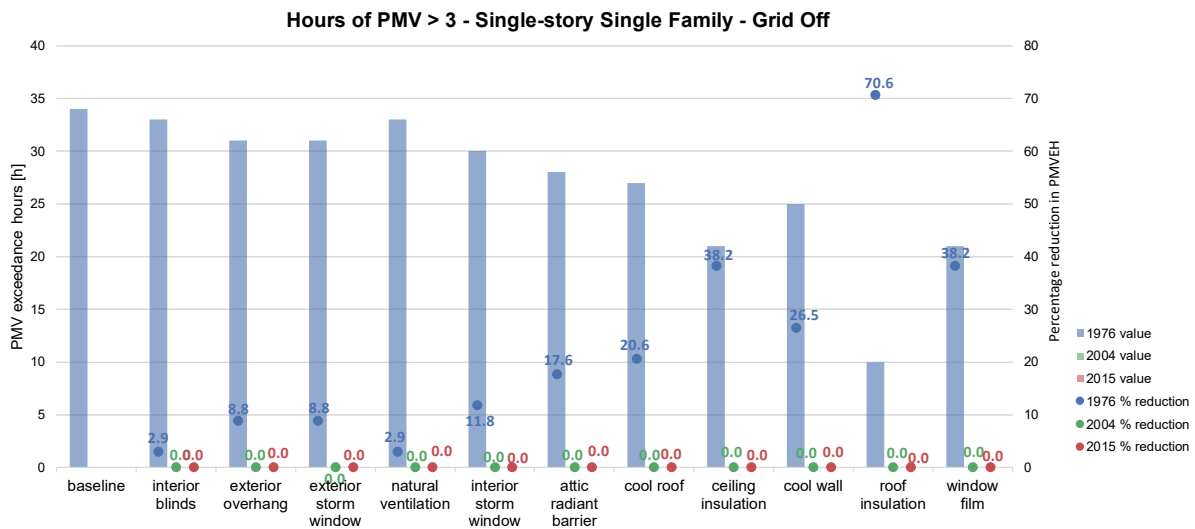


Figure A-3. Hours of PMV > 3 during the heat wave in the baseline case and after applying each ECM, show for single-family homes of different vintages in the grid-off scenario. Columns represent absolute values and the dots mark percentage reduction.

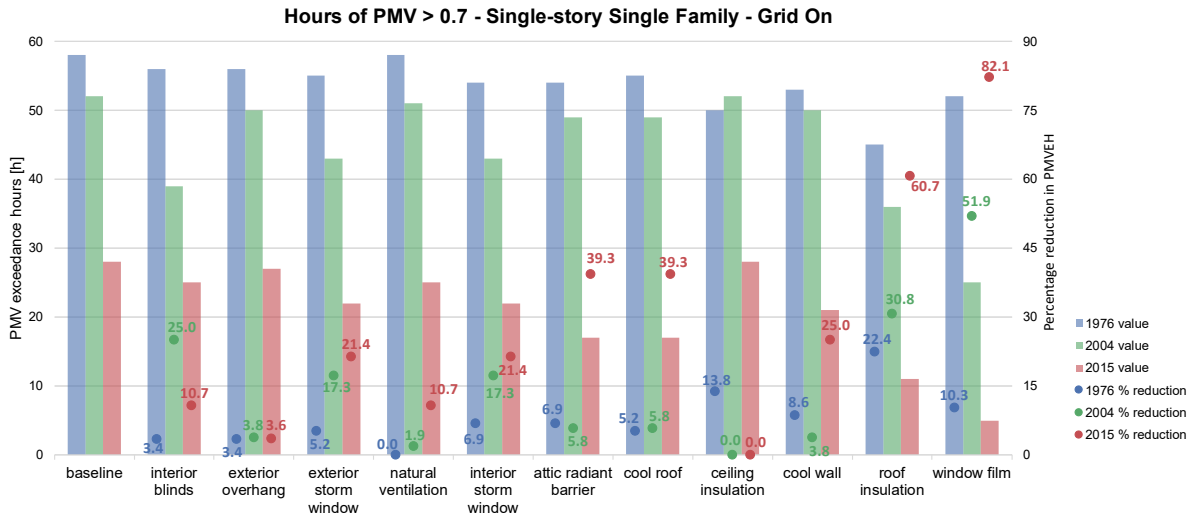


Figure A-4. Hours of PMV > 0.7 during the heat wave in the baseline case and after applying each ECM, show for single-family homes of different vintages in the grid-on scenario. Columns represent absolute values and the dots mark percentage reduction.

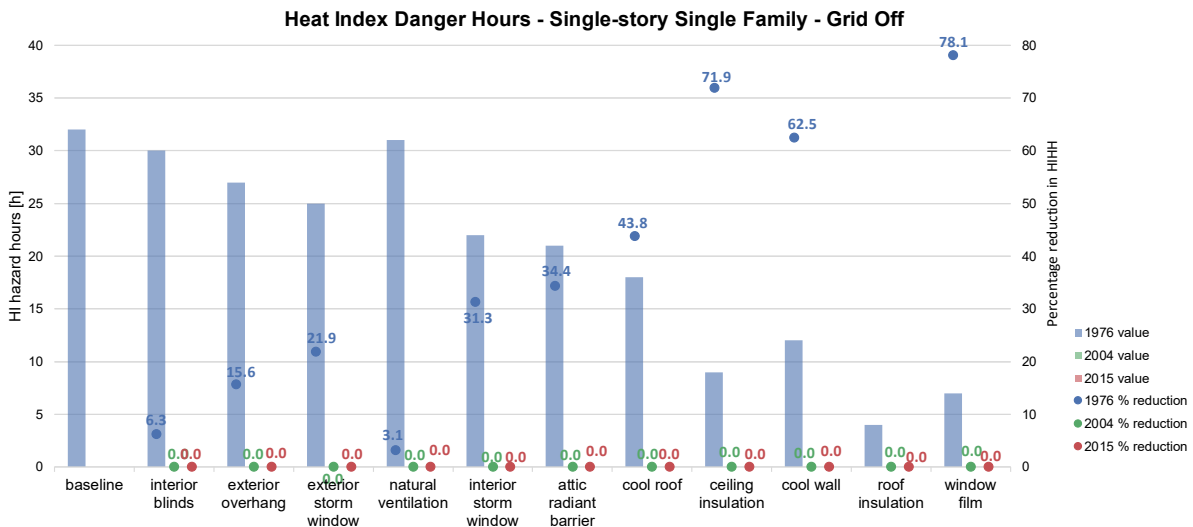


Figure A-5. Heat index danger hours during the heat wave in the baseline case and after applying each ECM, show for single-family homes of different vintages in the grid-off scenario. Columns represent absolute values and the dots mark percentage reduction.

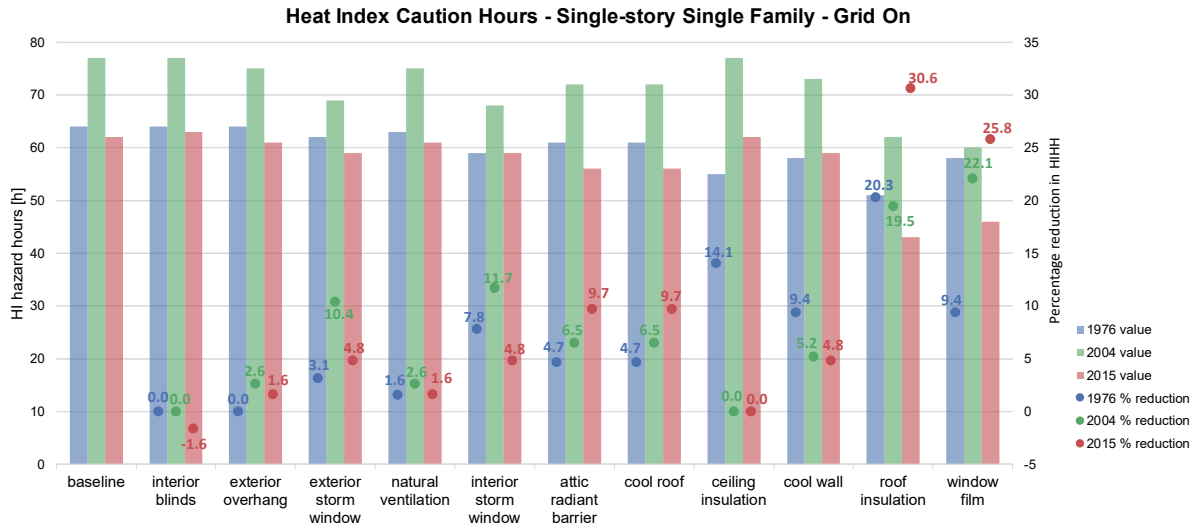


Figure A-6. Heat index caution hours during the heat wave in the baseline case and after applying each ECM, show for single-family homes of different vintages in the grid-on scenario. Columns represent absolute values and the blue mark percentage reduction.

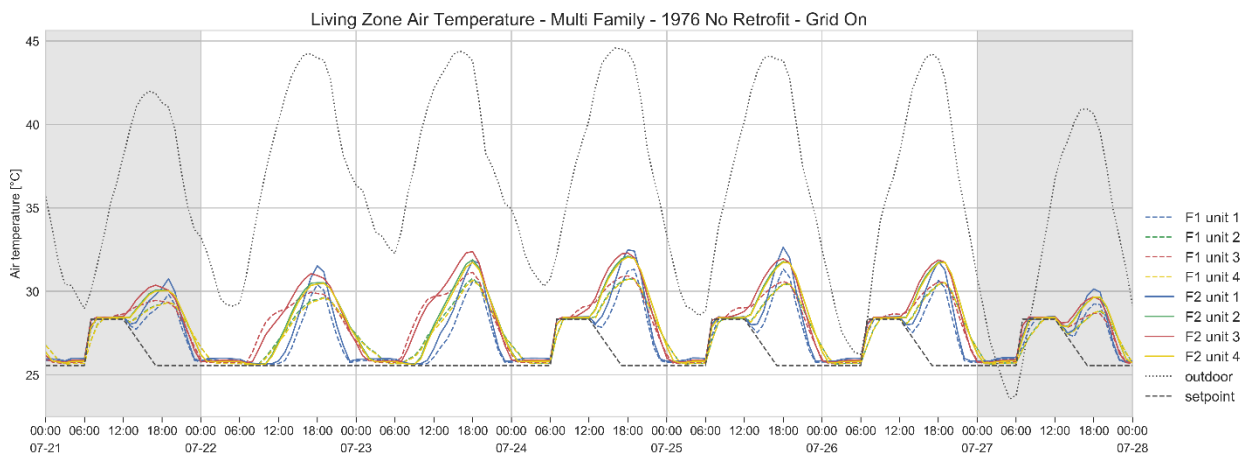


Figure A-7. Baseline air temperature of each unit of the multi-family home built in 1978 in the grid-on scenario. Labels "F1" and "F2" in the legend refer to units on the first and second floor, respectively. The temperatures for "unit 2" and "unit 4" are the same.

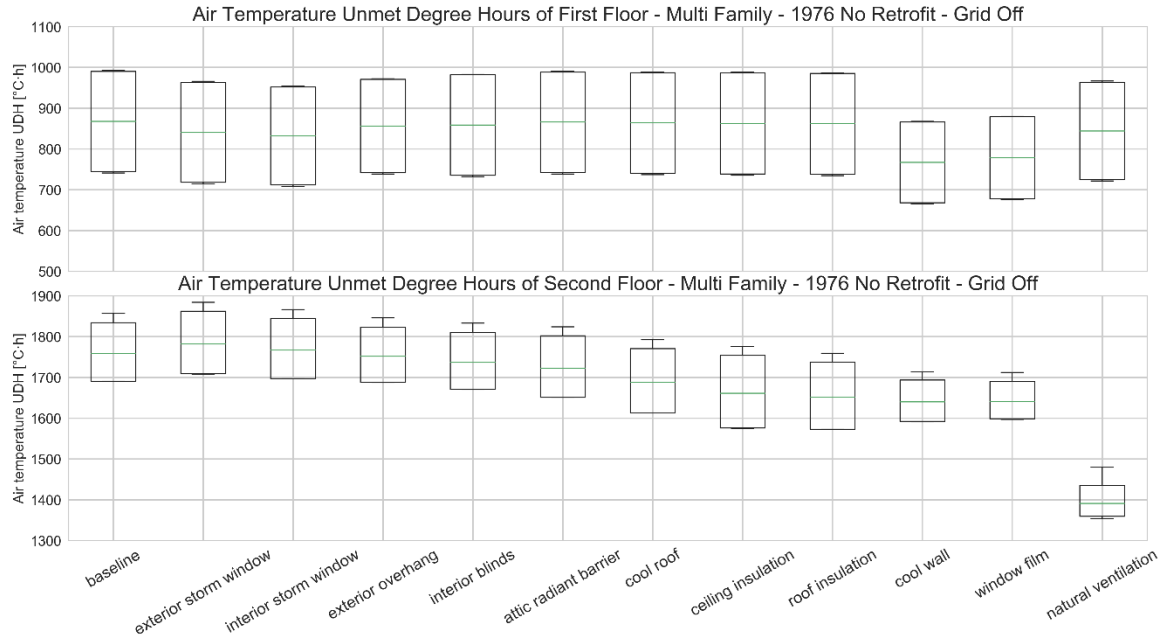


Figure A-8. Air temperature unmet degree hours during the heat wave in the baseline case and after applying each ECM, shown for the multi-family home built in 1976 in the grid-off scenario. Each box shows the distribution of different apartments within the multi-family home.

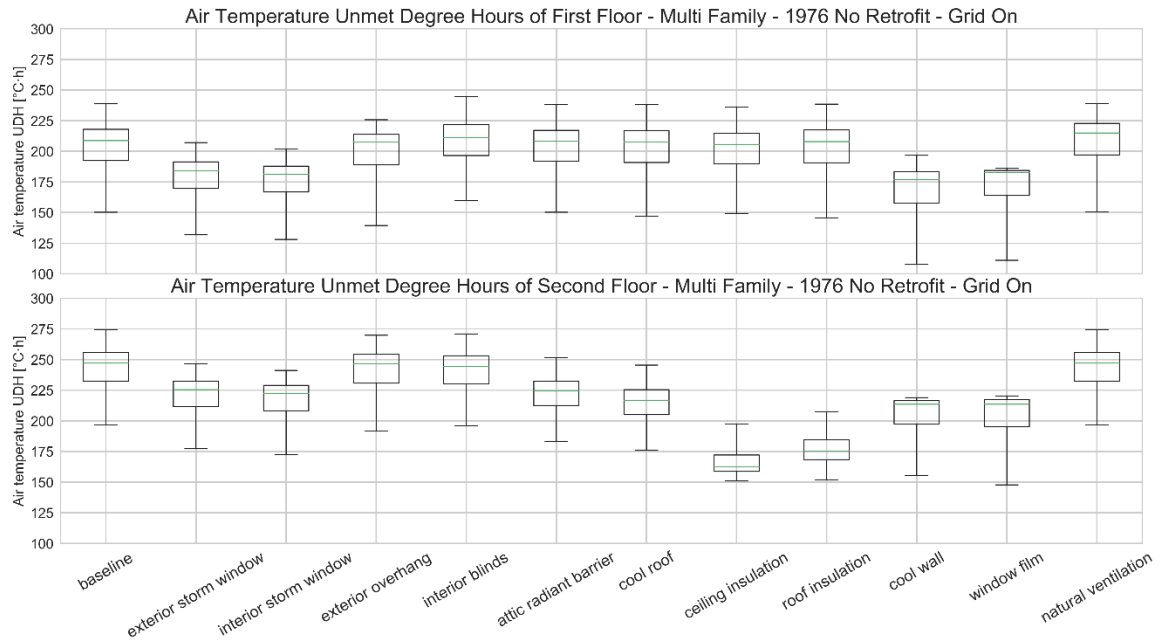


Figure A-9. Air temperature unmet degree hours during the heat wave in the baseline case and after applying each ECM, shown for the multi-family home built in 1976 in the grid-on scenario. Each box shows the distribution of different apartments within the multi-family home.

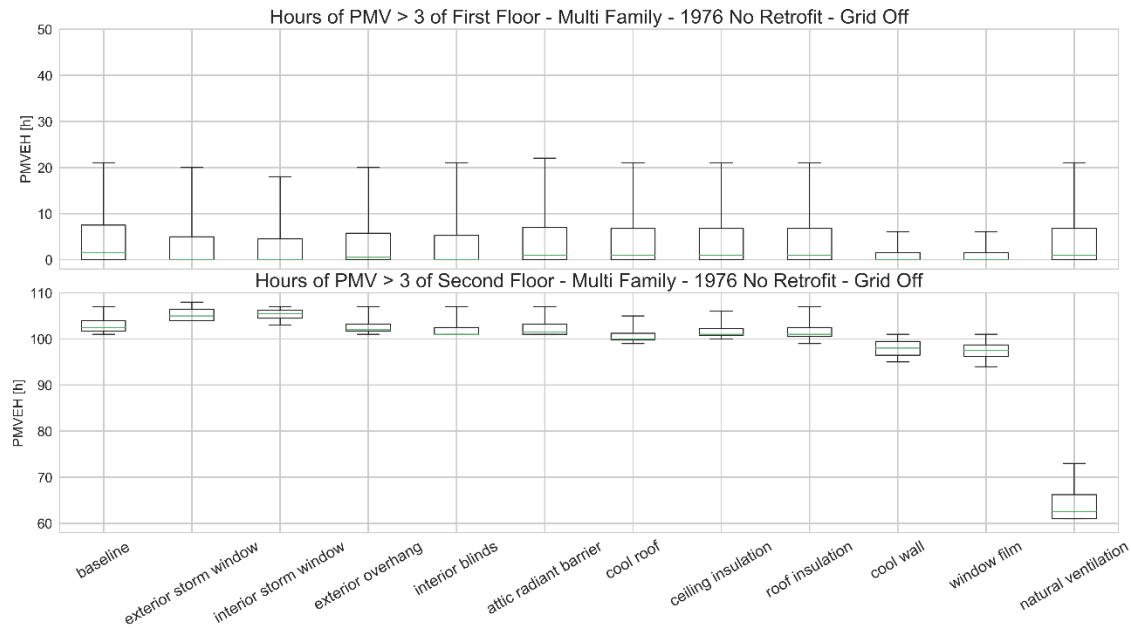


Figure A-10. Hours of PMV > 3 during the heat wave in the baseline case and after applying each ECM, shown for the multi-family home built in 1976 in the grid-off scenario. Each box shows the distribution of different apartments within the multi-family home.

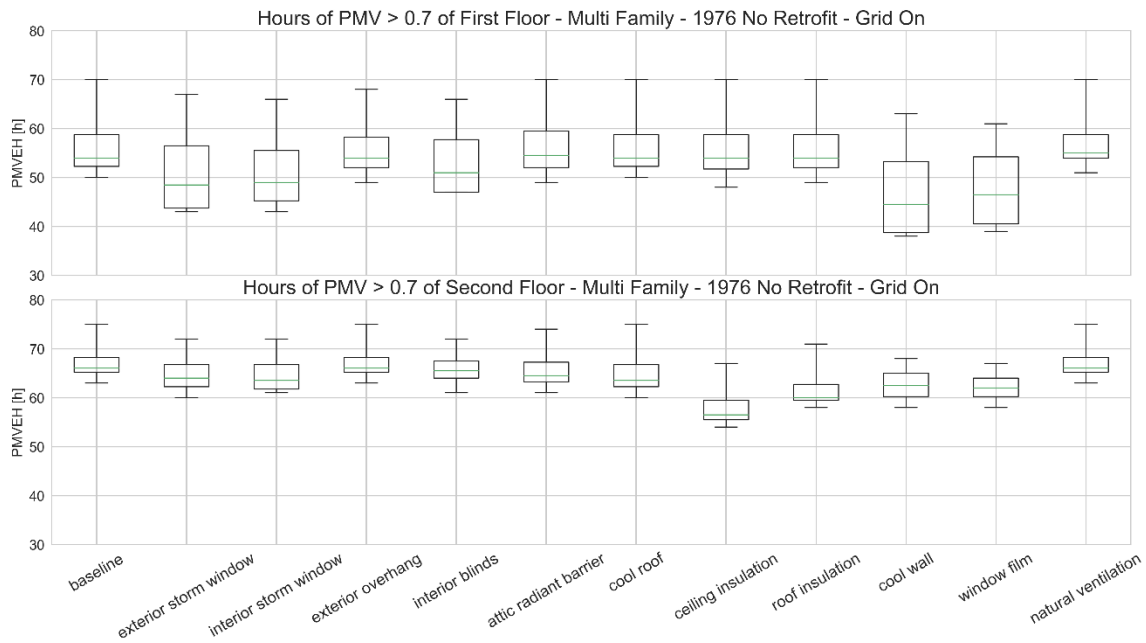


Figure A-11. Hours of PMV > 0.7 during the heat wave in the baseline case and after applying each ECM, shown for the multi-family home built in 1976 in the grid-on scenario. Each box shows the distribution of different apartments within the multi-family home.

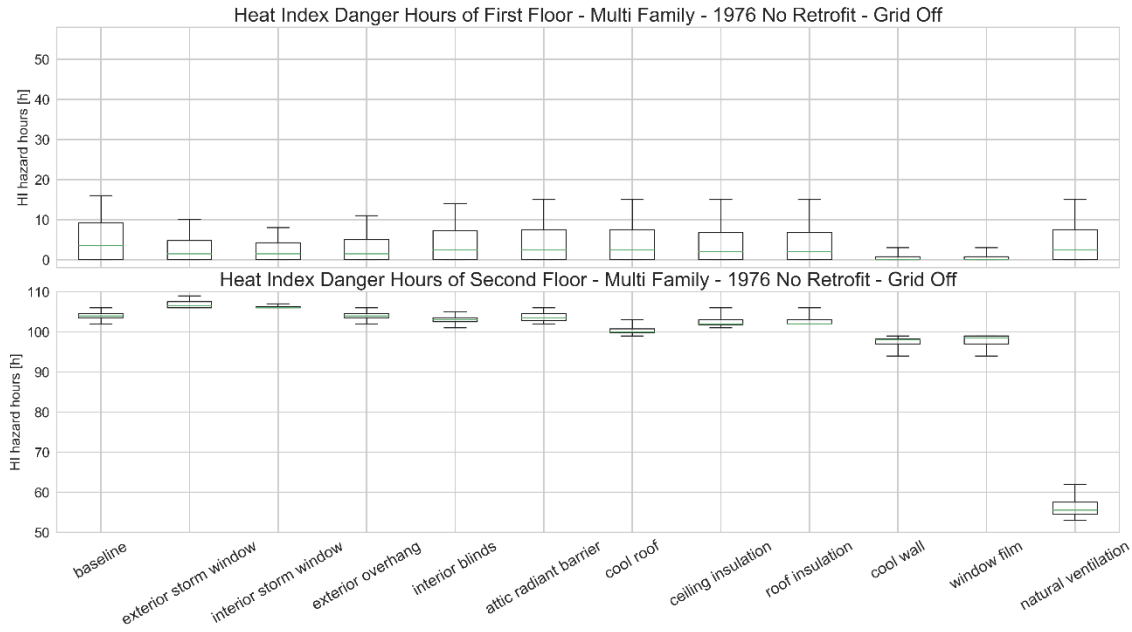


Figure A-12. Heat index danger hours during the heat wave in the baseline case and after applying each ECM, shown for the multi-family home built in 1976 in the grid-off scenario. Each box shows the distribution of different apartments within the multi-family home.

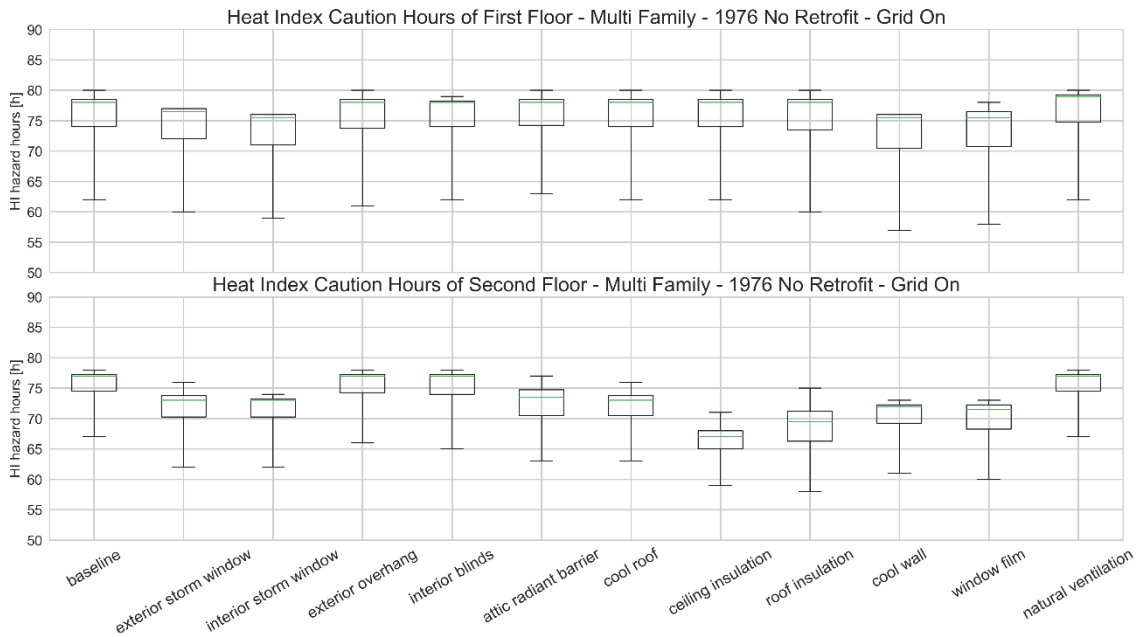


Figure A-13. Heat index caution hours during the heat wave in the baseline case and after applying each ECM, shown for the multi-family home built in 1976 in the grid-on scenario. Each box shows the distribution of different apartments within the multi-family home.

The vintage comparison for multi-family homes are illustrated by UDH and SETUDH to show the effects on the air temperature and other environmental variables.

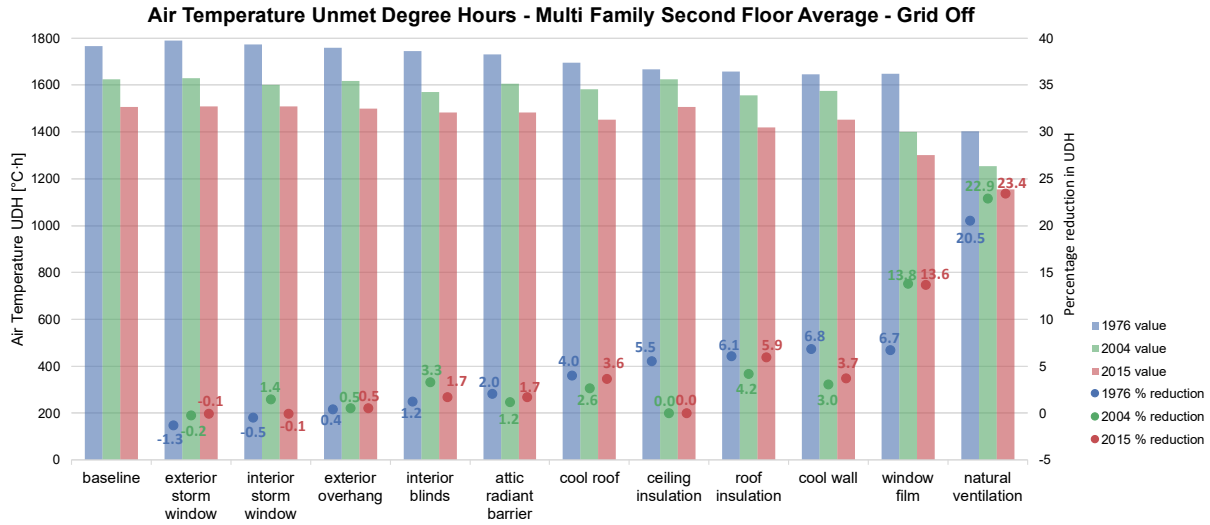


Figure A-14. Air temperature unmet degree hours during the heat wave in the baseline case and after applying each ECM, show for the average of the second-floor units in multi-family homes of different vintages in the grid-off scenario. Columns represent absolute values and the dots mark percentage reduction.

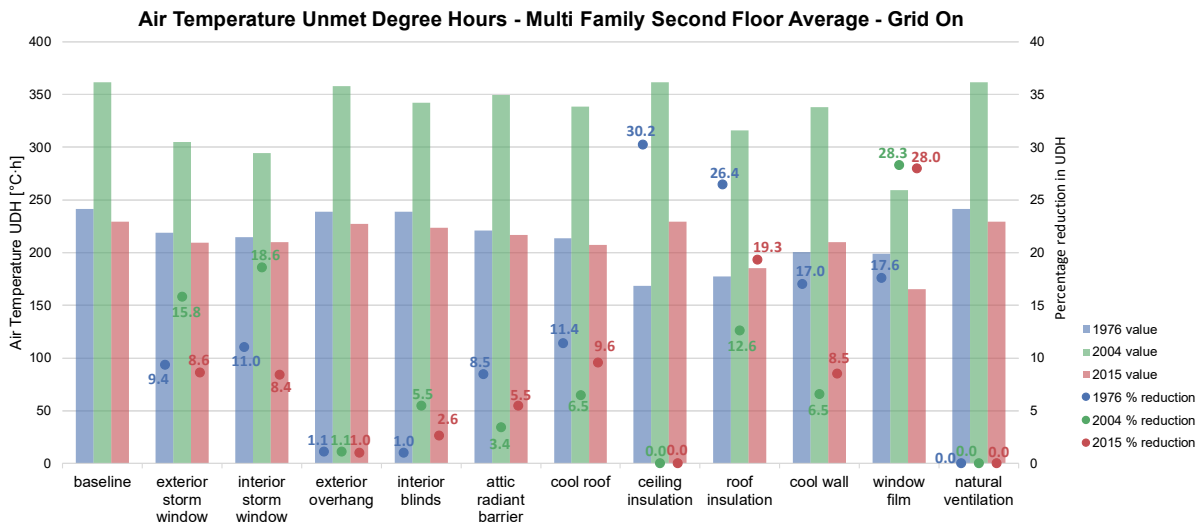


Figure A-15. Air temperature unmet degree hours during the heat wave in the baseline case and after applying each ECM, show for the average of the second-floor units in multi-family homes of different vintages in the grid-on scenario. Columns represent absolute values and the dots mark percentage reduction.

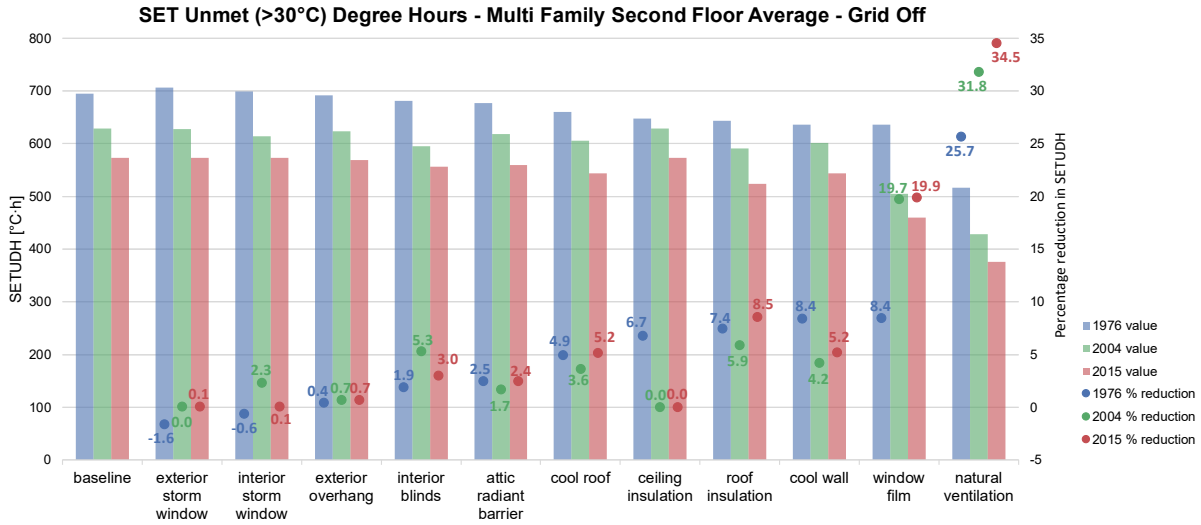


Figure A-16. Standard effective temperature unmet degree hours during the heat wave in the baseline case and after applying each ECM, show for the average of the second-floor units in multi-family homes of different vintages in the grid-off scenario. Columns represent absolute values and the dots mark percentage reduction.

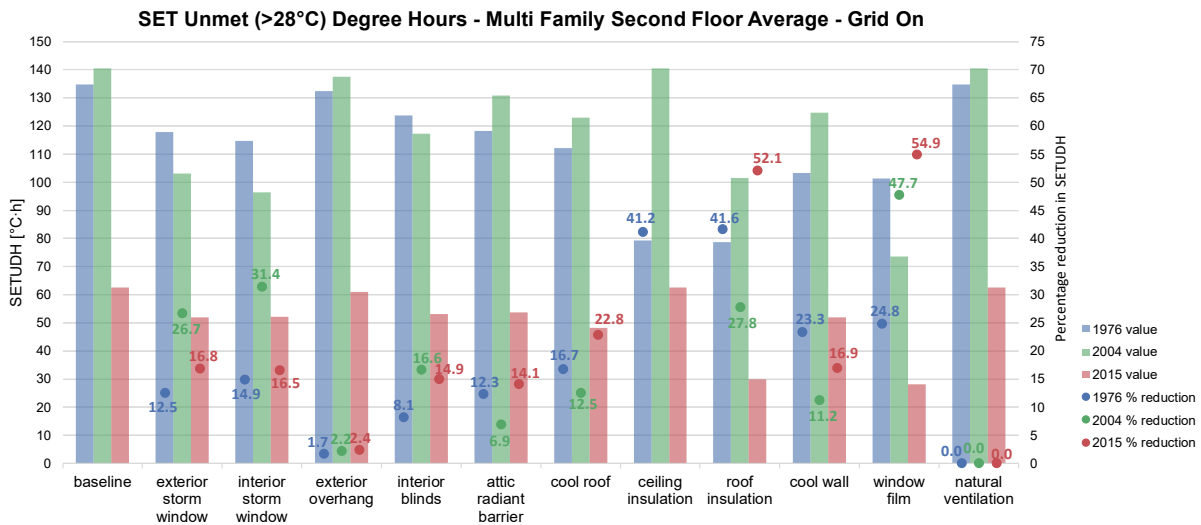


Figure A-17. Standard effective temperature unmet degree hours during the heat wave in the baseline case and after applying each ECM, show for the average of the second-floor units in multi-family homes of different vintages in the grid-on scenario. Columns represent absolute values and the dots mark percentage reduction.

Section B

This section shows the figures for metrics and scenarios of prototype houses that are not listed in Chapter 5.2.

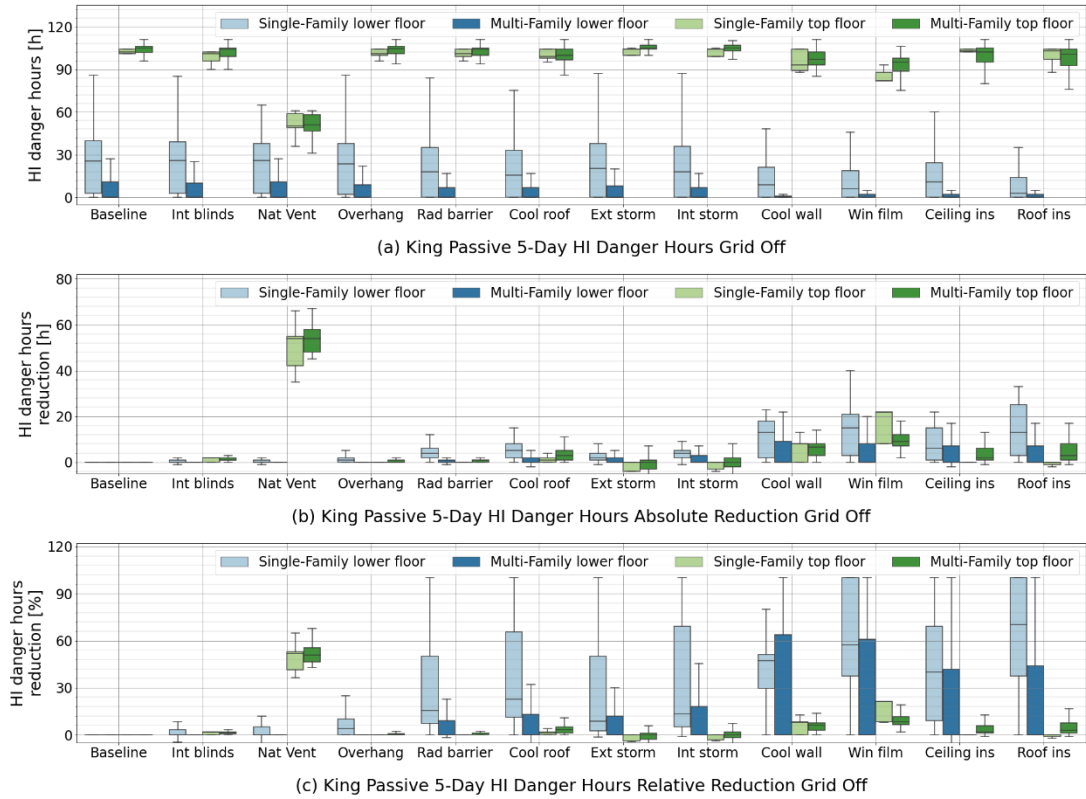


Figure B-1. Heat index danger hours during the heat wave in the baseline case and after applying each ECM for the grid-off scenario.

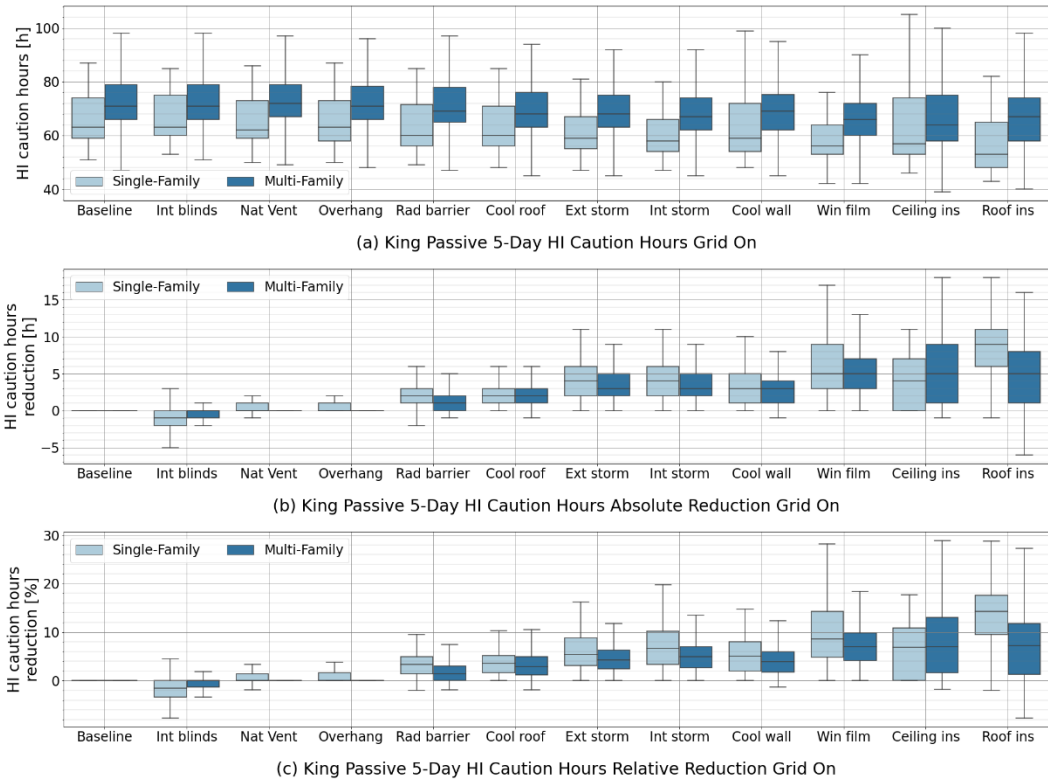


Figure B-2. Heat index caution hours during the heat wave in the baseline case and after applying each ECM for the grid-on scenario.



Figure B-3. Predicted mean vote exceedance hours (PMV > 3) during the heat wave in the baseline case and after applying each ECM for the grid-off scenario.

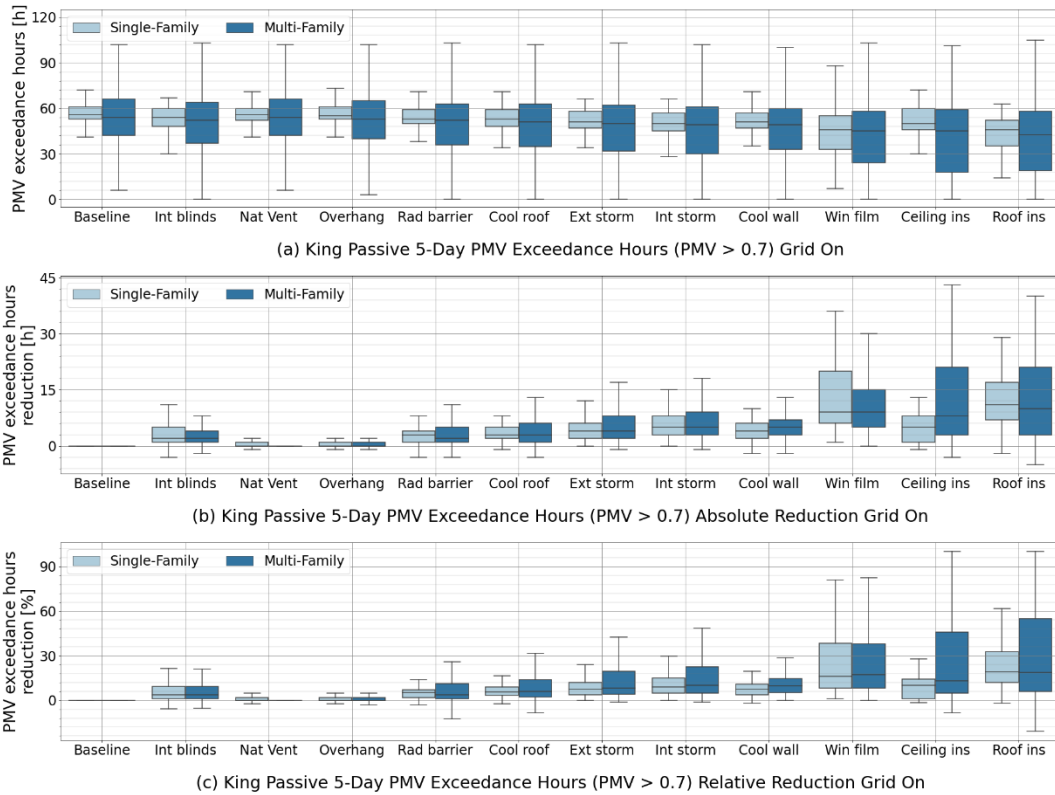


Figure B-4. Predicted mean vote exceedance hours (PMV > 0.7) during the heat wave in the baseline case and after applying each ECM for the grid-on scenario.

The results of HHH and PMVEH are similar to those of UDH and SETUDH, respectively. Thus, they will not be analyzed separately.